






Universitat Autònoma de Barcelona

ADVERTIMENT. L'accés als continguts d'aquesta tesi queda condicionat a l'acceptació de les condicions d'ús establertes per la següent llicència Creative Commons:  http://cat.creativecommons.org/?page_id=184

ADVERTENCIA. El acceso a los contenidos de esta tesis queda condicionado a la aceptación de las condiciones de uso establecidas por la siguiente licencia Creative Commons:  <http://es.creativecommons.org/blog/licencias/>

WARNING. The access to the contents of this doctoral thesis it is limited to the acceptance of the use conditions set by the following Creative Commons license:  <https://creativecommons.org/licenses/?lang=en>

**CHARACTERIZATION OF PLANT
CELLULAR RESPONSES UPON
PATHOGEN-INDUCED RNA
SILENCING SUPPRESSION**

Luis Manuel Villar Martin

Barcelona, December 2021

UNIVERSIDAD AUTÓNOMA DE BARCELONA

FACULTAD DE BIOCENCIAS

Dpto. BIOLOGÍA ANIMAL, BIOLOGÍA VEGETAL Y ECOLOGÍA

DOCTORADO EN BIOLOGÍA Y BIOTECNOLOGÍA VEGETAL

PhD. THESIS

CHARACTERIZATION OF PLANT CELLULAR RESPONSES UPON PATHOGEN-INDUCED RNA SILENCING SUPPRESSION

Dissertation presented by Luis Manuel Villar Martin for the degree of Doctor in biology and plant biotechnology by Universitat Autònoma de Barcelona.

This work was performed in Centre for Research in Agricultural Genomics (CRAG), Molecular Reprogramming and Evolution (MoRE) laboratory, Cerdanyola del Vallès (Barcelona)

Dr. Ignacio Rubio Somoza

Thesis director

Dr. Charlotte Poschenrieder

Tutor

Luis Manuel Villar Martin

Author

ACKNOWLEDGMENTS

Finalizada esta etapa de casi 5 años en mi vida, me gustaría dedicar unas palabras a todas las personas que han formado parte de esta experiencia dedicando unas palabras a cada una de ellas.

En primer lugar, a Ignacio Rubio (Nacho), por haberme abierto las puertas de su laboratorio y dejarme crecer como científico. Ha habido momentos de todo tipo estos años, pero conseguimos llegar al final. Gracias.

También me gustaría agradecer a todas las personas que han pasado por el Molecular Reprogramming and Evolution (MoRE) laboratory del CRAG. Íñigo, Álvaro, Albert, Tamara, Carlos, Paulina, Katelyn, Pooya, Simone, Will y Eric, gracias por vuestra ayuda y por compartir tantos momentos juntos, me habéis hecho el camino hasta aquí mucho más fácil. Porque de los buenos y malos vividos, todos hemos sacado grandes lecciones y eso nos han unido durante vuestra estancia en el laboratorio. Gracias.

Agradecer al Ministerio de Ciencia e Innovación por haberme dado la oportunidad de poder trabajar en este proyecto en el CRAG. Gracias.

A todos los servicios del CRAG: administrativos, informáticos, técnicos, secuenciación, genómica, imágenes e invernaderos. Me gustaría hacer una mención especial en este apartado a Montse, por haber compartido conmigo tantas horas en el confocal. También a Johanna, Victor y Martí por su ayuda en la realización de esta tesis. Y finalmente a la gente de invernaderos, por su paciencia cuando no encontrábamos la solución a los problemas de mis plantas. Gracias a todos.

A todos los investigadores que han colaborado en el Desarrollo de mi trabajo aportando material: Miguel Ángel Moreno Risueño, Idan Efroni, Juan Antonio García, Fernando Ponz, Sheng-Yang He, Brian Kvitko y, sobre todo, a Sebastian Schornack, por dejarme pasar dos meses en su laboratorio en Cambridge, en los que aprendí mucho de ciencia y por hacerme la vuelta a España todo lo fácil que se pudo en esos primeros meses de COVID...Gracias a todos.

A mis amigas de la Universidad de Zaragoza, Ana, Ester A., Ester M., Inés, Marta y Vicky, algunas de ellas compartiendo conmigo experiencia de doctorado en

Barcelona. Gracias a todas por los consejos y por las charlas sobre nuestras cosas de científicos en proceso. Porque somos tan complejos como una Ameba. Gracias a todas.

Para finalizar, pero no por ello menos importante, gracias a mis padres Mathilde y Pedro por hacer todo el esfuerzo posible para que sea quien hoy soy, a mis hermanos Nathalie y Rafael, por las confianzas y por hacerme el tío más feliz del mundo durante estos años de doctorado. A mis amigos del pueblo que han hecho la estancia en Barcelona mucho más fácil si cabe. Y por último gracias a ti Xavi, por aguantarme todo y más estos años, otra etapa más que cerramos.

Gracias a todos.

INDEX OF CONTENTS

SUMMARY	13
RESUMEN	15
INTRODUCTION	23
1. PLANTS AND THEIR SURROUNDING ENVIRONMENT	24
2. THE PLANT-PATHOGEN ARMS RACE	25
3. RNA SILENCING MACHINERY AS AN ANTIVIRAL DEFENCE MECHANISM	29
3.1 HELPER COMPONENT PROTEINASE (HC-PRO): EFFECTOR AND VSR FROM <i>POTYVIRIDAE</i> FAMILY	33
4. RNA SILENCING MACHINERY AS A TARGET FOR BACTERIAL SILENCING SUPPRESSORS (BSRs)	35
5. RNA SILENCING MACHINERY AS A TARGET FOR OOMYCETE EFFECTORS	37
6. RNA SILENCING MACHINERY AS A GENE REGULATORY SYSTEM	39
6.1 siRNA.....	40
6.1.1 HETEROCHROMATIC siRNAs (hc-siRNA)	41
6.1.2 SECONDARY siRNAs: pha-siRNAs and ta-siRNAs.....	41
6.1.3 NAT-siRNA	42
6.2 miRNA.....	42
6.2.1 PLANT miRNAs AND DEVELOPMENT	43
6.2.2 PLANT miRNA AND THEIR ROLE IN DEFENCE RESPONSES	44
6.2.3 PLANT miRNA-TFs AND THEIR ROLE IN PLANT DEFENCE .	45
OBJECTIVES	47
MATERIALS AND METHODS	49
1. PLANT MATERIAL AND GROWTH CONDITIONS	50
1.1 PATHOGEN INFECTIONS	50
1.2 PLANT TRANSFORMATIONS	51
1.3 VALIDATION OF THE REPORTER SYSTEMS.....	51
1.4 GUS STAINING	52

1.5	VALIDATION OF THE GR-LhG4-pOp TWO-COMPONENT SYSTEM AND SSs EXPRESSION	52
1.6	VALIDATION AND SETTING THE CONDITIONS FOR SILENCING SUPPRESSION TRIGGERED BY THE CONDITIONALLY EXPRESSION OF SSs.....	52
1.7	PROTOPLASTING	53
2.	PATHOGEN INFECTIONS.....	53
2.1	VIRUS, BACTERIA AND OOMYCETE STRAINS AND GROWTH CONDITIONS.....	53
2.2	INFECTION PROCEDURES	54
2.2.1	VIRAL INFECTIONS	54
2.2.2	PSEUDOMONAS SYRINGAE INFECTIONS	54
2.2.3	OOMYCETE INFECTIONS	55
2.3	INFECTION ANALYSIS	55
2.3.1	LUMINESCENCE MEASUREMENT	55
2.3.2	IMAGING.....	55
2.3.3	VIRAL CONCENTRATION.....	56
2.3.4	BACTERIAL CFU (COLONY FORMING UNIT) CALCULATION... ..	57
3.	CONSTRUCTS FOR PLANT TRANSFORMATION	57
3.1	REPORTER SYSTEM BASED ON THE REGULATION OF A FLUORESCENT PROTEIN GENE	58
3.2	GUS REPORTER GENE UNDER THE CONTROL OF CELL-TYPE SPECIFIC PROMOTERS	59
3.3	CONSTRUCTS FOR THE CONDITIONAL EXPRESSION OF SSs OR mSCARLET-I FLUORESCENT PROTEIN IN SPECIFIC CELL-TYPES....	61
3.4	CONSTRUCTS FOR THE CONSTITUTIVE EXPRESSION OF GFP IN SPECIFIC CELL-TYPES	62
4.	VALIDATIONS AND SETTING THE CONDITIONS FOR PROTOPLASTING AND CELL-SORTING.....	63
4.1	VALIDATION OF amiR REPORTER SYSTEMS	63
4.2	GENE EXPRESSION BY GUS STAINING	63

4.3	VALIDATION OF THE GR-LhG4-pOp TWO-COMPONENT SYSTEM AND SETTING THE CONDITIONS FOR DEXAMETHASONE TREATMENT	64
4.3.1	VALIDATION AND SETTING THE CONDITIONS FOR DEXAMETHASONE TREATMENT USING FLUORESCENCE.....	64
4.3.2	VALIDATION BY qPCR.....	64
4.4	VALIDATION AND SETTING THE CONDITIONS FOR SILENCING SUPPRESSION TRIGGERED BY THE CONDITIONALLY EXPRESSION OF SSs.....	65
5.	PROTOPLASTING AND CELL SORTING	65
5.1	PROTOPLASTS ISOLATION	65
5.2	CELL SORTING.....	66
6.	PROTOPLASTS RNA ISOLATION	66
7.	RNA SEQUENCING	67
7.1	PREPARATION OF cDNA LIBRARIES	67
7.2	RNA-seq DATA ANALYSIS	68
7.2.1	ILUMINA READS PREPROCESSING	68
7.2.2	TRANSCRIPT EXPRESSION QUANTIFICATION	68
7.2.3	GENE EXPRESSION QUANTIFICATION.....	69
7.2.4	SELECTION OF SAMPLES FOR DIFFERENTIAL EXPRESSION ANALYSIS.....	69
7.2.5	PCA PLOT OF SELECTED SAMPLES.....	69
7.2.6	DIFFERENTIAL EXPRESSION ANALYSIS (PAIRWISE COMPARISONS)	70
7.2.7	GO ANALYSIS	70
RESULTS		71
1.	THE RNA SILENCING MACHINERY IS DISMANTLED IN SPECIFIC CELL-TYPES UPON PATHOGEN INFECTION	72
1.1	OPTIMIZATION OF INFECTION CONDITIONS.....	72
1.1.1	PPV VIRAL INFECTION.....	73
1.1.2	P. SYRINGAE INFECTION	74
1.2	VALIDATION OF amiR REPORTER SYSTEMS	77

1.3	RNA SILENCING MACHINERY IS DISMANTLED IN MESOPHYLL AND VASCULAR BUNDLES UPON VIRUS INFECTION.....	81
1.4	RNA SILENCING MACHINERY IS DISMANTLED IN MESOPHYLL UPON BACTERIAL INFECTION	84
1.5	ASSAYING CELL-TYPE SPECIFICITY OF OOMYCETE-TRIGGERED SILENCING SUPPRESSION	88
2.	HOST CELL TYPE-SPECIFIC REPROGRAMMING IS TRIGGERED BY EFFECTORS WORKING AS SSs AGAINST THE RNA SILENCING MACHINERY.....	92
2.1	GENERATION OF PLANTS CONDITIONALLY EXPRESSING PATHOGEN SSs.....	92
2.2	KINETICS AND EFFICIENCY OF HOST SILENCING SUPPRESSION ARE SS-AND CELL-TYPE DEPENDENT	99
2.3	SILENCING SUPPRESSION LEADS TO SPECIFIC CELL-TYPE AND SS-DEPENDENT REPROGRAMMING.....	105
2.3.1	ISOLATION OF CELLS SHOWING sRNA MACHINERY DYSFUNCTIONS.....	105
2.3.2	HOPT1-1 INDUCTION HAS A LARGER IMPACT THAN HC-PRO IN TRANSCRIPTOME REPROGRAMMING IN MESOPHYLL CELLS 109	
2.3.3	HC-PRO TRIGGERS CELL-TYPE SPECIFIC REPROGRAMMING.....	114
3.	CONSEQUENCES OF SSs-TRIGGERED HOST REPROGRAMMING FOR PATHOGEN INFECTION.....	116
	DISCUSSION.....	121
	CONCLUSIONS.....	126
	BIBLIOGRAPHY.....	128
	ANNEX.....	150

INDEX OF FIGURES

Figure 1. Disease triangle.....	25
Figure 2. Plant immunity and the “arms-race”.....	29
Figure 3. VSRs and RNA silencing steps.....	34
Figure 4. Gene map of mScarlet-I reporter system.....	59
Figure 5. Gene map of GUS reporter gene under cell-type specific promoters.....	61
Figure 6. Gene map of the constructs for the conditionally expression of pathogen SSs or mScarlet-I in specific cell types.....	62
Figure 7. Gene map of the constructs for the constitutive expression of GFP in specific cell-types.....	62
Figure 8. MOCK treated and PPV-infected Arabidopsis plants.....	74
Figure 9. <i>Pseudomonas syringae</i> infection in Arabidopsis plants.....	76
Figure 10. Validation of the reporter systems by agroinfiltration in <i>N. benthamiana</i> leaves.....	78
Figure 11. Validation of the reporter systems in <i>A. thaliana</i> plants.....	80
Figure 12. PPV-infected Arabidopsis plants carrying the amiR-LUC reporter system 14 DAI.....	82
Figure 13. PPV-infected Arabidopsis plants carrying amiR-mScarlet-I reporter system 14 DAI.....	83
Figure 14. <i>Pseudomonas syringae</i> infection of Arabidopsis plants carrying the reporter systems 3DAI.....	86
Figure 15. <i>Phytophthora palmivora</i> infection of amiR-mScarlet-I reporter plant roots 24 hours after infection	89
Figure 16. <i>Phytophthora palmivora</i> infection of leaves from amiR-mScarlet-I reporter plants and plants constitutively expressing mScarlet-I in cell nuclei but lacking the amiR 24 hours after infection.....	90

Figure 17. Expression of GUS reporter gene under the control of the selected promoters in transgenic Arabidopsis plants.....	94
Figure 18. Plants conditionally expressing the mScarlet-I fluorescent protein in specific cell-types upon DEX treatment.....	97
Figure 19. Relative expression levels of the SSs Hc-Pro and HopT1-1 in two homozygous T2 plant lines conditionally expressing the SSs in the specific cell-types.....	98
Figure 20. Time course of miRNA dysfunction in mesophyll cells conditionally expressing SSs.....	100
Figure 21. Time course of miRNA dysfunction in different vascular cell-types conditionally expressing the VSR Hc-Pro.....	102
Figure 22. Plants conditionally expressing the mScarlet-I or SSs genes and constitutively expressing GFP gene in the specific cell-types not treated with DEX.....	107
Figure 23. Relative expression levels of the SSs Hc-Pro and HopT1-1 in heterozygous F1 lines of plants conditionally expressing the SSs in the specific cell types and constitutively expressing GFP in such cells.....	109
Figure 24. Hc-Pro showed higher expression levels after 24 HAI in mesophyll cells.	111
Figure 25. Transcriptome reprogramming resulting from HopT1-1 induction largely recapitulated changes observed upon Hc-Pro induction.....	112
Figure 26. GO classification of Biological Functions to which DEG found as consequence of HopT1-1 induction in mesophyll cells belong.....	113
Figure 27. Hc-Pro expression in mesophyll and vascular cells.....	114
Figure 28. Hc-Pro-triggered reprogramming is cell-type specific.....	115
Figure 29. Hopt1-1 induction in mesophyll cells leads to enhance resistance against TuMV.....	117

Figure 30. Hc-Pro induction in phloem companion cells had no effects in plant resistance against TuMV.118

Figure 31. Hc-Pro induction in bundle sheath cells had no effects in plant resistance against TuMV..... 119

Figure 32. Hopt1-1 induction in mesophyll cells leads to enhance resistance against *Pto* DC 3000..... 120

INDEX OF TABLES

Table 1. Diversity of sRNA, size, origin and mode of action.....	40
Table 2. Fluorescence protein mScarlet-I template, primers used for its amplification and GG destination vector.....	59
Table 3. Primers for amiR-mScarlet-I engineering by PCR reactions and template for PCRs.....	59
Table 4. Primers for promoter amplifications and cell domain expression.....	60
Table 5. Infection efficiencies achieved in <i>A. thaliana</i> plants grown on soil and <i>in vitro</i> using PPV-containing agrobacterium concentrations.....	73
Table 6. Infection efficiency in <i>A. thaliana</i> using different concentrations of <i>P. syringae</i>	75

SUMMARY

Plants have developed molecular mechanisms to defend themselves from pathogens. On the other hand, pathogens have evolved counter-measures (i.e. effector proteins) to elude plant defence programs, and thus ensues an ongoing “arms race” between plant and pathogen that contributes to their evolution. That tug of war depends on a delicate and highly dynamic balance between plants and pathogens. Plants must tightly regulate the timing and intensity of their immune responses to avoid undesired effects from defence-development trade-off. On the other hand, pathogens have to modulate host cell pathways by precisely controlling the production of different effectors for fully exploiting their host on their own benefit.

RNA-mediated gene silencing is an antiviral defence system and as such is the subject of an “arms race” between plants and pathogens. Pathogens such as viruses, bacteria and oomycetes, produce effectors working as silencing suppressors (SSs). Pathogen-produced SSs disrupt not only the plant defence system, but they also perturb other endogenous processes by releasing host transcripts from small RNA (sRNA) regulation. In the absence of functional sRNAs, the concomitant release of their target transcripts may facilitate the reprogramming of host defence and development.

This thesis comprises the study of the cell-type specific responses to pathogen-derived SSs and their role in the “arms race” between host and pathogens around RNA silencing. The work was performed in *Arabidopsis thaliana*. First, I established the cell-types targeted by pathogens for RNA silencing suppression in the course of infections. Unrelated pathogens, such as *Plum Pox Virus* (PPV) and *Pseudomonas syringae* pv. tomato DC3000 (*Pto* DC3000) bacteria, targeted leaf mesophyll cells for plant RNA silencing suppression. In addition, it was found that PPV colonized and impaired silencing suppression in vascular cell types.

On the other hand, cell-type specific transcriptional reprogramming as result of pathogen-triggered silencing suppression was studied. For that aim, the transcriptome changes from plants conditionally expressing the SS Hc-Pro from

Turnip Mosaic Virus (TuMV) in mesophyll and vascular cells and from plants conditionally expressing the SS HopT1-1 from *Pto* DC3000 in mesophyll cells were analysed. Transcriptome changes found in Hc-Pro expressing mesophyll cells were fewer than those found when HopT1-1 was induced. Furthermore, the latter cover most of the transcriptome changes found when Hc-Pro was induced.

That result suggested that HopT1-1 impact on host silencing was larger than that of Hc-Pro. Immunity, Proteasome activity and Endoplasmic Reticulum (ER) stress were found as the processes that were up-regulated, while photosynthesis, chloroplast and plastid organization and protein translation related processes were the most representative down-regulated processes. Among the up-regulated immunity related genes, there were elements involved both in pathogen triggered immunity (PTI) and effector triggered immunity (ETI). These results indicate that the presence of SSs in plant mesophyll cells triggers host defence counter-counter measures.

In vascular cells, Hc-Pro induction resulted in minor transcriptional changes in both cell types. These results indicate that Hc-pro induction led to cell-type specific reprogramming and that vascular cell types were more refractory to the presence of that SS than mesophyll cells.

Finally, the contribution to plant defence from the different events triggered by SS-mediated reprogramming was assayed by infecting plants conditionally expressing the different SSs with TuMV and *Pto* DC3000. Our results indicate that HopT1-1 induction in mesophyll cells results in counter-counter defence mechanisms that override both viral and bacterial infections.

Thus, pathogen-triggered host RNA silencing suppression enables a new layer of plant defence, in which host sRNA targets may play an important role, comprising counter-counter defence mechanisms and thus, ensues an “arms race” between host and pathogen around RNA silencing.

RESUMEN

Las plantas poseen mecanismos moleculares para defenderse de patógenos. Por otra parte, los patógenos han desarrollado contramedidas (por ejemplo, proteínas efectoras) para eludir dichos mecanismos de defensa. El resultado de dicha “carrera armamentística” condiciona de manera fundamental la co-evolución de ambas entidades biológicas, planta y patógeno. Dicha interrelación depende de un delicado, y altamente dinámico, balance entre planta y patógeno. Las plantas deben modular estrictamente la magnitud de su respuesta inmune para evitar efectos no deseados del “trade-off” defensa-desarrollo. Por otra parte, los patógenos tienen que regular la producción de distintos efectores para explotar completamente al huésped en su propio beneficio.

El silenciamiento génico mediado por ARN es un mecanismo de defensa antiviral y, como tal, está sometido a una carrera armamentística entre plantas y patógenos. Patógenos como virus, bacterias y oomicetos, producen efectores que actúan como supresores de silenciamiento (SSs). Los SSs no solo afectan al sistema de defensa de la planta, también afectan otros procesos endógenos liberando transcritos de la regulación por ARNs de pequeño tamaño (sRNA). En ausencia de sRNAs funcionales, la liberación de sus transcritos diana podría facilitar la reprogramación de la defensa y desarrollo del huésped.

Esta tesis abarca el estudio de respuestas específicas de tipo celular en *Arabidopsis thaliana* desencadenadas por SSs, y el papel de estas respuestas en la “carrera armamentística” entre planta y patógeno. En primer lugar, se establecieron los tipos celulares en los que se detectó una supresión del silenciamiento tras la infección con patógenos. En infecciones con patógenos no relacionados, como *Plum Pox Virus* (PPV) y *Pseudomonas syringae* pv. Tomato DC3000 (*Pto* DC3000), la supresión del silenciamiento se vio afectada en células de mesófilo. Además, se vio que PPV coloniza y afecta la supresión del silenciamiento en vasculatura.

Por otra parte, se estudió la reprogramación transcripcional específica de tipo celular como resultado de la supresión de silenciamiento desencadenada por patógenos. Para ello, se analizaron los cambios en el transcriptoma de

plantas que expresan de manera inducible el SS Hc-Pro de *Turnip Mosaic Virus* (TuMV) en mesófilo y vasculatura y de plantas que expresan de manera inducible el SS HopT1-1 de *Pto* DC3000 en mesófilo. Los cambios en el transcriptoma encontrados en células de mesófilo que expresan Hc-Pro fueron menores que los cambios observados cuando se expresa HopT1-1, que además estaban incluidos en estos últimos.

Este resultado sugiere que el impacto en el silenciamiento del huésped de HopT1-1 es mayor que el de Hc-Pro. Entre los procesos activados se encontraron: inmunidad, actividad del proteosoma y estrés del retículo endoplasmático. Entre los procesos inhibidos, se encontraron: fotosíntesis, organización de cloroplastos y plastidios y traducción proteica. Entre los genes de inmunidad cuyos niveles se vieron aumentados, hay varios involucrados en inmunidad activada por constituyentes de patógenos (PTI) e inmunidad activada por efectores (ETI). Estos resultados indican que la presencia de SSs en células de mesófilo desencadena contra-contra-medidas en la planta.

En células de vasculatura, la inducción de Hc-Pro resultó en menor cambio transcripcional. Estos resultados indican que la inducción de Hc-Pro lleva a una reprogramación específica de tipo celular y que las células de vasculatura apenas responden a la presencia de SSs.

Finalmente, se estudió la contribución a la defensa de la planta de los diferentes eventos desencadenados por la reprogramación mediada por SSs. Nuestros resultados indican que la inducción de HopT1-1 en células de mesófilo desencadena mecanismos de contra-contra-defensa, combatiendo las infecciones por virus y bacterias.

Por tanto, la supresión de silenciamiento de ARN desencadenada por patógenos activa en la planta un nuevo nivel de defensa, en la que las dianas de sRNA de la planta podrían desempeñar un papel importante.

ABREVIATIONS

ADK Adenosine kinase

AGO ARGONAUTE

amiR Artificial miRNA

ARR Age-Related Resistance

Avr Avirulence

AvrPto Avirulence Pto

AvrPtoB Avirulence Pto B

BAK1 BRI1-ASSOCIATED RECEPTOR KINASE 1

BCTV *Beet curly top virus*

BIK 1 BOTRITIS INDUCED KINASE 1

BPH Brown Plant Hopper

BSRs Bacterial Suppressors of RNA Silencing

CAB3 Chlorophyll A/B Binding Protein

CaMV *Cauliflower Mosaic Virus*

CDC2A CELL DIVISION CONTROL 2A

CER6 3-Ketoacyl-Coa Synthase 6

CERK1 CHITIN ELICITOR RECEPTOR KINASE 1

CFU Colony forming unit

CMV *Cucumber mosaic virus*

CNLs Coiled-coil (CC) type NLRs

CP Coat protein

DAI Days after infection

DAMPs Damage-associated molecular patterns

DCL Dicer-like

DDL RNA-binding protein DAWDLE

DEG Differentially Expressed Genes

DEX Dexamethasone

DRBs dsRNA-binding proteins

dsDNA Double stranded DNA

dsRBD dsRNA binding domain

dsRNA double stranded RNA

EFR BACTERIAL ELONGATION FACTOR Tu RECEPTOR

EF-Tu BACTERIAL ELONGATION FACTOR Tu

ER Endoplasmic reticulum

ETI Effector-triggered immunity

FCW Fungal Cell Wall

Fig Figure

Flg22 22-aminoacid peptide from bacterial flagellin

FLS2 FLAGELLIN SENSING 2

FTIP FT-interacting protein 1

GFP Green Fluorescent Protein

GG GreenGate

GO Gene ontology

GRF GROWTH-REGULATING FACTOR

GW glycine/tryptophan

HAI Hours After Induction

Hc-Pro Helper Component Proteinase

Hc-siRNA Heterochromatic siRNA

HEN1 S-adenosylmethionine-dependent methyltransferase Hua Enhancer 1

HopN1 Hrp outer protein N1

HopT1-1 Hrp outer protein T1-1

Hpa *Hyalosporonospora arabidopsidis*

HR Hypersensitive Response

HST HASTY

HTR5 HISTONE THREE RELATED 5

HYL1 HYPONASTIC LEAVES 1

JA Jasmonate

LD Long Day

LRR Leucine-rich repeat

LUC Firefly Luciferase gene

LYK5 LYSIN MOTIF RECEPTOR KINASE 5

MAPK Mitogen-Activated Protein Kinase

MET2 METHYLTRANSFERASE 2

miRNA micro RNA

MIRs miRNA genes

MS Murashige-Skoog

NAT-siRNA Natural antisense transcript-derived siRNA

NB Nucleotide binding

NIA Nuclear Inclusion A

NLRs Nucleotide-binding domain leucine-rich repeat containing receptors

NLS Nuclear Localization Signal

PAMPs Pathogen-associated molecular patterns

PAZ Piwi/Argonaute/Zwille

PBL1 PBS-LIKE 1

Pha-siRNA Phased siRNA

PINP1 PSR1-Interacting protein 1

PoLV Photos Latent Virus

PPR Pentatricopeptide Repeat

PPV *Plump Pox Virus*

PR1 PATHOGENESIS-RELATED 1

pre-miRNA Precursor-miRNA

pri-miRNA Primary miRNA transcripts

PRR Pattern Recognition Receptor

PRSV *Papaya ringspot virus*

PSR1 Phytophthora Suppressor of RNA silencing 1

PSR2 Phytophthora Suppressor of RNA silencing 2

PTI Pattern-triggered immunity

Pto DC3000 *Pseudomonas syringae* pv. tomato DC3000

PVA *Potato Virus A*

RBCS Ribulose Bisphosphate Carboxylase Small Subunit

RBCS1A Ribulose Bisphosphate Carboxylase Small Chain 1A

RDR RNA-dependent RNA polymerase

RIN RNA integrity number

RISC RNA-induced silencing complex

RLCK Receptor-like cytoplasmic kinase

RLKs Receptor-like kinases

RLPs Receptor-like proteins

RNA Pol II RNA Polymerase II

RNLs Resistance to powdery mildew 8-like domain (RPW8)-type NLR

ROS Reactive Oxygen Species

Ros1 *Anthirrium majus* MYB-related Rosea 1

RSA Rye sucrose agar

SA Salicylic acid

SCMV *Sugarcane mosaic virus*

SCR Scarecrow

SD Short Day

SDNs SMALL RNA DEGRADING NUCLEASEs

SE SERRATE

SERK3 SOMATIC EMBRYOGENESIS RECEPTOR KINASE 3

SGS3 Suppressor of Gene Silencing-3

siRNA Small Interfering RNA

SNARE Soluble NSF Attachment Protein

SOD Superoxide Dismutase

SPCSV *Potato Chlorotic Stunt Crinivirus*

SPL6 Squamosa promoter-binding-like protein 6

SPMMV *Sweet Potato Mild Mottle Virus*

sRNA Small RNA

SS Silencing Suppressor

ssRNA Single stranded RNA

SUC2 Sucrose-Proton Symporter 2

Sultr2;2 Sulphate Transporter 2;2

SVP SHORT VEGETATIVE PHASE

T2SS Type II Secretion System

T3SS Type III Secretion System

Ta-siRNA Trans-acting siRNA

TCV *Turnip Crinkle Virus*

TEV *Tobacco etch virus*

TF Transcription Factor

TGMV *Tomato Golden Mosaic Virus*

TNLs Toll/interleukin-1 receptor/Resistance protein (TIR)-type NLR

TOE1 TARGET OF EAT1

TOE2 TARGET OF EAT2

TPM Transcripts per million

TuMV *Turnip Mosaic Virus*

TYLCV *Tomato Yellow Leaf Curl Virus*

vsRNA Virus-derived small interfering RNAs

VSR Viral Suppressors of RNA Silencing

X-Gluc 5-bromo-4-chloro-3-indolyl glucuronide

ZYMV *Zucchini yellow mosaic virus*

INTRODUCTION

1. PLANTS AND THEIR SURROUNDING ENVIRONMENT

Plants live in complex and highly dynamic ecosystems where they interact with a myriad of other organisms dealing simultaneously with the presence of different sources of abiotic stresses. Those interactions have different natures: beneficial (competition, mutualism, commensalism) or detrimental (parasitism) for maintaining plant homeostasis.

Interactions with pathogens constitute a major threat for plant survival and reproduction. Pathogenic relationships lead to plant disease when a susceptible host interrelates with a pathogen under favourable environmental conditions, as defined by the 'Disease Triangle' (Waqar, 2018) (Fig.1). Accordingly, three factors placed at the corners of a triangle must meet to cause plant disease: a susceptible host, a pathogen and a favourable environment. Without the right host in a favourable environment, pathogens cannot cause any harm.

In order to survive, plants need to differentiate between foes and folks. Accordingly, plants have developed sophisticated molecular mechanisms to perceive and defend themselves from pathogen invaders. In response, pathogens have evolved counter-measures to elude host defence programs, and thus ensues an ongoing arms race between host and pathogen that largely determines their evolution. Such tug-of-war depends on a delicate and highly dynamic balance between pathogen and host. While pathogens have to precisely modulate host cell pathways to fully exploit their host in their own benefit avoiding host defences, hosts must finely control the timing and intensity of their defence responses to limit undesired self-inflicted damage as result of the defence-growth trade off.

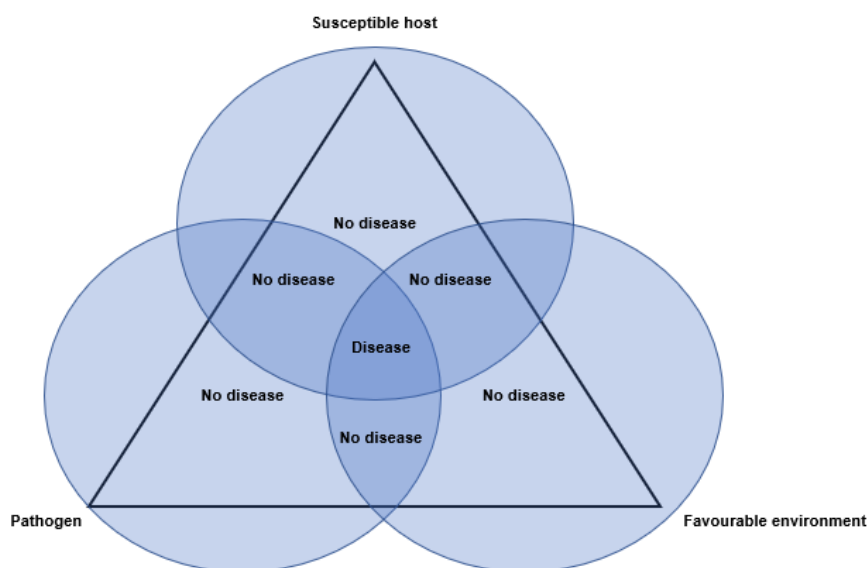


Figure 1. Disease triangle. Plant disease illustrated as the interior of a triangle with three essential factors (susceptible host, favourable environment and pathogen) at the vertices. These factors must interact to cause disease.

2. THE PLANT-PATHOGEN ARMS RACE

In order to survive and reproduce, plants need to perceive the presence of potential pathogens and protect themselves against them. Plants lack specialized mobile immune cells and an adaptive immune system like other organisms. Nonetheless, plants have developed innate immune responses to ward off damage by pathogens. Immune responses rely on extracellular and intracellular monitoring mechanisms, which are highly specialized on detecting pathogen-derived molecules and/or their impact on cellular processes and constituents. Thus, immune responses against pathogens initiate upon sensing at the cellular level via surface-localized pattern recognition receptors (PRRs) and intracellular nucleotide-binding domain leucine-rich repeat containing receptors (NLRs) (J. M. Zhou et al., 2020), leading to pattern-triggered immunity (PTI) and effector-triggered immunity (ETI), respectively (Fig. 2).

PTI plays an important role in preventing pathogen invasion and maintaining the homeostasis required for commensal microbiota, which is essential for plant growth and health (Chen et al., 2020). PTI is triggered upon PRRs perception of the so-called elicitors, which are molecules that have the

ability of eliciting PTI responses. These molecules are divided into pathogen-associated molecular patterns (PAMPs) and host molecules released by pathogen damage, named as damage-associated molecular patterns (DAMPs). PAMPs and DAMPs are broadly conserved molecules that include proteins, carbohydrates, lipids and small molecules, such as ATP (Bartels et al., 2015). PRRs are classified into two types, receptor-like kinases (RLKs) and receptor-like proteins (RLPs) (Boutrot et al., 2017). RLKs contain an ectodomain for ligand binding, a transmembrane domain and a cytoplasmic kinase domain. RLPs have similar domains but a short cytoplasmic tail instead of a kinase domain (Boutrot et al., 2017). Ectodomains depend on the class of ligand they bind to, and are divided into leucine-rich repeat (LRR) domains for protein ligands, LysM domains for glycans, lectin domains for carbohydrates and epidermal growth factor-like repeat domains for oligogalacturonides released from plant cell walls upon fungal infection (Saijo et al., 2018). Upon binding to their specific ligands, RLKs and RLP receptors recruit co-receptors to form a complex, which leads to the phosphorylation of cytoplasmic kinases that activate a variety of substrate proteins. Activation of receptor and co-receptor pairs triggers diverse physiological outputs, including Reactive Oxygen Species (ROS) production, stomatal closure, Ca^{2+} influx, production of defence hormones and the phosphorylation of Mitogen-Activated Protein Kinase (MAPK). Examples in *Arabidopsis thaliana* are the BRI1-ASSOCIATED RECEPTOR KINASE 1/SOMATIC EMBRYOGENESIS RECEPTOR KINASE 3 (BAK1/SERK3) and its homolog BAK1-LIKE1 (BKK1/SERK4) that function as co-receptors for LRR-RLK-type PRRs like FLAGELLIN SENSING 2 (FLS2) that recognizes a conserved 22-aminoacid peptide (flg22) from bacterial flagellin (Chinchilla et al., 2007) and the BACTERIAL ELONGATION FACTOR Tu (EF-Tu) RECEPTOR (EFR), that recognizes a 18-aminoacid peptide (elf18) of EF-Tu (Roux et al., 2011). The receptor-like cytoplasmic kinase (RLCK) BOTRITIS INDUCED KINASE 1 (BIK 1) and its close homolog PBS-LIKE 1 (PBL1), constitutively associate with FLS2/EFR and BAK1. Upon flg22 recognition, BIK1 is rapidly phosphorylated by BAK1 and released from the receptor complex, which leads to the activation of ROS production and MAPK phosphorylation (Roux et al., 2011). MAPK activation results in callose deposition, stomatal closure, production of hormones and the activation of transcription factors (TFs), all of them hallmarks

of PTI (W. Lin et al., 2014). Another example of RLK that recruits a co-receptor forming phosphorylation complexes is the LYSIN MOTIF RECEPTOR KINASE 5 (LYK5). Fungal cells are encased within a complex matrix of interconnected polysaccharides and proteins, which constitutes the fungal cell wall (FCW). The inner part of the FCW is a chitin–glucan-rich interconnected matrix. Upon fungal chitin perception, LYK5 associates with LysM-RLK CHITIN ELICITOR RECEPTOR KINASE 1 (CERK1), inducing the phosphorylation of the CERK1 kinase domain (Cao et al., 2014). CERK1 is essential for the recognition of fungal chitin and bacterial peptidoglycans. Following ligand binding, RLCK PBL27 is phosphorylated by LYK5-CERK1 and connects chitin perception to MAPK activation (Yamada et al., 2016). The expression of PRRs have been shown to be cell-type and developmental-stage specific (F. Zhou et al., 2020). FLS2 expression is confined to specific cell-types both in above and below ground tissues and it is responsive to hormones, damage and biotic stress (Emonet et al., 2021). FLS2 is highly expressed in cells and tissues vulnerable to bacteria attack, such as stomata, hydathodes and lateral roots (Beck et al., 2014). On the other hand, different bacterial isolates can evade recognition accumulating mutations in their flg22 epitopes (Parys et al., 2021).

The intracellular immune survey system relies on NLR receptors to recognize pathogen effectors, or their action, leading to ETI. Effectors are essential virulence proteins secreted by pathogens as a counter-measure strategy to avoid immune responses like PTI. Once inside of host cells, effectors manipulate physiological processes or signalling pathways for pathogen benefit (Deslandes et al., 2012). ETI responses are qualitatively similar to PTI, but differs in their magnitude and kinetics and are often associate with localized cell death named as hypersensitive response (HR) (Jones et al., 2006). Plant NLRs can detect effectors directly or indirectly by monitoring the homeostasis or modification of host proteins that are fundamental in cellular processes and that are targeted by effectors. Most of NLRs consist on a variable N-terminal domain, a central nucleotide binding (NB) domain and a carboxyl-terminal LRR domain (Monteiro et al., 2018). Based on the composition of their N-terminal domain, NLRs can be classified into three types: coiled-coil (CC) type NLRs (CNLs), Toll/interleukin-1 receptor/Resistance protein (TIR)-type NLR (TNLs) and the

Resistance to powdery mildew 8-like domain (RPW8)-type NLR (RNLs) (Monteiro et al., 2018). During effector recognition, NLRs function as 'sensors' or 'helpers' (Jubic et al., 2019). Recent advances in NLR biology have vastly advance our knowledge about NLR evolution, interaction in supramolecular protein complexes and mode of action.

Some pathogens are able to defeat ETI by losing their recognizable effectors, gaining new effectors or changing their subcellular location (Asai et al., 2018). On the other hand, plants have evolved to recognize new effectors, re-establishing ETI. This co-evolution between plants and their pathogens, which also includes PTI defeat and activation of ETI, was early explained by the classical two branches of the plant immune system called Zig-Zag model proposed by Dangl and Jones (Jones et al., 2006). The Zig-Zag model is based on the distinction of PTI and ETI and has been widely accepted, as it explains the plant immune system capturing the co-evolutionary dynamics of the 'arms race' between host and pathogen. However, increasing evidence suggests that PTI and ETI share signalling components and are interrelated. As said before, multiple down-stream responses can be activated during PTI and more strongly during ETI, including influx of Ca^{2+} , ROS burst, activation of MAPK, defence gene induction and biosynthesis of defence phytohormones (such as Jasmonate (JA) and Salicylic acid (SA)). That suggests that both immune responses are functionally linked. As an example, PTI coreceptors BAK1 and BIK1 in Arabidopsis are required for ETI mediated by TNLs RPP2 and RPP4 against *Hyalosporonospora arabidopsidis* (*Hpa*) (Roux et al., 2011). Consistently, ETI resistance against *Pseudomonas syringae* pv tomato (*Pto*) DC 3000 that deploy avirulence (Avr) effectors is compromised in different PRR or coreceptor mutants (Yuan et al., 2021). Additionally, activation of PRR signalling by PAMP can promote the expression of effectors recognized by NLRs in an HR-mediated manner (Yuan et al., 2021). In addition to HR, other ETI responses like ROS burst and activation of MAPK cascade are also modulated by PRR signalling supporting the idea that PTI co-regulates multiple ETI responses in a NLR type-specific manner [20, 21].

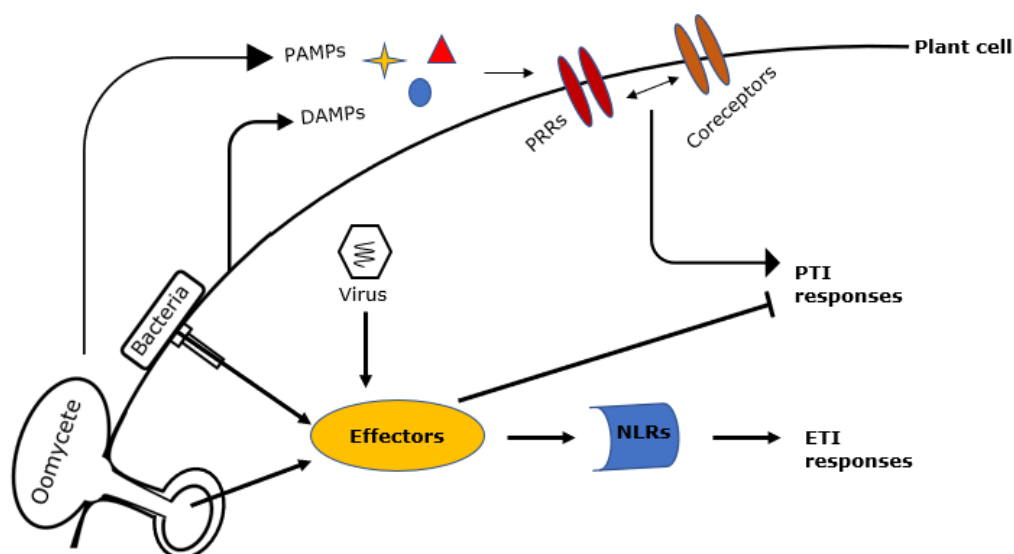


Figure 2. Plant immunity and the “arms race”. PAMPs recognized by PRRs elicit PTI responses. Pathogens deliver effector proteins into the host cell that suppress PTI. These effectors are recognized by NLRs, which induce ETI.

3. RNA SILENCING MACHINERY AS AN ANTIVIRAL DEFENCE MECHANISM

Besides a universal regulatory mechanism in eukaryotes, RNA-mediated gene silencing is also an antiviral defence mechanism in plants and invertebrates, being currently accepted that is also active in vertebrates including humans (Ding et al., 2007; Yang Li et al., 2016). Viruses cause almost half of the reported emerging infectious diseases in plants (Aranda et al., 2017), resulting on a severe impact on agriculture. Viruses are intracellular pathogens which genome is packed into virions. Viral genomes are formed by single stranded (ss) or double stranded (ds) RNA or DNA. ssRNA viruses can be further divided into positive-sense (+) and negative-sense (-). All the diverse type of viruses (ssRNA, dsRNA or DNA) produce highly stable double-stranded RNA intermediates during their life cycle. Those dsRNA structures are recognized and processed by host Dicer-like (DCL) and accessory proteins (i.e. Double Strand RNA Binding proteins, also known as DRBs). DCL enzymes have different domains: dsRNA binding, RNA helicase, RNase III and a small RNA (sRNA) binding PAZ (Piwi/Argonaute/Zwille).

dsRNA cleavage generates sRNAs called Virus-derived small interfering RNAs (vsiRNA). vsiRNAs are further stabilized and loaded into the RNA-induced silencing complex (RISC), in which members of the ARGONAUTE (AGO) gene family are the central components. AGO proteins contain a PAZ domain and a PIWI endonucleolytic domain to cleave target RNAs (Ding et al., 2007). sRNA loaded RISC complexes find the source of viral dsRNA through sequence homology abrogating infection, mainly through target RNA degradation (RNA viruses) and by epigenetic modifications in the genome of DNA viruses. This antiviral defence system is also subjected to an 'arms race' between host and pathogens. Viral genomes encode effectors that manipulate physiological processes or signalling pathways to evade host defence responses. Among them, Silencing Suppressors (SSs), called viral suppressors of RNA silencing (VSRs) in viruses, interfere with multiple steps of host's RNA silencing pathway, such as dsRNA recognition and dicing, RISC assembly, RNA targeting and amplification of antiviral silencing (Fig.3) (Burguán et al., 2011). Besides, VSRs can also interfere with epigenetic modifications.

Viruses need to tightly control their silencing suppression ability to avoid host counter-counter defence (Pruss et al., 2004).

a. dsRNA recognition and dicing

VSRs can interfere with the processing of dsRNA templates into vsiRNAs. It has been shown that two viral proteins, P14 from *Photos Latent Virus* (PoLV) and P38, the capsid from *Turnip Crinkle Virus* (TCV), prevent vsiRNA biogenesis targeting that step at the silencing process (Méraï et al., 2005; T et al., 2017). On the other hand, VSRs could affect ds-sRNA processing by the interaction with components of sRNA-processing complex. *Rice stripe virus* suppressor NS3 interacts with OsDRB1, a component of the micro RNA (miRNA)-processing complex (L. Zheng et al., 2017). *Cauliflower Mosaic Virus* (CaMV) can also interfere with vsiRNA processing by the interaction of P6 VSR with dsRNA-binding protein 4 (DRB4), required for vsiRNA processing (Haas et al., 2015).

b. RISC assembly

VSRs are able to impede RISC assembly by the interaction with essential known components of the complex as sRNAs or AGO proteins in different ways.

Otherwise, other undiscovered components of the RISC complex may be targets of viral suppressors, leading to a wide variety of suppression strategies.

Small Interfering RNA (siRNA) sequestration is the most common strategy in a large number of viral genera, preventing the correct RISC complex assembly and action. One of the most characterized VSR is the *Tombusvirus* P19 protein, which preferentially binds to siRNA duplexes with a high affinity depending on size, preventing the loading of siRNAs into AGO1 (Kontra et al., 2016).

A different strategy is used by *Potato Chlorotic Stunt Crinivirus* (SPCSV). This virus encodes a RNAase III endonuclease (CSR3) that cleaves 21-24 nt vsiRNA into 14 nt products preventing the antiviral response (Linping Wang et al., 2021). CSR3 is the target of antiviral drugs that prevent Sweet potato virus disease (Linping Wang et al., 2021).

VSRs could also interact with different components of the RISC complex. The 2b protein from *Cucumber mosaic virus* (CMV), binds to dsRNAs of various sizes through its nucleolar localization signal encoded within the 61–amino acid N-terminal double-stranded RNA (dsRNA) binding domain (dsRBD) (Duan et al., 2012) but also interacts with the PAZ and PIWI domains of AGO1 and AGO4, blocking AGO/RISC slicer activity (Duan et al., 2012).

VSRs could bind to AGO through the glycine/tryptophan (GW/WG) motif required for the interaction with AGO in RISC complexes. As an example, *Sweet Potato Mild Mottle Virus* (SPMMV) VSR P1 targets AGO1 through three WG/GW motifs (Giner et al., 2010). On the other hand, P38, in addition to RNA binding, contains two GW repeats that allows the interaction with AGO1 (Azevedo et al., 2010). Another coat protein encoded by *Pelargonium line pattern virus*, P37, has a conserved GW motif, which permits interaction with AGO1 (Pérez-Cañamás et al., 2015).

AGO1 homeostasis in plants depends on miRNA 168 (miR168)-guided AGO1 mRNA cleavage and translational inhibition (Várallyay et al., 2017). miR168 accumulation is triggered by VSRs in early-infections and this activity is associated with the control of the endogenous AGO1 protein level (Várallyay et al., 2013). These has been shown in infections with different virus genera

indicating that miR168 control of AGO1 is an important invasion strategy in several plant-virus interactions (Várallyay et al., 2013).

c. RNA targeting and amplification of antiviral silencing

VSRs could affect host plant defence downstream to RISC formation. As an example, P1 besides of inhibiting de novo-formed RISCs, could interfere with sRNA-loaded RISC (Giner et al., 2010).

Host RNA-dependent RNA polymerases (RDRs), such as RDR1 and RDR6, amplify vsiRNAs leading to an increase of the RNA silencing and a spread of the antiviral signal by the formation of secondary vsiRNA. Its production is inhibited by CMV 2b VSR, which interferes with RDR-dependent antiviral silencing through 2b-AGO interaction (Fang et al., 2016). Inhibition of RDR action was observed also in V2 from Tomato *Yellow Leaf Curl Virus* (TYLCV), which interacts with Arabidopsis suppressor of gene silencing-3 (SGS3), cofactor of RDR6, blocking silencing amplification (Glick et al., 2008).

d. Epigenetic modifications

Plants use epigenetic modifications to protect themselves against DNA viruses, such as geminiviruses. Geminiviruses replicate their genome inside the nucleus generating dsDNA replicative strands that associate with histones (Preiss et al., 2003). Several DNA viruses encode VSRs that are able to alter DNA/histone methylation leading to the inhibition of gene silencing. *Tomato Golden Mosaic Virus* (TGMV) AL2 and *Beet curly top virus* (BCTV) L2 VSRs inhibit adenosine kinase (ADK), which sustains the methyl cycle and therefore S-adenosyl-methionine-dependent methyltransferases, leading to the indirectly block of the viral genome epigenetic modification (Raja et al., 2008). It has also been recently described that V2 protein from TYLCV directly interacts with host AGO4 in cajal bodies to suppress methylation of the viral genome (Liping Wang et al., 2020).

3.1 HELPER COMPONENT PROTEINASE (HC-PRO): EFFECTOR AND VSR FROM *POTYVIRIDAE* FAMILY

Viral genomes can encode more than one protein with the ability to suppress host RNA silencing. Viruses from the *Potyviridae* family are the most dangerous threats for socio-economical important crops, such as pepper or melon, causing serious diseases leading to significant losses in agriculture (A. Valli et al., 2015). Accordingly, viruses from this family are the main targets of investigation studies around the world. This family of (+) ssRNA viruses is divided in eight genera (*Brambyvirus*, *Bymovirus*, *Ipomovirus*, *Macluravirus*, *Poacevirus*, *Potyvirus*, *Rymovirus* and *Tritimovirus*), which differ on genome composition and structure, RNA sequence and vectors for transmission (A. Valli et al., 2015). Their RNA genome is encapsulated in filamentous virus particles by several units of a single coat protein (CP) (Kendall et al., 2008). Inside host cells, viral genome is uncoated and translated into a polyprotein that is processed by viral proteinases, into the following 9 viral gene products: P1 (protein with serine proteolytic activity responsible for cleavage), P3, 6K1 (6-kDA peptide), CI (cytoplasmatic inclusion), 6K2 (6-kDA peptide), NIa (Nuclear Inclusion A protease), Nib (viral replicase), CP (capsid protein) and Hc-Pro (Helper Component Proteinase). Additionally, potyvirus genome can produce the P1N-PISPO VSR by a polymerase slippage mechanism (Mingot et al., 2016).

Hc-Pro seems to be the most conserved VSR among different potyviruses (Hu et al., 2020). Hc-Pro is a multifunctional protein involved in all the essential steps of the viral infection cycle. Hc-Pro has three independent functions: viral plant-to-plant transmission, polyprotein maturation and silencing suppression (A. A. Valli et al., 2018). Regarding silencing suppression function, Hc-Pro was the first VSR described in the *Potyviridae* family (Anandalakshmi et al., 1998). Within *Potyviridae* family, only the Hc-Pro from genera *Potyvirus* and *Rymovirus* have RNA silencing suppression activity.

Hc-Pro is able to counteract multiple steps of the host's RNA silencing pathway. Similar to P19 from *Tombusvirus*, Hc-Pro from *Tobacco etch virus* (TEV) (Lakatos et al., 2006), *Plump Pox Virus* (PPV) (A. Valli et al., 2015), *Papaya*

ringspot virus (PRSV) (Shibolet et al., 2007), *Zucchini yellow mosaic virus* (ZYMV) (Jamous et al., 2011) and *Turnip Mosaic Virus* (TuMV) (Garcia-Ruiz et al., 2015) impedes the loading of vsiRNA into the RISC complexes by binding to these molecules depending on size. sRNA sequestration by Hc-Pro is thought to prevent cell-to-cell movement of vsiRNA which otherwise would surpass the infection front contributing to abrogate virus spread (Lakatos et al., 2006).

Additionally, Hc-Pro can interfere with 3' vsiRNA methylation, required for vsiRNA stabilization, by inhibiting the methionine cycle as Hc-Pro from *Potato Virus A* (PVA) (Ivanov et al., 2016) or by the interaction with the S-adenosylmethionine-dependent methyltransferase Hua Enhancer 1 (HEN1) enzyme, in case of ZYMV Hc-Pro (Jamous et al., 2011). Hc-Pro intervention on HEN1-dependent sRNA stabilization has been recently shown to be conserved in non-vascular plants (P.-C. Lin et al., 2016; Sanobar et al., 2021).

Hc-Pro can also directly interact with AGO1 through GW motifs as described for PVA (Ivanov et al., 2016; Pollari et al., 2020). Likewise, Hc-Pro from TEV disrupts miR168-dependent AGO1 by triggering its expression (Várallyay et al., 2013).

An additional role of Hc-Pro from *Sugarcane mosaic virus* (SCMV) is to interfere with the amplification of the RNA silencing by the down-regulation of RDR6 mRNA (Xiaoming Zhang et al., 2008).

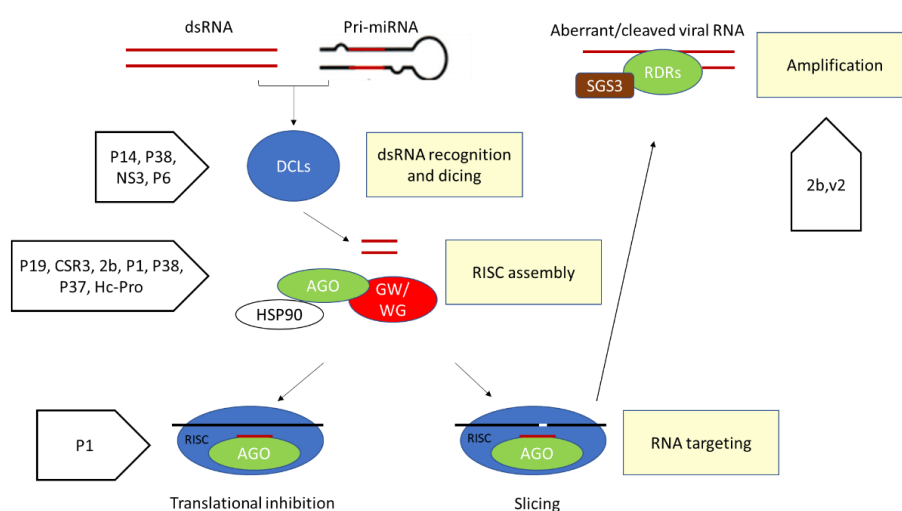


Figure 3. VSRs and RNA silencing steps. VSRs can interfere with multiple steps of RNA silencing in plants as dsRNA recognition and dicing, RISC assembly, RNA targeting and amplification.

4. RNA SILENCING MACHINERY AS A TARGET FOR BACTERIAL SILENCING SUPPRESSORS (BSRs)

The implications of RNA silencing in host defence seem to be broader than anticipated and not restricted to viral infections. Like viruses, bacteria have evolved to overcome host's immune responses by deploying effector proteins through a variety of secretion systems (Pfeilmeier et al., 2016). As an example, type II secretion system (T2SS) delivers apoplasmic effectors and plant cell wall-degrading enzymes (Cianciotto et al., 2017; Pfeilmeier et al., 2016). On the other hand, the type III secretion system (T3SS) is an elaborated mechanism for delivering effector proteins into the cytoplasm of plant cells (Alfano et al., 2004; Pfeilmeier et al., 2016). The presence of these effectors inside plant cells alter a variety of host cellular components and molecular functions, affecting plant cell transcriptome and proteome and making plants more susceptible to infections (Deslandes et al., 2012).

The Arabidopsis miRNA pathway is essential for PTI defence response and suggest that bacterial effectors have evolved to suppress this small RNA pathway to cause disease (see 6.2.2). *Pseudomonas syringae* infection of *A. thaliana* mutant lines defective in components of RNA silencing pathways showed that miRNA pathways play an important role in PTI responses against bacteria (Navarro et al., 2008). Alike viruses, bacteria produce effectors, known as Bacterial Suppressors of RNA silencing (BSRs), with the ability to interfere with the host RNA silencing suppression machinery, allowing bacteria to overcome sRNA-mediated plant defence (Navarro et al., 2008).

Pseudomonas syringae pv. Tomato (*Pto*) DC3000 is the best-characterized bacterial pathogen in the context of RNA silencing. *Pto* DC3000 produces and injects BSRs through the T3SS into the host's cellular space that target the miRNA silencing pathway: Avirulence Pto B (AvrPtoB), Avirulence Pto (AvrPto), Hrp outer protein N1 (HopN1) and Hrp outer protein T1-1 (HopT1-1) (Navarro et al., 2008). The presence of these BSRs could affect miRNA transcription, biogenesis or activity.

AvrPtoB is an effector with E3-ubiquitin ligase activity which promotes protein ubiquitination and degradation (Janjusevic et al., 2006). Its role as BSR was shown by the quantification of primary miRNA transcripts (pri-miRNAs; see 6.2). Pri-miR393a and pri-miR393b, PAMP-responsive pri-miRNAs, decrease after the expression of AvrPtoB in *Arabidopsis* without affecting other PAMP-insensitive pri-miRNA (Navarro et al., 2008). Besides, AvrPtoB was proposed to suppress miR393a and miR393b transcription independently of E3-ubiquitin ligase activity (Navarro et al., 2008).

AvrPto is an effector that interacts and inhibits the kinase activity of several PRR (Xiang et al., 2008). The reduced levels of PAMP-sensitive and insensitive miRNA after AvrPto delivery in *Arabidopsis* showed its function as BSR. AvrPto reduce the accumulation of unrelated miRNAs at the post-transcriptional level since AvrPto did not alter pri-miRNA transcripts (Navarro et al., 2008). For this reason, it was proposed that AvrPto interferes with some miRNA precursors through an alteration in miRNA processing by DCL proteins (Navarro et al., 2008).

HopN1 is a cysteine protease effector which inhibits the production of ROS and callose deposition, associated with defence responses (Rodríguez-Herva et al., 2012). In addition, HopN1 also affects mature miRNA accumulation without affecting pri-miRNA levels. On the other hand, it also affects the accumulation of trans-acting (ta-siRNA; see 6.1.2) tas255, probably affecting a conserved process in sRNAs processing (Navarro et al., 2008).

The type-III secreted Hrp outer protein T1-1 (HopT1-1) was initially described as a transcriptional repressor of a gene involved in PAMP defence (X. Li et al., 2005). Later on, HopT1-1 was described as an essential *Pto* DC3000 effector, working as a BSR, which enhances bacterial pathogenicity and growth affecting the AGO1-dependent miRNA pathway (Navarro et al., 2008; Thiébeauld et al., 2021). Lines overexpressing HopT1-1 are smaller than wild-type, suggesting a general suppression of sRNAs that in turns affects plant development (Navarro et al., 2008). Additionally, mRNA levels of miRNA targets raise in these plants, mimicking the effects of AGO-mutated plants (Navarro et al., 2008). As well, in these lines, miRNAs decrease moderately without affecting pri-miRNA levels (Thiébeauld et al., 2021). This observation suggested that the

BSR function of HopT1-1 mainly interferes with RISC complex function instead of biogenesis or stability of miRNAs (Navarro et al., 2008; Thiébeauld et al., 2021).

HopT1-1 physically interacts with AGO1 through two conserved AGO-binding GW/WG motifs, also present in some VSRs (Azevedo et al., 2010; Giner et al., 2010; Pérez-Cañamás et al., 2015; Thiébeauld et al., 2021). These motifs are not only essential for the ability of HopT1-1 to suppress miRNA but are also essential to interfere with PTI responses. HopT1-1 is able to suppress PTI responses as H₂O₂ production and callose deposition during bacterial infection and this suppression is compromised in bacteria deploying HopT1-1 mutated in GW motifs (Thiébeauld et al., 2021). This suggests that HopT1-1 activity couples silencing suppression activity with virulence function by the activation of negative regulators of PTI controlled by miRNA and/or by the suppression of AGO1-directed reprogramming and early PTI signalling (Thiébeauld et al., 2021).

Taken together, all this information leads to determine that HopT1-1 has evolved specifically to target AGO1 protein (Thiébeauld et al., 2021).

5. RNA SILENCING MACHINERY AS A TARGET FOR OOMYCETE EFFECTORS

Oomycetes are an important class of filamentous eukaryotic pathogens of animals and plants. Among them, more than 60% of known oomycetes are pathogens of plants (Thines Marco et al., 2010). Oomycete secrete effector proteins that are delivered inside (cytoplasmic) or can act outside (apoplastic) to promote infection and colonization of plant tissues, affecting host immunity (S. Wang et al., 2017). These effectors include hydrolytic enzymes that are involved in degradation of host cell components, enabling oomycete penetration in host cells through haustoria. Oomycete infection encompass a convoluted defence-counterdefence crosstalk due to the large amount of effector proteins secreted by oomycetes (McGowan et al., 2017).

The oomycete genus *Phytophthora* encompasses some of the most important crop pathogens, causing plant diseases largely affecting staple production and natural ecosystems (Kroon et al., 2012). The majority of *Phytophthora* species synthesize cytoplasmic effectors carrying a RXLR motif (RXLRs) (McGowan et al., 2017). RXLRs containing proteins are characterized by a highly conserved RXLR motif in the N-terminal domain, followed by a downstream EER motif. The RXLR motif has been predicted to act as a translocation signal, targeting the protein for delivering into the host cell (Whisson et al., 2007).

A large screen for the identification of the RXLRs-containing effectors with silencing suppression activity from *Phytophthora Sojae* led to the identification of Suppressors of RNA silencing 1 and 2 (PSR1 and PSR2) (Qiao et al., 2013). PSR1 affects sRNA biogenesis by the binding to a nuclear protein containing a DEAH box RNA helicase domain, called PSR1-Interacting protein 1 (PINP1). This protein regulates the accumulation of miRNA and other sRNAs by affecting the assembly of DICER like complexes (Qiao et al., 2015). PSR1 carries a WY motif following the RXLR, required for RNA silencing suppression activity in some plant species (P. Zhang et al., 2019). Through the search for effectors carrying RXLR and WY motifs, PpPSR1L from *Phytophthora parasitica* and PiPSR1L from *Phytophthora infestans* were identified as PSR1-like effectors, having silencing suppression activity (Qiao et al., 2015).

PSR2 suppresses the ta-siRNA pathway (see 6.1.2), which leads to a decrease on the expression of NLRs and other genes involved in plant defence, leading to host damage (Qiao et al., 2013). PSR2 is highly expressed in early infection, modifying plant gene regulation during the biotrophic phase for the pathogen's benefit (Vries et al., 2017). PSR2 belongs to a conserved and widespread effector family in *Phytophthora*. PSR2 homologs have been identified in *P. infestans* (PiPSR2) and in *P. parasitica* (PpPSR2) (Vries et al., 2017; Xiong et al., 2014).

P. infestans have at least another effector (Pi14054) which also suppress RNA silencing in *N. benthamiana* (Vetukuri et al., 2017). The host proteins that

potentially interact with Pi14054 and how it might affect host defence are still unknown.

To date, all studies aiming to identify oomycete SSs have focused on a subset of *phytophthora* species. Thus, it is possible that future research in other species will contribute to the characterization of additional SSs.

6. RNA SILENCING MACHINERY AS A GENE REGULATORY SYSTEM

RNA silencing is not only a defence mechanism but also an ancient universal gene regulation system in eukaryotes that regulates many fundamental processes, such as development and stress responses. Hence, pathogen SSs disrupt not only the host's defence system but also perturb other endogenous processes by releasing host transcripts under sRNA regulation.

Like vsiRNAs, biogenesis and action of endogenous sRNAs in plants encompasses three sequential molecular phases: formation of dsRNA, processing of dsRNA templates into sRNA and RISC-mediated inhibitory action of the sRNA acting on partially or fully complementary RNA or DNA.

Plant sRNA can be classified in two different groups, based on the nature of their dsRNA precursors and its mode of action: siRNAs and miRNAs (Table 1) (Axtell, 2013).

sRNA CLASS	sRNA SUBCLASS		SIZE	CHARACTERISTIC FEATURES	MODE OF ACTION
Small interfering RNA (siRNA) Formed by the processing of two complementary and perfectly-paired ssRNA.	Heterochromatic siRNA (Hc-siRNA)		23-24	Transcript from intergenic or repetitive regions of the genome	Regulates chromatin structure
	Secondary siRNA	Phased siRNA (Pha-siRNA)	21-22	Formed by the transcription of non-coding or coding gene regions	mRNA cleavage
		Trans-acting siRNA (Ta-siRNA)	21-22	Formed by the transcription of non-coding gene regions	mRNA cleavage
	Natural antisense transcript-derived siRNA (NAT-siRNA)		21-24	Formed by hybridization of complementary RNAs separately transcribed	mRNA cleavage
Micro RNA (miRNA) Formed by the processing of a dsRNA from a ssRNA that self-hybridize			21-24	Expressed from miRNA genes.	Translation repression and mRNA cleavage

Table 1. Diversity of sRNA, size, origin and mode of action.

6.1 siRNA

siRNAs are a subclass of sRNAs with a length between 20-24 nt. siRNA are formed by the processing of two complementary and perfectly-paired RNA strands. Except of natural antisense transcript-derived siRNA (NAT-siRNA), the dsRNA precursor of siRNA is formed through the antisense transcription of a RNA template by a RDR. siRNA can be classified in different groups according to their biogenesis and/or function (Table 1) (Axtell, 2013). That classification includes heterochromatic siRNA (hc-siRNA), secondary siRNA and NAT-siRNA. Secondary siRNA can be further subdivided into phased (pha-siRNA) and trans-acting (ta-siRNA) siRNA (Axtell, 2013).

6.1.1 HETEROCHROMATIC siRNAs (hc-siRNA)

Hc-siRNA are 23-24 nt siRNA generated from intergenic or repetitive regions of the genome, such as those found in transposons, repeat elements and heterochromatin regions. Hc-siRNAs lead to RNA-dependent DNA methylation to maintain genome integrity by suppressing the expression of transposable elements (Matzke et al., 2009). Their biogenesis and action is dependent on a unique set of RDR, DCL and AGO family members: RDR2, DCL3 and AGO4 (Matzke et al., 2009).

6.1.2 SECONDARY siRNAs: pha-siRNAs and ta-siRNAs

Secondary siRNAs are 21-22 nt siRNAs. Pha-siRNA are secondary siRNA derived from protein-coding loci in many plant genomes, such as MYB transcription factors (Arikiti et al., 2014), pentatricopeptide repeat (PPR) genes (Arikiti et al., 2014) or NLR (Zhai et al., 2011). On the other hand, pha-siRNA can be also generated from non-coding loci (pha-siRNA-producing loci, PHAS loci) (Fei et al., 2013). The production of pha-siRNA relies on an upstream miRNA trigger and subsequent RDR activity. miRNA targeting of the primary transcript leads to recruitment of an RDR, which in turn triggers the synthesis of the complementary RNA strand and “in phase” processing of the resulting dsRNA into pha-siRNAs (Allen et al., 2005). The production of pha-siRNA starts in a specific nucleotide of a consistent dsRNA and are produced in a head-to-tail arrangement.

Some secondary siRNAs repress one or more targets distinct from their locus of origin (Fei et al., 2013). These secondary siRNAs are termed ta-siRNAs. Many of the known trans-acting siRNAs are also phased, and are generated from the same locus than pha-siRNA.

Ta-siRNAs are generally generated from noncoding TAS transcripts from TAS genes. TAS transcripts are targeted by an AGO1/7-miRNA complex that recruits RDR6 for the synthesis of a complementary strand. The resulting dsRNA molecule is processed by DCL4 to trigger the production of 21 nt ta-siRNAs (Fei

et al., 2013). Ta-siRNAs are then loaded into AGO1 and inhibit the expression of additional mRNA targets, some of them involved in plant development (Peragine et al., 2004).

6.1.3 NAT-siRNA

NAT-siRNA are 21-24 nt siRNA. Unlike the other types of siRNA, dsRNA precursors of NAT-siRNA are formed by the hybridization of complementary RNAs separately transcribed from opposite strands of the same locus (cis-NAT-siRNAs) or from genes that possess no overlap (trans-NAT-siRNAs). Only the first ones have been described in plants. Cis-NAT-siRNA are involved in developmental and biotic and abiotic stresses (Borsani et al., 2005; Held et al., 2008; Katiyar-Agarwal et al., 2006).

6.2 miRNA

miRNAs are the second most abundant class of plant sRNAs and have a length between 21-24nt (Table 1).

With the exception of mirtrons, originated from spliced out introns from protein-coding genes (Meng et al., 2012), the majority of plant miRNA are independent transcriptional units located between protein-coding genes. miRNA genes (MIRs) have their own promoters and are transcribed by RNA Polymerase II (RNA Pol II). MIR promoters have regulatory elements which interacts with many transcriptional regulators, leading to a multicomponent mode of regulation of MIR transcription (Rogers et al., 2013). Primary miRNA transcripts (pri-miRNA) are ssRNAs able to fold back and self-hybridize forming highly stable dsRNA hairpins. The RNA-binding protein DAWDLE (DDL) stabilizes pri-miRNA in nuclear processing centres called D-bodies. Subsequently, DCL proteins (mainly DCL1), assisted by accessory proteins like HYPONASTIC LEAVES 1 (HYL1) and SERRATE (SE), catalyse a two-steps processing of pri-miRNA into an intermediate precursor-miRNA (pre-miRNA) to finally release 21-24 nt miRNA/miRNA* duplexes (Rogers et al., 2013).

Like for all sRNAs, miRNA duplexes are further stabilized by HEN1 preventing their degradation by SMALL RNA DEGRADING NUCLEASES (SDNs), a class of exonucleases (Budak et al., 2015). Initially, the exportin HASTY (HST), an ortholog of the animal Exportin 5 that transports animal pre-miRNAs to the cytoplasm (Zeng et al., 2004), was considered to participate in miRNA shuttling from nucleus to cytoplasm. Nevertheless, recent studies have shown that an important body of miRNA duplexes are loaded in nuclear AGO1 which is translocated to the cytoplasm (Bologna et al., 2018).

Additional recent studies have shown that HST has other functions in the miRNA pathway in Arabidopsis. HST directly interacts with DCL1 through its N-terminal domain, acting as a scaffold to facilitate the recruitment of DCL1 to genomic miRNA loci, boosting transcription and processing of pri-miRNA (Cambiagno et al., 2021). HST has also been reported to regulate cell-to-cell and vascular miRNA movement (Brioudes et al., 2021).

Once in the cytoplasm, miRNA/miRNA* separates and the guide strand targets AGO1-containing RISC complexes to mRNAs with high sequence complementarity. Target mRNAs are prevented from their expression through two co-existing mechanisms, cleavage and translational inhibition (Rogers et al., 2013). The contribution from both miRNA-triggered silencing mechanisms has been shown to be cell-type, developmental stage and temperature dependent (Born et al., 2018; Grant-Downton et al., 2013).

The repertoire of plant miRNA and their targets within a cell is specific to its identity and maturation stage (Breakfield et al., 2012; Brosnan et al., 2019). Furthermore, populations of miRNA and targets can diverge between plant species (Smith et al., 2015).

6.2.1 PLANT miRNAs AND DEVELOPMENT

Most of our knowledge about the role of plant miRNAs is related to their role in development. Similar to what was found in *Caenorhabditis elegans* (Miska et al., 2007), about 20% of Arabidopsis miRNA families regulate targets involved in plant physiology and development (Todesco et al., 2010). The inactivation of miRNAs that control the expression of genes with regulatory functions, such as

F-box proteins and TFs, resulted in plant developmental defects, similar to those observed by the constitutive expression of SSs from different pathogens (Navarro et al., 2008; Qiao et al., 2015; Shibolet et al., 2007; Todesco et al., 2010). miRNA-targeted TFs coordinate plant developmental plasticity by interacting in common regulatory protein complexes that converge on the regulation of shared downstream targets (Rubio-Somoza et al., 2011). Combinations of different miRNA-targeted TFs within the same regulatory complexes result in different developmental outcomes in different plant species (Rubio-Somoza et al., 2014).

6.2.2 PLANT miRNA AND THEIR ROLE IN DEFENCE RESPONSES

MiRNA implication in PTI responses was initially demonstrated in *A. thaliana*. Arabidopsis plants increase the production of miR393 upon the presence of flg22. In turn, miR393 represses the expression of F-box auxin receptors essential for auxin signalling, conferring resistance to *P. syringae* (Navarro et al., 2006). That way, miRNAs involved in defence against pathogens seem to regulate plant defence directly or indirectly through the control of hormone signalling. Besides, both mature miRNAs from the miR393/miR393* duplex are functional: miR393 regulates auxin signalling and miR393* regulates the expression of MEMB12, which encodes a Golgi protein Soluble NSF Attachment Protein (SNARE) involved in transport and secretion of the antimicrobial PATHOGENESIS-RELATED 1 (PR1) protein when loaded in AGO2 (Navarro et al., 2006; Xiaoming Zhang et al., 2011a).

Analysis of flg22 responsive miRNAs in Arabidopsis, led to the identification of additional miRNAs involved in defence. miR160a was found to positively regulate callose deposition, while miR398b and miR773 negatively regulate this PTI response upon *P. syringae* infection (Yan Li et al., 2010). Besides, miR398 and miR395 regulates the expression of Superoxide Dismutase (SOD) transcripts CSD1 and CSD2. SOD are involved in ROS detoxification, protecting cells against oxidative stress (L. Li et al., 2017). On the other hand, the overexpression of miR773 and silencing of its target METHYLTRANSFERASE 2 (MET2) increased the susceptibility to fungal pathogens in *A. thaliana* (Salvador-Guirao et al., 2017).

Additionally, plant miRNAs directly and indirectly regulate core defence elements such as NLR genes (Shivaprasad et al., 2012). Despite both miRNAs and NLRs are present in the genomes of unicellular algae, their regulatory relationship can only be traced back to Gymnosperms (Y. Zhang et al., 2016). miRNAs regulating NLRs are commonly targeting sequences within the highly conserved and functionally important P-loop domain. miRNA-binding to NLR transcripts results in the production of RDR6-dependent dsRNAs that in turn are substrates for DCL4. DCL4-dependent secondary siRNAs are loaded in AGO1-containing RISC complexes to target additional members of the NLR family expanding the repertoire of NLRs subjected to silencing suppression (Zhai et al., 2011).

The *Arabidopsis* genome bears two different miRNAs that regulate different sets of NLRs, miR472 (CNLs) and miR825-5p (TNLs). Mature miRNA levels from both loci, have been shown to decrease upon perception the perception of PAMPs from bacteria (flg22) and fungi (chitin). Inhibition of those miRNAs and the concomitant increase on their NLR targets was found to lead to an enhanced resistance against viral, bacterial and fungi infections (Boccaro et al., 2014; López-Márquez et al., 2021; Nie et al., 2019; Niu et al., 2016).

Core members of the antiviral RNA silencing machinery are also regulated by different miRNAs. Among those, AGO1 and AGO2 genes are the two principal components of antiviral RISC complexes are regulated by miR168 and miR403 (Harvey et al., 2011; Manacorda et al., 2021; Vaucheret et al., 2004). AGO2 additionally participates in antibacterial defence (Xiaoming Zhang et al., 2011b).

6.2.3 PLANT miRNA-TFs AND THEIR ROLE IN PLANT DEFENCE

In the plant model organism *A. thaliana*, around 20% of miRNA families regulate TFs, although only 3% of the estimated repertoire of TFs is under miRNA regulation. The study of transcriptome changes in mutants with overexpressed or lacking specific miRNAs showed that miRNA-TFs regulate genes involved in cell differentiation, hormone signalling, cell cycle, DNA repair, metabolism and defence (unpublished results).

miRNA-targeted TFs can regulate both transcription and action of different NLRs (unpublished results, Padmanabhan et al., 2013). miR156-targeted Squamosa promoter-binding-like protein 6 (SPL6) can interact with a NLR in *N. benthamiana* and *A. thaliana* plants and regulate defence responses against virus and bacteria (Padmanabhan et al., 2013). Besides, other miR156 targets, such as SPL9, are also involved in defence responses. *A. thaliana* plants overexpressing miR156 showed an enhanced resistance against *Pto* DC3000, since the overexpression of miR156 leads to an accumulation of ROS (Yin et al., 2019). miR156 and miR172 are core regulators in the transition throughout life cycle in several plant species from juvenile to adult and reproductive phases. Since plant immunity varies with age, they can contribute to age-dependent defence mechanisms. Thus, levels of miR156 decrease as plants mature, in turn rice plants with low levels of miR156 show enhanced resistance to brown plant hopper (BPH) (Ge et al., 2018). Likewise, Arabidopsis miR172b affects the transcription of the PRR FLS2 through the regulation of the TFs TARGET OF EAT1 (TOE1) and TOE2, which binds to FLS2 promoter and inhibits its activity. miR172b expression increases during seedling development enhancing PTI immunity due to the increase of FLS2 expression (Zou et al., 2018). Other example of the role of miRNA-targeted TFs in age-related resistance (ARR) is SHORT VEGETATIVE PHASE (SVP). SVP is regulated in *A. thaliana* by miR396 but also in different plant species (Yang et al., 2015). miR396 also targets members of GROWTH-REGULATING FACTOR (GRF) family that participate in plant defence against bacteria and fungi both in *A. thaliana* and Rice (Chandran et al., 2019; Soto-Suárez et al., 2017).

In addition, another miRNA targeting TF that has been related to plant immunity against virus is miR159. miR159 modulates the TF GAMYB, which is a positive regulator of the gibberellin signal. The inhibition of miR159 in *N. tabacum* and rice showed developmental defects but also resulted in increased resistance to *Phytophthora* infection, unravelling an important role of miR159 in plant immunity (Z. Zheng et al., 2020).

OBJECTIVES

RNA silencing is not only a defence mechanism but also a universal gene regulation system in eukaryotes that orchestrates many fundamental processes, such as development and stress responses. Hence, pathogen-produced SSs disrupt not only a host's defence system, but they also perturb other endogenous processes by releasing host transcripts from sRNA regulation. In the absence of functional sRNAs, the concomitant release of their target transcripts may facilitate the reprogramming of host defence and development. Thus, impaired sRNA regulation could be used by the host to translate the presence of an intracellular threat into the need of self-reprogramming to cope with it by enabling counter-counter defensive measures. Linking the failure of the sRNA-mediated post-transcriptional regulation to defence would enable a rapid host reprogramming in response to the presence of intracellular threats. In support of that hypothesis, it has been found that lack of specific miRNAs in *Arabidopsis thaliana* plants leads to enhanced resistance to different pathogens (virus, bacteria and fungi). The aim of this work is to study the cell-type specific responses to pathogen-derived silencing suppressors and their role in the arms race between host and pathogens around RNA silencing. To that end, three objectives were pursued:

1. Establishing the specific host cell-types that pathogens target for RNA silencing suppression in the course of infection.
2. Determining cell-type specific transcriptional reprogramming as result of pathogen-triggered silencing suppression.
3. Study of the contribution of cell-type reprogramming to counter-counter defence mechanisms.

MATERIALS AND METHODS

1. PLANT MATERIAL AND GROWTH CONDITIONS

1.1 PATHOGEN INFECTIONS

Arabidopsis thaliana ecotype Col-0 was used to perform the infections.

For the optimization of infection conditions in Objective 1, *A. thaliana* wild-type (WT) plants were used for infection assays. For viral infections, 40 *Arabidopsis* plants were grown on soil in long day (LD) conditions: 16 h light, 8 h darkness, 100 $\mu\text{E}/\text{m}^2/\text{sec}$ light intensity, 22 °C, 60 % relative humidity. Infection assays were performed on plants 10 days after sowing. For viral infections performed in plants grown *in vitro*, 40 plants were grown in 0.5 MS (2,2 g/L Murashige-Skoog media with vitamins + 0,25 g/L MES buffer + 10 g/L agar) plates in LD conditions. Infection assays were performed on plants 10 days after germination. For bacterial infections, 40 plants were grown on soil in short day (SD) conditions: 8 h light, 16 h darkness, 100 $\mu\text{E}/\text{m}^2/\text{sec}$ light intensity, 22 °C, 60 % relative humidity. Infection assays were performed on 4-5 weeks old plants.

Reporter lines to establish the spatiotemporal pattern of pathogen infections and to monitor the efficiency of the silencing machinery were used for infections in Objective 1. The first reporter line carried the Firefly Luciferase gene (LUC) under the control of the 35S promoter from CaMV, and an artificial miRNA (amiR) against the LUC gene under the control of the very same promoter (amiR-LUC reporter system) (Manavella et al., 2012). For viral infections, 10 plants carrying the amiR LUC reporter system were grown on soil in SD conditions. Cotyledons from 10 days old seedlings were infected. For bacterial infections, 10 plants were grown on soil during 4-5 weeks in SD conditions.

Additionally, for viral, bacterial and oomycete infections in Objective 1, a second reporter line was used. The second reporter line carried a nuclear location signal (NLS, derived from the *Simian Virus 40* Nuclear Localization Signal SV40 viral sequence) translationally fused to a plant codon optimized mScarlet-I gene under the control of the constitutive HISTONE THREE RELATED 5 (HTR5; At4g40040) promoter from *A. thaliana*, and an amiR against mScarlet-I gene, under the control of the same promoter (amiR-mScarlet-I reporter system) (see 3.1). For viral infections, 10 plants carrying the amiR-mScarlet-I reporter system

were grown on soil in SD conditions and infected 10 days after sowing. For bacterial infections, 10 plants were grown on soil in SD and infected 4-5 weeks after sowing. For oomycete infections in Objective 1, 10 plants were grown in 0.5 MS plates in SD conditions. Infection assays were performed on plants 2 weeks after germination.

For viral infections in Objective 3, a set of plants conditionally expressing the SSs TuMV Hc-Pro or mScarlet-I fluorescent protein in mesophyll, phloem companion and bundle sheath cells and HopT1-1 in mesophyll cells, were used (see 3.3). 10 plants were grown on soil in SD conditions and infected 10 days after sowing. For bacterial infections in Objective 3, only plants conditionally expressing the SSs or mScarlet-I protein in mesophyll cells were used. 10 plants were grown on soil in SD conditions and infected 4-5 weeks after sowing.

1.2 PLANT TRANSFORMATIONS

Arabidopsis thaliana ecotype Col-0 were used to perform plant transformations.

20 *Arabidopsis* plants for each construct were grown on soil in LD conditions for 4 weeks. At this time, fully flowered plants were transformed with the constructs (see section 3) by the floral dip method (Xiuren Zhang et al., 2006).

Transgenic plants were selected in 0.5 MS plates using the corresponding antibiotics or herbicides.

1.3 VALIDATION OF THE REPORTER SYSTEMS

For agroinfiltrations, *Nicotiana benthamiana* plants were grown on soil in LD conditions at 23 °C and 65 % humidity. ~3 weeks old *N. benthamiana* plants were used to perform agroinfiltrations.

Validation of reporter lines in *A. thaliana* was carried out by crossing homozygous parental lines containing either amiR-LUC or amiR-mScarlet-I reporter systems with those constitutively expressing TuMV Japanese Hc-Pro

under the 35S promoter. F1 generations were grown on soil under LD conditions for 2~3 weeks.

1.4 GUS STAINING

For the GUS staining, one set of *A. thaliana* plants carrying GUS-reporter constructs (see 3.2) were grown on plates containing 0.5 MS + BASTA during 2 weeks under LD conditions.

Additionally, another set of plants carrying GUS-reporter constructs were grown on soil during 3 weeks under LD conditions for inflorescence staining.

1.5 VALIDATION OF THE GR-LhG4-pOp TWO-COMPONENT SYSTEM AND SSs EXPRESSION

The validation of the GR-LhG4-pOp two-component system and the analysis of the SSs expression was performed in 2~3-weeks-old *Arabidopsis* plants carrying the constructs in 3.3 grown on soil under LD conditions.

1.6 VALIDATION AND SETTING THE CONDITIONS FOR SILENCING SUPPRESSION TRIGGERED BY THE CONDITIONALLY EXPRESSION OF SSs

Arabidopsis plants conditionally expressing the SSs in the specific cell-types and carrying the amiR-mScarlet-I reporter system, generated by the crossing of stable lines expressing each construct, were grown on soil during 2 weeks under LD conditions.

1.7 PROTOPLASTING

36 plants conditionally expressing the SSs or the mScarlet-I gene in specific cell-types that also expressed GFP in the same cell-types, generated by the crossing of stable lines expressing each constructs (see 3.3; 3.4), were grown on soil during 10 days under LD conditions.

2. PATHOGEN INFECTIONS

2.1 VIRUS, BACTERIA AND OOMYCETE STRAINS AND GROWTH CONDITIONS

PPV and TuMV from the *Potyviridae* family were used for viral infections (Lansac et al., 2005; Bedoya et al., 2012). Viral genomes are contained in *Agrobacterium tumefaciens* strains that serve as vectors for plant inoculation. PPV is labelled with the Green Fluorescent Protein gene (GFP). The GFP gene is integrated in the genome and is expressed together with the rest of viral proteins (Lansac et al., 2005). TuMV carries the *Anthrrium majus* MYB-related Rosea 1 (Ros1) TF. The expression of Ros1-TF leads to the accumulation of anthocyanins, inducing pigment accumulation detectable by naked eye (Bedoya et al., 2012). Both viral genomes carry the TuMV Japanese VSR Hc-Pro.

Pto DC3000 was the strain used for bacterial infection experiments (obtained through a collaboration with Sheng-Yang He Laboratory at Michigan State University, USA). This strain is also labelled with GFP, carrying the GFP gene integrated in the bacterial chromosome at the attTn7 locus. Additionally, a *Pto* DC3000 strain lacking the T3SS secretion system (*Pto* DC3000 hrcC-) was also used. Both *P. syringae* strains carry the BSR HopT1-1 in its genome.

Oomycete *Phytophthora palmivora* (isolate LILI) was used for oomycete infection experiments. The line used expresses an endoplasmic reticulum (ER)-targeted yellow fluorescent protein (YFP) (Carella et al., 2019).

Pseudomonas and *agrobacterium* cells were stored in glycerol 30 % at -80°C and grown in the same manner. For the experiments, strains were refreshed

on LB (Peptone 10 g/L, Yeast extract 5 g/L and NaCl 5 g/L) media plates containing the corresponding selective antibiotics. Plates were incubated at 28°C for 48h.

P. palmivora was maintained long-term on petri plates of rye sucrose agar (RSA) containing G418 (1.5 % agar, 50 µg of G418 per millilitre) in a Conviron growth cabinet set to 25°C with constant light conditions. For infection assays, a piece of mycelium from the growing edge of a *P. palmivora* colony on RSA was transferred to the centre of a V8 agar plate, (1.5 % agar, 50 µg of G418 per millilitre). V8 plates were grown for 5 to 7 days to allow sporulation.

2.2 INFECTION PROCEDURES

2.2.1 VIRAL INFECTIONS

Plates containing the Agrobacterium strain carrying the PPV-GFP or the TuMV-Ros1 genomes were scraped off and re-suspended in infiltration buffer (10 mM MgCl₂, 10 mM MES pH5.7, 150 µM acetosyringone). Agrobacterium concentration was measured and adjusted to the OD₆₀₀ required by adding infiltration buffer.

Infections were performed by piercing in the two cotyledons using a needle previously soaked in the agroinfiltration solution.

The set of plants conditionally expressing the SSs in specific cell-types infected with TuMV-Ros1 were sprayed with 10 µM dexamethasone + 0.02 % surfactant Sylwet L-77 one day after infection and they were treated every 4-5 days during 2 weeks until symptoms appeared.

2.2.2 PSEUDOMONAS SYRINGAE INFECTIONS

For infections in Objective 1, plates containing *Pto* DC3000 bacteria were scrapped off and re-suspended in 10mM MgCl₂. OD₆₀₀ was measured and adjusted to the required to perform the infections. Right before the infection, surfactant Sylwet L-77 was added to the solution to a final concentration of 0.05

%. Then, plants were sprayed with the solution. Trays were abundantly watered and covered overnight with a transparent plastic film, in order to keep a high relative humidity and allow the entrance of bacteria into the plant tissues through the stomata.

For infections in Objective 3, plates containing *Pto* DC3000 bacteria were scrapped off and re-suspended in 10 mM MgCl₂. Solution-containing *Pto* DC3000 was adjusted to OD₆₀₀ 0.001 in 10 mM MgCl₂ and leaves 7 and 8 were infiltrated.

2.2.3 OOMYCETE INFECTIONS

For oomycete infections in *A. thaliana* roots and leaves, 5 to 7 days V8-*P. palmivora* plates were flooded with sterile water and incubated at room temperature for 1 hour under continuous light, to induce the release of zoospores. For infection assays, zoospores were used at a concentration of 50000 spores per millilitre, adding the solutions directly to the plates containing the Arabidopsis seedlings.

2.3 INFECTION ANALYSIS

2.3.1 LUMINESCENCE MEASUREMENT

Infected plants carrying the AmiR-LUC reporter system were sprayed with Luciferin (luciferase substrate) 1,25 mM and Triton 0,01 % (v/v) and after 5 minutes, images were taken using a LAS-4000 Luminescent Image Analyser (Fujifilm). Images were taken using high-resolution mode and μ minutes of exposure and then processed using the software Fiji 1.0.

2.3.2 IMAGING

PPV-GFP viral infections were observed under a magnifying glass attached to a UV light source and using a filter that allows to observe GFP signal. An Olympus DP71 fluorescence device was used together with Cell[^]D software

(Olympus) to take pictures of the plants. Images were taken using the high resolution mode, ISO200 and 50 seconds of exposure.

P. syringae and *P. palmivora* infections were observed under the confocal microscope, which allows clearly distinguishing individual GFP-labelled bacteria or YFP-labelled oomycete and its localization inside tissues and cells. Images were taken with a Leica Confocal Microscope SP5 and treated with the LAS X (Leica) software package.

All infected plants were imaged using a Nikon camera

All images were further analysed using Fiji 1.0 software.

2.3.3 VIRAL CONCENTRATION

For the quantification of viral concentration in the set of plants conditionally expressing the SSs in specific cell-types, infected with TuMV-Ros1, a qPCR was performed.

8 infected plants were randomly collected 3 weeks after infection and its RNA was isolated by the Phenol-based RNA isolation protocol (Box et al., 2011). Then, the cDNA was generated using the RevertAid First Strand cDNA Synthesis kit of ThermoFisher Scientific™ following manufacturer instructions. After that, a qPCR using the Roche's LightCycler® 480 SYBR Green I Master kit was performed, following manufacturer instructions, in a LightCycler® 480 instrument, using the following primers:

qRT-TuMV.s	5'-GATGCGCGTGCCAAGATACGAG-3'
qRT-TuMV.as	5'-GCTCCGGCGTGTATAGGATTAGATG-3'
qRT-Actin.s	5'-CTAAGCTCTCAAGATCAAAGGCTTA-3'
qRT-Actin.as	5'-ACTAAAACGCAAACGAAGCGGTT-3'

TuMV gene expression was normalized to the expression of actin (At3g18780) as housekeeping gene expression. qPCR data analysis was performed using R software.

2.3.4 BACTERIAL CFU (COLONY FORMING UNIT) CALCULATION

Right after the infection and 3 days after infection (DAI), 2 leaf discs of 1 cm² were taken from infiltrated leaves and placed into 2 ml Eppendorf tubes containing 1ml of 5mM MgCl₂. Samples were grinded using a TissueLyser. Then, a serial dilution was done until 10⁻⁶ and 10 µl of each dilution were plated in a square plate containing LB ½ NaCl with the appropriate antibiotics. After that, plates were incubated at 28 °C for 1.5 or 2 days.

Once the colonies had the right size, they were counted and the CFU/cm² was calculated.

Data analysis was performed using Excel software.

3. CONSTRUCTS FOR PLANT TRANSFORMATION

All plant transformation constructs were made using the GreenGate (GG) cloning system, based on the Golden Gate method (Lampropoulos et al., 2013). GG system depends on six types of insert modules: plant promoter, N-terminal tag, coding sequence, C-terminal tag, plant terminator and plant resistance cassette. GG system allows the assembling of the different modules in one binary destination vector, using one type of IIS restriction endonuclease and a ligase.

Modules here used were from the collection of GG pre-cloned building blocks or from modules previously available in the laboratory. Those needed and not available were generated by adding the corresponding ligation ends to PCR products. Then PCR products were inserted in GG empty entry vectors by Eco31-I digestion and T4-DNA ligase ligation reactions.

All final constructs were introduced in *Escherichia coli* TOP 10 competent cells for its validation by colony PCR, miniprep and plasmid digestion and sanger sequencing. Then, plasmids were introduced by electroporation in *Agrobacterium tumefaciens* strains GV3101 or ASE carrying the pSOUP helper plasmid.

3.1 REPORTER SYSTEM BASED ON THE REGULATION OF A FLUORESCENT PROTEIN GENE

A reporter system based on a constitutive expressed amiR designed to regulate a constitutive expressed fluorescent protein, mScarlet-I, located in the nucleus, were made using the GG system (Fig.4).

HTR5 promoter, *Simian Virus 40* Nuclear Localization Signal (SV40 NLS) and Ribulose Bisphosphate Carboxylase Small Subunit gene (RBCS) terminator sequences were obtained from the GG collection. Plant codon optimized mScarlet-I gene sequence was amplified through PCR and added the properly end bases for its insertion in the corresponding empty vector from the GG collection (Table 1).

AmiR targeting the mScarlet-I gene sequence were obtained using the WMD3 web app, which allows the automated design of artificial microRNAs. WMD3 web delivered 4 oligonucleotide sequences (I to IV), which were used to engineer amiR into the endogenous miR319a precursor by site-directed mutagenesis, following the web app instructions. The template for the PCRs was the plasmid pRS300, which contains the miR319a precursor in pBSK (Table 3).

In order to add the properly ends to insert the resulting amiR sequences into pGGB000 empty vector, amiR sequences were amplified using the following primers:

amiR.B.s 5'-AAAGGTCTCAAACAACAAACACACGCTCGG-3'

amiR.C.as 5'-AAAGGTCTCAAGCCCATGGCGATGCCTTAAATAAAG-3'

Once all blocks were generated, all inserts were combined by Eco31-I digestion and T4-DNA ligase ligation reactions in intermediate GG empty vectors, (pGGM000 and pGGN000) and then in the final GG empty vector pGGZ003.

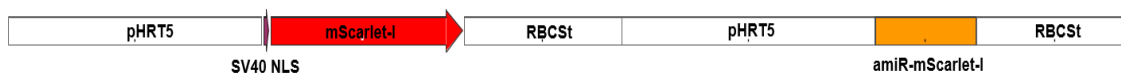


Figure 4. Gene map of mScarlet-I reporter system. HISTONE THREE-RELATED 5 promoter (HTR5p; At4g40040), Simian Virus 40 (SV40) nuclear localization signal (SV40 NLS), mScarlet-I gene, Ribulose Bisphosphate Carboxylase Small Subunit gene terminator (RBCSt), artificial micro RNA designed to regulate mScarlet-I gene (amiR-mScarlet-I).

Gene	Template	Primers (5'→3')	Destination Vector
mScarlet-I	P2P3-mScarlet	aacaGGTCTCaggctcaacaatggtgagcaagggcg aacaGGTCTCtctgattactgtacagctcgtccatg	pGGC000

Table 2. Fluorescence protein mScarlet-I template, primers used for its amplification and GG destination vector.

amiR	Template	Primers for amiR engineering (5'→3')
amiR-mScarlet-I	pRS300	I. gaTCTGCACGGGCTTCTTGGCCActctctttgtattcca II. agTGGCCAAGAAGCCCGTGCAGAtcaaagagaatcaatga III. agTGACCAAGAAGCCGGTGCAGTtcacaggtcgtgatag IV. gaACTGCACCGGCTTCTTGGTCActacatatatattccta

Table 3. Primers for amiR-mScarlet-I engineering by PCR reactions and template for PCRs

3.2 GUS REPORTER GENE UNDER THE CONTROL OF CELL-TYPE SPECIFIC PROMOTERS

A set of constructs carrying the GUS gene under the control of 7 cell-type specific promoters (Table 4; Fig. 5) were generated using the GG system. Promoters drive the expression to phloem companion cells (Sucrose-Proton Symporter 2 (SUC2; At1g22710) promoter), bundle sheath cells (Sulphate Transporter 2;2 (Sultr2;2; At1g77990) promoter), Scarecrow (SCR; At3g54220) promoter), mesophyll cells (Chlorophyll A/B Binding Protein (CAB3; At1g29910) promoter), Ribulose Bisphosphate Carboxylase Small Chain 1A (RBCS1A;

At1g67090) promoter), epidermal cells (3-Ketoacyl-Coa Synthase 6 (CER6; At1g68530) promoter) and proliferating tissues (CELL DIVISION CONTROL 2A (CDC2A; At3g48750) promoter).

Promoters were searched in literature (Cui et al., 2014; Ranjan et al., 2011; Sawchuk et al., 2008; Serna et al., 1997; Takahashi et al., 2000; Ursache et al., 2018), amplified from Arabidopsis genes and added the properly ends for its insertion in pGGA000 empty vector.

Those promoters carrying restriction sites for Eco31I inside its sequence were mutated, substituting Eco31I target bases by homologous non-target bases.

Promoter	Primers (5'→3')	Cell domain
SUC2	GGTCTCaACCTCTAATGTTTTGGAATTAA GGTCTCtTGTTATTTGACAAACCAAGAA	phloem
Sultr2;2	AACAGGTCTCAACCTAACCTATTATTTTATAGCAATTTTACATA AATATATTTAGATATTG AACAGGTCTCTTGTTTCAGCTCTCTCTCTAGATATATATTA CTTTTTT	bundle sheath
SCR	AACAGGTCTCAACCTCCAAACAGATATTTGCATTTGGG AACAGGTCTCTTGTTGGAGATTGAAGGGTTGTTGG	bundle sheath
CAB3	GTGGTCTAGAAATGCTTTGG CATTTCTAGACCACATGTTGC	mesophyll
RBCS1A	AACAGGTCTCAACCTATTAGAAACATCTTATTATGATATGTG GGTAC AACAGGTCTCTTGTTTGTCTTCTTTACTCTTTGTGTGAC	mesophyll
CER6	GGTCTCaACCTCAAATGTGAATTATATTT GGTCTCtTGTTCTCGGAGAGTTTTAATG	epidermal cells
CDC2A	GGTCTCaACCTGTTTTGAAGATATATATATCG GGTCTCtTGTTCAATTCCTGAATAATAAAG	proliferating tissues

Table 4. Primers for promoter amplifications and cell domain expression.



Figure 5. Gene map of GUS reporter gene under cell-type specific promoters. Cell-type-specific promoters (pSUC2, pSultr2;2, pSCR, pCAB3, pRBCS1A, pCER6 or pCDC2A), GUS gene (GUS), RBCS terminator (RBCSt).

3.3 CONSTRUCTS FOR THE CONDITIONAL EXPRESSION OF SSs OR mSCARLET-I FLUORESCENT PROTEIN IN SPECIFIC CELL-TYPES

A set of constructs for the conditional expression of the VSR Hc-Pro, the BSR HopT1-1 or the mScarlet-I fluorescent protein were created using the GG system (Fig. 6). The constructs carried the GR-LhG4-pOp two-component system (Craft et al., 2005; López-Salmerón et al., 2019) driven by the specific cell-type promoters pCAB3, pSUC2 and pSultr2;2, which drove GR-LhG4 expression to mesophyll, phloem and bundle sheath respectively. The GR-LhG4-pOp two-component system is based on a chimeric transcription factor and a cognate pOp-type promoter ensuring tight control of expression levels of genes under the control of the pOp promoter (Craft et al., 2005). In normal conditions, the GR-LhG4 chimeric protein is located in the cytoplasm but when plants carrying this system are treated with dexamethasone, the complex is translocated to the nucleus and the expression of the genes under the control of pOp promoter is activated.

On the other hand, the constructs carried the sequence of the VSR TuMV Hc-Pro (for its expression in mesophyll and vascular cells), the BSR *Pto* DC300 HopT1-1 (for its expression in mesophyll), or the sequence of mScarlet-I fluorescent protein (for its expression in mesophyll and vascular cells), all of them under the control of the pOp promoter (Fig. 6).

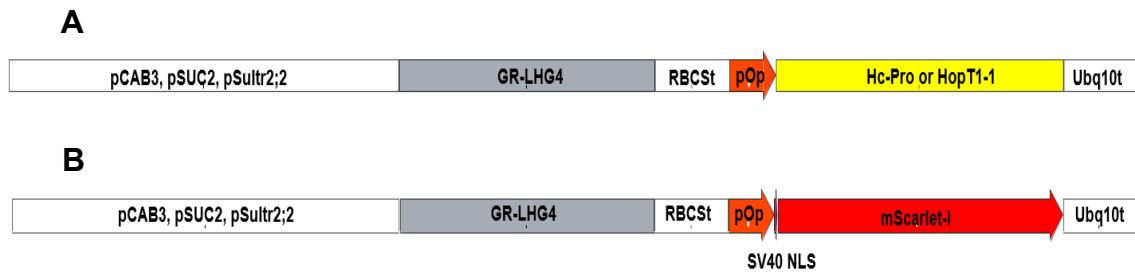


Figure 6. Gene map of the constructs for the conditional expression of **A.** pathogen SSs or **B.** mScarlet-I fluorescent protein in specific cell types.

A. CAB3, SUC2, Sultr2;2 promoters, chimeric protein GR-LHG4 (GR-LHG4), RBCS terminator (RBCSt), pOp promoter, Hc-Pro or HopT1-1 sequence, Ubiquitin 10 terminator (Ubq10ter).

B. CAB3, SUC2, Sultr2;2 promoters, chimeric protein GR-LHG4 (GR-LHG4), RBCS terminator (RBCSt), promoter pOp (promoter module 6xOP), nuclear localization signal (SV40 NLS), mScarlet-I gene, Ubiquitin 10 terminator (Ubq10t).

3.4 CONSTRUCTS FOR THE CONSTITUTIVE EXPRESSION OF GFP IN SPECIFIC CELL-TYPES

3 different constructs were generated using the GG system for the expression of GFP fluorescent protein in mesophyll and vascular bundles (Fig. 7). The constructs carried the GFP sequence under the control of CAB3p, SUC2p and Sultr2;2p cell-type specific promoters (Fig. 7).

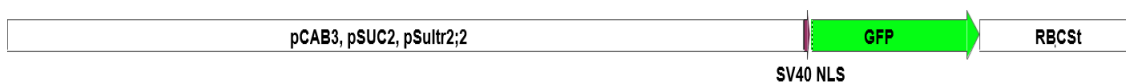


Figure 7. Gene map of the constructs for the constitutive expression of GFP in specific cell-types. CAB3, SUC2, Sultr2;2 promoters, nuclear localization signal (SV40 NLS), GFP gene (GFP), RBCS terminator (RBCSt).

4. VALIDATIONS AND SETTING THE CONDITIONS FOR PROTOPLASTING AND CELL-SORTING

4.1 VALIDATION OF amiR REPORTER SYSTEMS

AmiR-LUC and amiR-mScarlet-I reporter systems were validated through agroinfiltration (10mM MgCL₂, 10mM MES pH5.7, 150uM Acetosyringone; OD₆₀₀ 0.6) in *Nicotiana benthamiana* leaves. The validation consisted on the agroinfiltration of the different constructs together with a construct for the constitutive expression of Hc-Pro or an EV as negative control.

AmiR-LUC agroinfiltrated leaves were infiltrated with Luciferin (luciferase substrate) 1,25 mM and Triton 0.01 % (v/v) and after 5 minutes, images were taken using a LAS-4000 Luminescent Image Analyser (Fujifilm). Images were taken using high-resolution mode and 10 minutes of exposure and then processed using the software Fiji 1.0.

AmiR-mScarlet-I agroinfiltrated leaves were observed after 3 days under the confocal microscope. Images were taken with a Leica Confocal Microscope SP5 and treated with the LAS X (Leica) software package.

4.2 GENE EXPRESSION BY GUS STAINING

Plants carrying the constructs from section 3.2 were grown on 0.5 MS + the corresponding herbicide for 2 weeks, collected and prefixed 20 minutes in 90% acetone. On the other hand, inflorescences from 3-weeks-old plants grown on soil, were collected and prefixed in the same manner. All samples were washed with GUS staining buffer without 5-bromo-4-chloro-3-indolyl glucuronide (X-Gluc) (0.2 % Triton X-100, 50 mM NaPO₄ pH 7.2, 2 mM K-Ferri, 2 mM K-Ferro) and then infiltrate with cold staining buffer containing 2 mM X-Gluc. After an incubation at 37°C overnight, samples were washed with ethanol series (20 %, 35 %, 50 %) during 30 minutes with low agitation, fixed 30 minutes with FAA solution (50 % ethanol, 5 % formaldehyde, 10 % acidic acid glacial) and washed with ethanol 70 %.

GUS stained samples were observed under the magnifying glass Olympus DP71 fluorescence device and analyzed with Cell^{AD} software (Olympus). Images were taken using the high-resolution mode, ISO200 and 50 seconds of exposure.

4.3 VALIDATION OF THE GR-LhG4-pOp TWO-COMPONENT SYSTEM AND SETTING THE CONDITIONS FOR DEXAMETHASONE TREATMENT

4.3.1 VALIDATION AND SETTING THE CONDITIONS FOR DEXAMETHASONE TREATMENT USING FLUORESCENCE

The system was validated in plants carrying the GR-LhG4-pOp two-component system and expressing mScarlet-I in specific cell-types (see 3.3; Fig. 6B). 2~3 weeks old plants grown on soil under LD conditions were sprayed with 10 μ M dexamethasone + 0.02 % Silwet L-77.

During the following days, leaves were imaged under a Leica Confocal Microscope SP5 and analysed with the LAS X (Leica) software package.

4.3.2 VALIDATION BY qPCR

The system was further validated in plants carrying the GR-LhG4-pOp two-component system and also expressing the SSs Hc-Pro or HopT1-1 in specific cell-types (see 3.3; Fig. 6A). 2~3 weeks old plants grown on soil under LD conditions were sprayed with 10 μ M dexamethasone + 0.02 % Silwet L-77.

3 pools of 3 random leaves each one, from treated and non-treated plants bearing each construct, were collected at the times established in 4.3.1 and its RNA isolated by the Phenol-based RNA isolation protocol (Box et al., 2011). Then, the cDNA was generated using the RevertAid First Strand cDNA Synthesis kit of ThermoFisher ScientificTM following manufacturer instructions. After that, a qPCR using the Roche's LightCycler[®] 480 SYBR Green I Master kit was performed, following manufacturer instructions, in a LightCycler[®] 480 instrument using the following primers:

qRT Hc-Pro.s 5'- CCGCGTCGGAGCTGCATAC-3',

qRT Hc-Pro.as 5'- GAGTGCGTAATCTGGGACGTCG-3'

qRT HopT1-1.s 5'-GGCTAGCGAAAGTCGTGAAC-3'

qRT HopT1-1.as 5'-AACCCCTTATCGAAGCCCACT-3'.

Hc-Pro and HopT1-1 gene expression was normalized to actin housekeeping gene expression. qPCR data was analysed using Microsoft Excel software.

4.4 VALIDATION AND SETTING THE CONDITIONS FOR SILENCING SUPPRESSION TRIGGERED BY THE CONDITIONALLY EXPRESSION OF SSs

2-weeks-old *A. thaliana* stable lines conditionally expressing the silencing suppressors in the specific cell-types and carrying the amiR-mScarlet-I reporter system, were treated with 10 µM dexamethasone + 0.02 % Silwet L-77. During the following days, the fluorescence changes were analysed by the observation of the corresponding leaves with a Leica Confocal Microscope SP5. Then, the images were analysed with the LAS X (Leica) software package.

5. PROTOPLASTING AND CELL SORTING

5.1 PROTOPLASTS ISOLATION

36 plants conditionally expressing the SSs (Hc-Pro or HopT1-1) or mScarlet-I gene in the specific cell-types and also expressing GFP in the same domains, were grown on soil under LD conditions. 10-days old seedlings were sprayed with 10 µM dexamethasone + 0.02 % Sylwet L-77. 24 hours (for plants expressing the constructs in mesophyll) and 96 hours (for plants expressing the constructs in vascular bundles) after induction, protoplasts from 15 number 3 leaves were isolated. Leaves were cut into 0.5-1mm strips with a clean scalped blade, and the pieces were transferred and submerged into the enzyme solution (0.4 M Mannitol, 20 mM KCl, 20 mM MES buffer pH 5.7, 1.5 % Cellulose R-10,

0.4 % Macerozyme R-10, 0.35 % Pectolyase Y-23, 10 mM CaCl₂, 0.1 % BSA). After an incubation of 1 hour and 30 minutes at 80 rpm in a continuous light chamber, protoplasts were released by gentle circular agitation of the plate and the solution was filtered through a 100 or 70 µm filter, depending on the origin of the protoplasts (mesophyll or vascular bundles, respectively). Protoplasts were washed with W5 solution (154 mM NaCl, 125 mM CaCl₂, 5 mM KCl, 2 mM MES buffer pH5.7). After a centrifugation for 3 minutes at 1000 rpm at room temperature, protoplasts were washed one more time and resuspended in 500 µl of W5 solution.

5.2 CELL SORTING

2000 GFP-expressing protoplasts were isolated using the MoFlo XDP cell sorted located in the The Bellvitge Biomedical Research Institute (IDIBELL), L'Hospitalet de Llobregat, Barcelona, Spain. Protoplasts were collected in Eppendorf tubes containing RLT buffer (QIAGEN RNeasy Micro Kit) with 1 % of β-mercaptoethanol and kept in dry-ice.

6. PROTOPLASTS RNA ISOLATION

Total RNA from protoplasts was isolated using the columns and buffers provided in the QIAGEN RNeasy Micro Kit, with changes in manufacturer instructions. Eppendorf tubes containing RLT buffer and protoplasts were thawed in hands and 4 °C 70 % ethanol were added to the tubes. The resulting solution was added to the MinElute column and centrifuged at 1000 g for 1 minute, then 10000 g for 30 seconds. Flow-through was reapplied and centrifuged 10000 g for 30 seconds. Elutes were collected in a low-binding Eppendorf. Then, RW1 buffer was added to each column and centrifuged at 10000 g for 30 seconds. Elutes were added to the low-binding Eppendorf containing the first elute from each sample, and stored at -80°C for sRNA recovery.

After that, RPE buffer was added to the column and centrifuged 10000 g for 30 seconds. 80 % ethanol at room temperature was added to the column and centrifuged 10000 g for 30 seconds. 80 % ethanol at room temperature was

added to the columns and centrifuged at 10000 g for 2 minutes. The column was next placed in a new collection tube and centrifuged with open cap 5 minutes at maximum speed. Later on, the column was transferred to a pre-labelled 1.5 mL tube and 12 μ L of nuclease free water were added. After 2 minutes of incubation time, all samples were spined 1000 g for 1 minute, then 16000 g for 1 minute. Finally, the samples were reapplied to the filter and centrifuged 16000 g for 1 minute in a 4°C centrifuge. The elute was collected in low binding Eppendorf tubes and kept at -80°C.

Total RNA quality and concentration were assayed using bioanalyzer RNA Pico chips. The RNA integrity number (RIN) was used to assigning integrity values to RNA measurements and RNAs used for library preparation were RIN>8.

7. RNA SEQUENCING

7.1 PREPARATION OF cDNA LIBRARIES

cDNA libraries were obtained from 500 picograms of total RNA using the SMART-Seq® v4 Ultra® Low Input RNA Kit for Sequencing from Takara, using 16 cycles of amplification. cDNA quality and concentration were assayed using bioanalyzer High sensitivity chips and a Qubit Fluorometer. cDNA was fragmented by sonication using a Covaris device to enrich in 300 bps fragments (Duty cycle: 10 %; Intensity: 5; Cycles/Burst: 200; time: 5 minutes). Fragmentation was assayed using bioanalyzer high sensitivity chips. Then, cDNA concentration was established using a Qubit fluorometer and 2 nanograms were used as starting material for generating multiplexed libraries with ThruPLEX DNA-seq 48D Kit from Takara, following instructions from manufacturer. Final library concentrations were adjusted to a final concentration of 5 nM and pooled in two lanes (20 libraries each) of an Illumina High seq device for sequencing.

7.2 RNA-seq DATA ANALYSIS

7.2.1 ILLUMINA READS PREPROCESSING

Each set of sequencing reads was first processed with Trim Galore! v0.6.1 software. In a first step, this software trims low-quality bases from the 3' end of the reads. Then, adaptor sequences were removed from those same ends. Last, any sequence that becomes shorter than 20 bp as a consequence of the previous steps were removed. Both reads of a read-pair need to be longer than 19 bp to retain the pair, otherwise both were removed.

Then, SortMeRNA v4.3.2 software was used to detect and remove rRNA reads. Again, when one member of a read-pair was detected as rRNA, the complete pair was removed.

7.2.2 TRANSCRIPT EXPRESSION QUANTIFICATION

Cleaned reads together with the transcriptome of *Arabidopsis thaliana* were used to quantify gene expression at transcript level using Salmon v1.5.1 software. For this, the file AtRTD2_19April2016.fa, containing the transcriptome was downloaded from <https://ics.hutton.ac.uk/atRTD/>, while the file Arabidopsis_thaliana.TAIR10.dna.toplevel.fa, containing the genome, was downloaded from <https://plants.ensembl.org/info/data/ftp/index.html> (as of 05-Mar-2021).

The transcriptome file was modified by adding the transcript sequences from HopT1-1, TuMV Hc-Pro and mScarlet-I. This new file, together with the genome sequence were indexed using *Salmon index* and then used as input for *Salmon quant*, which was ran with parameters -l A, --validateMappings, --recoverOrphans, --rangeFactorizationBins 4, --seqBias, and --gcBias.

Mapping rate were found to be in the 93.4%-97.1% range.

7.2.3 GENE EXPRESSION QUANTIFICATION

Salmon's output contains quantification of gene expression at transcript-level. The quant.sf output files provide information of TPM and counts for all sequences included in the transcript file. In order to aggregate counts at gene-level, the R program tximport v1.14.2 was used.

7.2.4 SELECTION OF SAMPLES FOR DIFFERENTIAL EXPRESSION ANALYSIS

Upon inspection of the estimated gene expression levels of HopT1-1 and Hc-Pro transgenes across all samples, it was decided to select three replicates and remove the most likely outlier candidate for each sample type. To this end, a Grubb's test was applied (<https://www.graphpad.com/quickcalcs/Grubbs1.cfm>).

7.2.5 PCA PLOT OF SELECTED SAMPLES

The function *DESeqDataSetFromTximport* from the R package DESeq2 v1.26.0 was used to create an R object with count data information of the 21 selected samples along with the information regarding cell, mutant and time characteristics of each sample. In addition, the experimental design was set to 'design = ~group', where group was a combination of cell, mutant, and type (e.g. CAB3pHop24 or SUC2pScarlet96).

Then, a low-expression filter was applied to remove any gene with less than 10 counts across all 21 analysed samples. The filtered object consisted of 26386 genes (of a total of 33684 found in the original list of quantified genes, including the HopT1-1, Hc-Pro and mScarlet-I transgenes).

Then, the *DESeq* function, which, among other things, computes size factors for sample normalization, was applied to the filtered object. Last, DESeq2's *rlog* function was used to transform count data to the log₂ scale while minimizing for differences between samples for low-expressed genes. DESeq2's

plotPCA function was used to visualize a PCA plot of the filtered, normalized and transformed count data.

7.2.6 DIFFERENTIAL EXPRESSION ANALYSIS (PAIRWISE COMPARISONS)

The analysis of differential expression was done using DESeq2's *results* function with the filtered and normalized object as input, $\alpha = 0.05$, and specifying *contrast=c("group", "X", "Y")*, where X and Y were the names of any of the ten groups the samples were classified into.

Functional information was added to the obtained results using the R package biomaRt. An R object was produced by using the *useMart* function with parameters *biomart = "plants_mart"*, *host = "plants.ensembl.org"*, *dataset = "athaliana_eg_gene"*. Then, the function *getBM* was used to produce an object with the list of analyzed genes together with their ENSEMBL identifier, gene name and description if available. Last, this object is merged with the output of the *results* function.

7.2.7 GO ANALYSIS

Gene Ontology analysis were performed using the ShinyGO v0.741 (<http://bioinformatics.sdstate.edu/go/>) tool with default parameters (FDR<0.05) and selecting the option of showing 30 top pathways to show.

RESULTS

1. THE RNA SILENCING MACHINERY IS DISMANTLED IN SPECIFIC CELL-TYPES UPON PATHOGEN INFECTION

Unrelated pathogens have different lifestyles and strategies to colonize their hosts. Although they target common cellular processes, which allows pathogens to divert resources from the host on their own benefit, the production and delivery of effectors from different pathogens is tightly controlled. That delivery might take place at different points of infection and targeting distinct host cells, according to the nature of the invader (Vries et al., 2017).

As part of plant defence, the plant RNA silencing machinery is targeted by pathogen SSs. sRNAs and their targets are characteristics of the different cell-types that constitute each plant organ. Therefore, SSs-triggered host cell reprogramming will be also characteristic depending on the targeted cell-type.

In order to determine which are the plant cell types targeted for the action of pathogen-derived SSs, infections of plants carrying an artificial reporter system that sensitively monitors the activity of the miRNA machinery were performed. Infections were carried out using three pathogens labelled with fluorescent proteins: a GFP-labelled virus (PPV) (Lansac et al., 2005), a GFP-labelled bacteria (*Pseudomonas syringae*) and a YFP-labelled oomycete (*Phytophthora Palmivora*) (Carella et al., 2019).

1.1 OPTIMIZATION OF INFECTION CONDITIONS

The optimal conditions to establish sub-lethal pathogen infections for PPV and *P. syringae* bacteria were firstly determined. Different scenarios were tested according to pathogen concentration and plant growth conditions. Macroscopic symptoms and GFP signal imaging were used to validate the best conditions to perform further studies.

1.1.1 PPV VIRAL INFECTION

Viruses are mainly considered non-living organisms. They are obligate parasites which need living cells to survive and multiply. During natural infections, viruses spread through vectors, as insects or tools used by farmers. In both cases, the first layer of plant defence, the wax cuticle, is skipped easily since the originated wounds permits viruses to reach plant tissues. In order to mimic natural conditions, viral infections were performed by cotyledon piercing with a needle impregnated in a solution in which the virus-containing *Agrobacterium* was resuspended.

The optimal conditions for virus infection were determined by using different viral concentrations assayed in *A. thaliana* WT plants grown on soil and on 0.5 MS plates (Table 5). Presence of PPV-GFP was assayed by GFP tracking under microscopy. The best infection conditions (90% of infected plants) were obtained when the PPV-GFP-containing *Agrobacterium* inoculum was OD₆₀₀ 1.5 and plants were grown on soil. Furthermore, this viral concentration was enough to infect plants without killing them in a few days. For this reason, these conditions were used in the following experiments, including TuMV infections.

Infection efficiency	PPV-GFP	
	Soil	<i>In vitro</i>
OD ₆₀₀ 0.5	N/A	10 %
OD ₆₀₀ 1	N/A	10 %
OD ₆₀₀ 1.5	90 %	30 %

Table 5. Infection efficiencies achieved in *A. thaliana* plants grown on soil and *in vitro* using PPV-containing agrobacterium concentrations.

Plants infected with PPV-GFP presented macroscopic disease symptoms 10 DAI, such as smaller leaves and reduced leaf turgor. At this time, infection was confirmed by the virus-derived GFP signal, which was systemically observed in the midrib and petiole of one or few leaves of infected plants. 14 DAI, symptoms

were more evident when compared to MOCK treated plants (Fig. 8 A), showing curly leaves, growth inhibition and chlorosis in some individuals (Fig. 8 B).

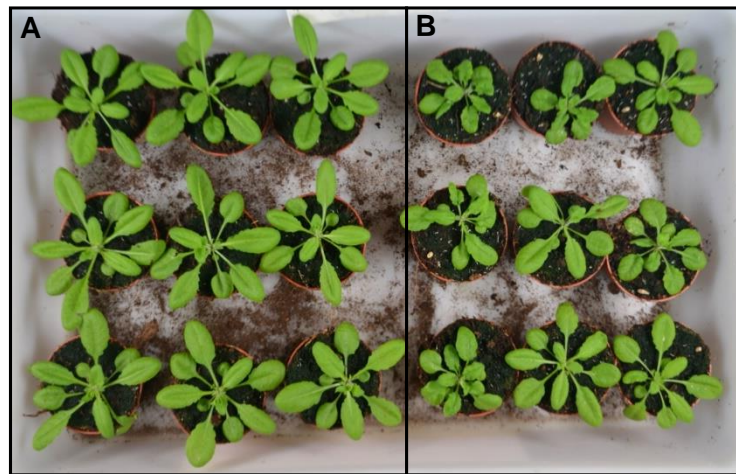


Figure 8. MOCK treated and PPV-infected Arabidopsis plants.

A. MOCK treated plants 14 DAI.

B. PPV-infected plants 14 DAI. Plants showed curly leaves, growth inhibition and chlorosis in some of them.

1.1.2 *P. SYRINGAE* INFECTION

P. syringae is one of the most common and deadly plant pathogens that infect the phyllosphere. *P. syringae* is often associated to water environments and has been found in rain and snow. Thus, it is believed that rain is an important vector for the spread of this species (Morris et al., 2007). Once over the leaves, the bacteria enter into the plant internal space through stomata. Spraying bacteria suspension over plant leaves would mimic what is happening in natural infections, in contrast to the generally performed inoculation method consisting on infiltrating a big amount of pathogen in the internal space of the leaves.

Optimal conditions for infections were determined by spraying three different *Pto* DC3000 concentrations in *A. thaliana* WT plants grown on soil (Table 6). OD₆₀₀ 0.4 was the optimal concentration, since 95 % of the plants were infected but the effects of infections were not so intense to impede plant observation or their dead after few days.

Bacteria concentration	Infection efficiency	Symptoms observed
OD₆₀₀ 0.2	0 %	None
OD₆₀₀ 0.4	95 %	Intense at 4 DAI
OD₆₀₀ 0.8	95 %	Plant death at 4 DAI

Table 6. Infection efficiency in *A. thaliana* using different concentrations of *P. syringae*.

Macroscopic disease symptoms were readily observed at 4 DAI being more intense at to 7 DAI when compared to MOCK treated plants (Fig. 9 A). Disease symptoms included chlorosis and necrosis (Fig. 9 B). Upon confocal microscope inspection, *Pto DC3000* bacteria were localized in the intercellular space forming clusters around plasmatic membranes (apoplast) from mesophyll cells (Fig. 9 C, 9 D). Bacteria disposition around membranes is necessary to inject effectors (including BSRs) in the plant cell cytoplasm through T3SS.

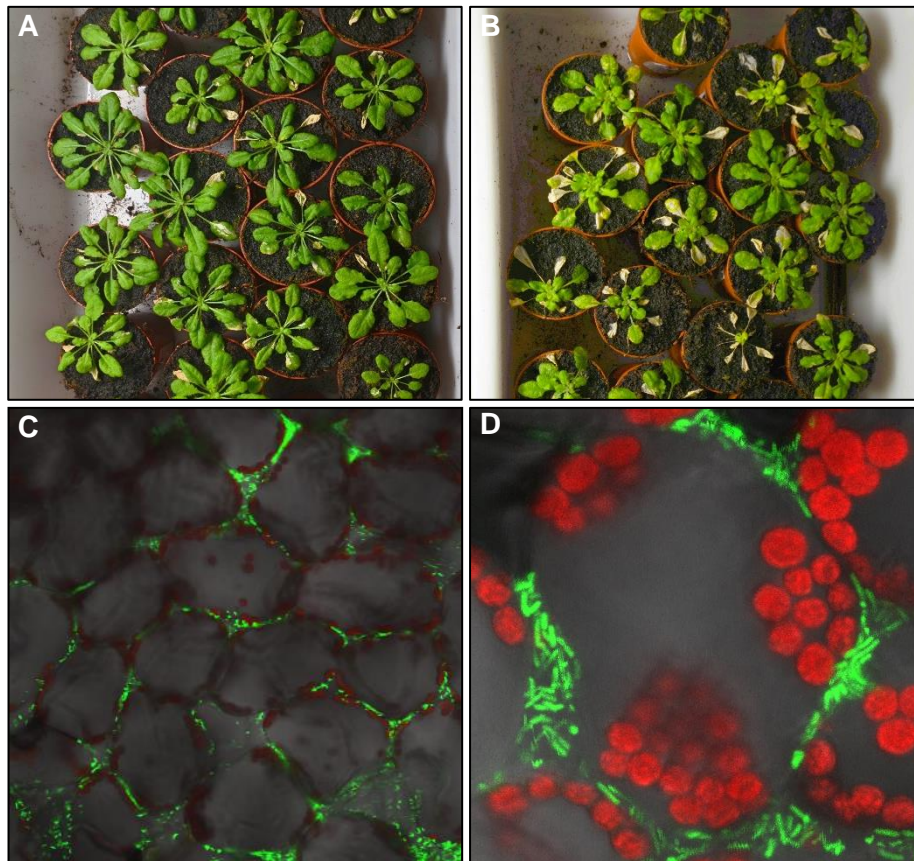


Figure 9. *Pseudomonas syringae* infection in Arabidopsis plants.

A. Representative sample of MOCK treated plants 7 days after treatment.

B. Representative sample of *Pto* DC3000-infected plants 7 DAI. Symptoms observed included chlorosis and necrosis

C. Distribution of *Pto* DC3000 (green) in the apoplast of Arabidopsis mesophyll cells (greys). Images represent Z-stacks obtained under confocal laser scanning microscope.

D. Close up view of *Pto* DC3000 (green) in the apoplast of a mesophyll cell (grey). Image represent Z-stacks obtained under confocal laser scanning microscope. Red signal corresponds to chlorophyll.

1.2 VALIDATION OF amiR REPORTER SYSTEMS

In order to establish the pattern of silencing suppression during pathogen infections, reporter plants that had previously shown to be sensitive to the lack of active miRNA-dependent silencing suppression were used. That reporter system consisted on an artificial miRNA (amiR) designed to uniquely target a luciferase gene (Firefly) (Manavella et al., 2012). Additionally, another reporter system based on the regulation of a nuclear localized mScarlet-I fluorescent protein was built following the same principle than the one applied for the amiR-LUC sensor.

Both reporter systems were validated by *Agrobacterium*-mediated transient expression in *Nicotiana Benthamiana* leaves, in the presence or absence of the VSR Hc-Pro. Leaves expressing the amiR-LUC reporter system presented higher levels of luciferase signal 3 days after infiltration when co-expressed with Hc-Pro, confirming the impairment of amiR-mediated silencing (Fig. 10 A, 10 B).

Similarly, mScarlet-I signal was higher under confocal microscopy in the nuclei from *Nicotiana* leaf cells when Hc-Pro was present (Fig. 10 C-F). Those results validated that both reporter systems are suitable to monitor the presence of pathogen-derived SSs *in planta*.

Those reporter systems were further validated in stable lines of *Arabidopsis thaliana* plants constitutively expressing the reporter systems. Plants constitutively expressing the amiR-LUC reporter system and the Hc-Pro were sprayed with luciferin solution. As shown in transient expression, the luciferase signal was lower in control plants (plants constitutively expressing amiR-LUC reporter system and an empty vector) (Fig. 11 A) when compared to plants constitutively expressing Hc-Pro along the amiR-LUC reporter system (Fig. 11 B), thus validating the amiR-LUC reporter system in *A. thaliana* plants.

Likewise, the amiR-mScarlet-I reporter system was also validated in *A. thaliana* plants constitutively expressing the amiR-mScarlet-I reporter system and Hc-Pro. While nuclei from epidermal and mesophyll cells in control plants constitutively expressing amiR-mScarlet-I reporter system and an empty vector

(Fig. 11 C, E) presented a faint mScalet-I signal, fluorescence intensity was higher when Hc-Pro was expressed (Fig. 11 D, F).

According to the results observed, we validated both reporter systems for its use in pathogen infections of *A. thaliana*.

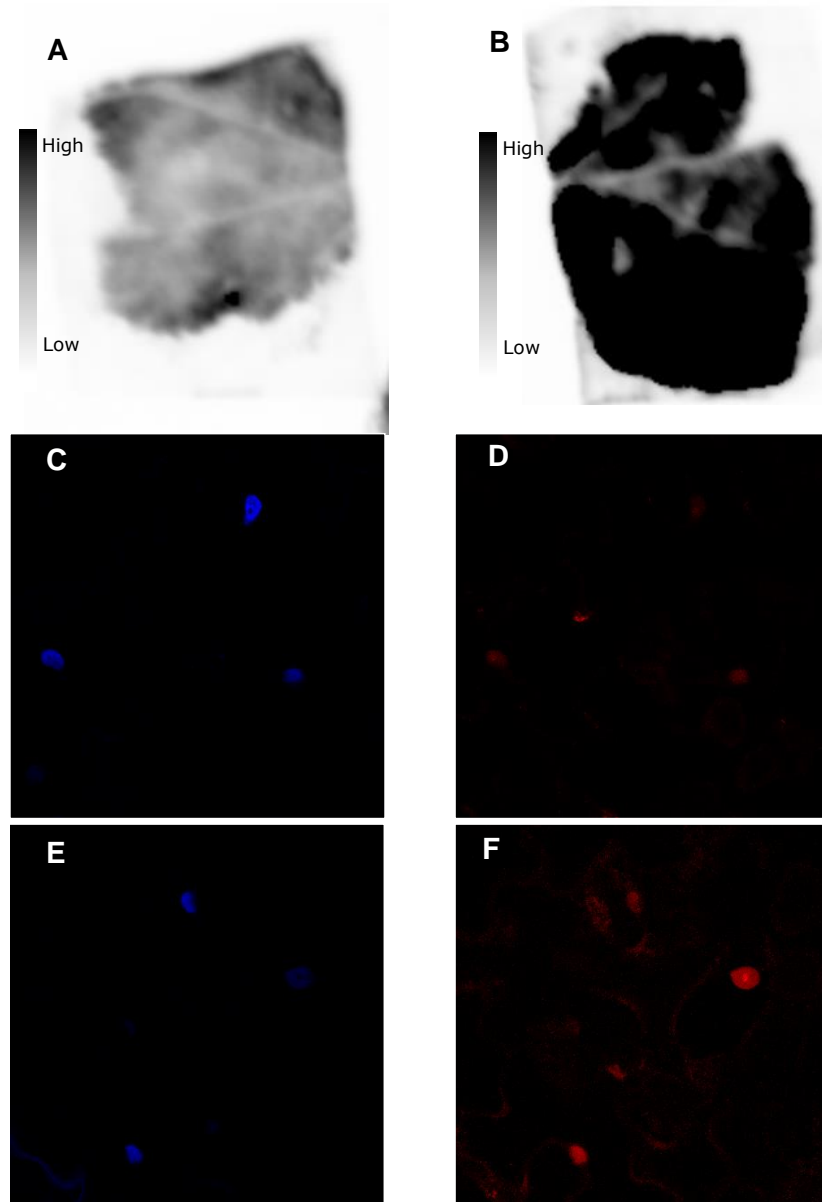


Figure 10. Validation of the reporter systems by agroinfiltration in *N. benthamiana* leaves.

A. Luciferase activity from an agroinfiltrated leaf with the amiR-Luc reporter system in the presence of a construct constitutively expressing GUS. Luciferin solution was applied 5 minutes before imaging. Exposure time: 10 min.

B. Luciferase activity from an agroinfiltrated leaf with the amiR-Luc reporter system together with p35s::Hc-Pro. Luciferase signal was higher than in **A** due to the presence of the VSR. Luciferin solution was applied 5 minutes before imaging. Exposure time: 10 min

C. Confocal laser scanning microscopy images showing DAPI-dyed nuclei (blue) from an agroinfiltrated leaf with the amiR-mScarlet-I reporter system in the presence of a construct constitutively expressing GUS. Image shows UV channel.

D. Same as C but showing mScarlet-I channel. Red signal corresponds to leaf cell nuclei.

E. Confocal laser scanning microscopy images showing leaf cell nuclei (blue) from an agroinfiltrated leaf with the amiR-mScarlet-I reporter system together with p35s::Hc-Pro. Leaf was DAPI-dyed before imaging. Image shows UV channel.

F. Same as C but showing mScarlet-I channel. Red signal corresponds to leaf cell nuclei. Fluorescence signal is higher than in D, due to the presence of the VSR.

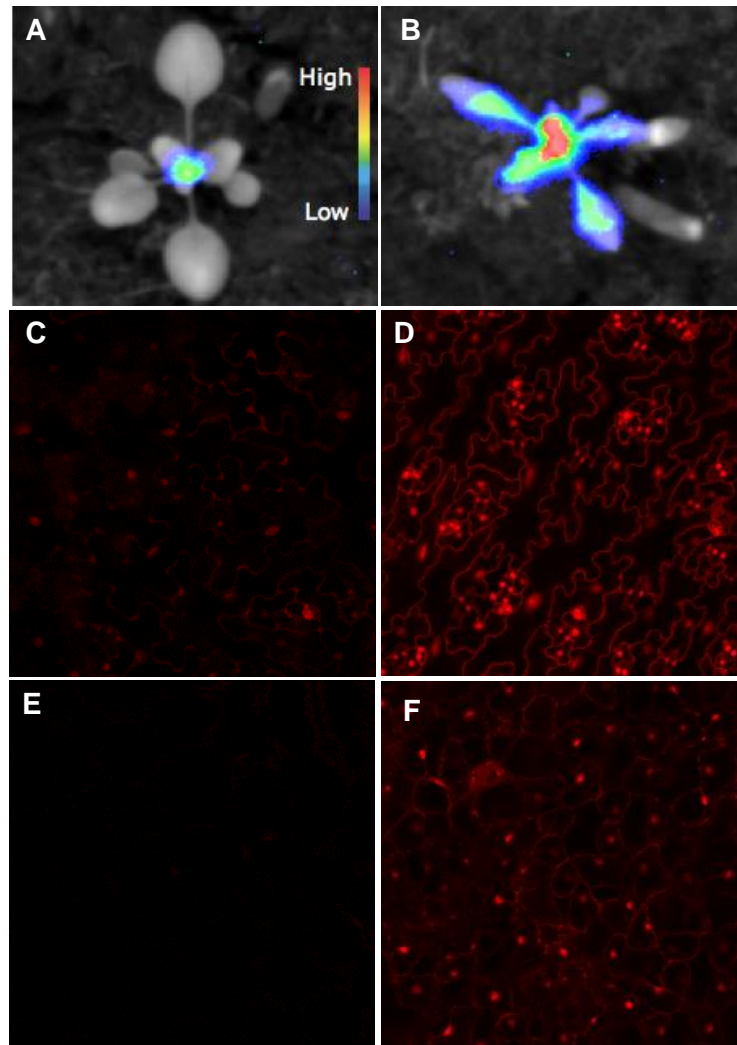


Figure 11. Validation of the reporter systems in *A. thaliana* plants.

A. Luciferase activity from a plant constitutively expressing the amiR-Luc reporter system and an empty vector. Luciferin solution was applied 5 minutes before imaging. Exposure time: 10 min.

B. Luciferase activity from a plant constitutively expressing the amiR-Luc reporter system and p35s::Hc-Pro. Luciferase signal was higher than in **A**, due to the presence of the VSR. Luciferin solution was applied 5 minutes before imaging. Exposure time: 10 min.

C. Confocal laser scanning microscopy image showing nuclei from epidermal cells (red) in a plant constitutively expressing the amiR-mScarlet-I reporter system and an empty vector. Image shows mScarlet-I channel.

D. Confocal laser scanning microscopy image showing nuclei from epidermal cells (red) in a plant constitutively expressing the amiR-mScarlet-I reporter system and p35s::Hc-Pro. The fluorescence signal was higher and more intense than in **C**, validating the system in epidermal cells of *A. thaliana* plants. Image shows mScarlet-I channel.

E. Confocal laser scanning microscopy image showing mesophyll cell nuclei (red) from amiR-mScarlet-I reporter plants crossed to empty vector plants. Image shows mScarlet-I channel.

F. Confocal laser scanning microscopy image showing mesophyll cell nuclei (red) from a plant constitutively expressing the amiR-mScarlet-I reporter system and p35s::Hc-Pro. The fluorescence signal was higher and more intense than in **E**, validating the system in mesophyll cells from *A. thaliana* plants. Image shows mScarlet-I channel

1.3 RNA SILENCING MACHINERY IS DISMANTLED IN MESOPHYLL AND VASCULAR BUNDLES UPON VIRUS INFECTION

In order to establish the spatiotemporal pattern of viral infections and the dynamics of the synthesis and delivery of SSs, *Arabidopsis* plants carrying the luciferase reporter system were grown on soil under SD conditions and infected with PPV and TuMV-containing agrobacterium OD_{600} 1.5 10 days after germination.

PPV and TuMV encode in their genome, the Hc-Pro VSR, which is able to interfere with miRNA action. After luciferin spraying, MOCK treated plants showed basal luminescence signal (Fig. 12 A) while several leaves from PPV-infected plants showed stronger luminescence in the vascular bundles 14 DAI (Fig. 12 B), due to the impairment of amiR-mediated silencing. This observation correlated with the absence (Fig. 12 E) or presence (Fig. 12 F) of PPV-GFP. Those results suggested that the production of VSRs is constitutive and intrinsic to the virus presence.

The amiR-LUC reporter system is very instructive to establish the temporal pattern of pathogen infection and to determine the spatial pattern at a whole plant

or tissue level. On the other hand, amiR-mScarlet-I reporter system is more suited to finely define the cell-types targeted by pathogens. In order to determine the cell-types targeted by PPV, 10-days-old *Arabidopsis* plants carrying the amiR-mScarlet-I reporter system grown on soil under SD conditions were infected with PPV-containing agrobacterium OD₆₀₀ 1.5. As shown in figure 13, the virus was present in vascular cells (Fig. 13 A, B) but also in mesophyll cells (Fig. 13 C, D), in which 14 DAI an activation of the fluorescence signal was observed (Fig. 13 E-G).

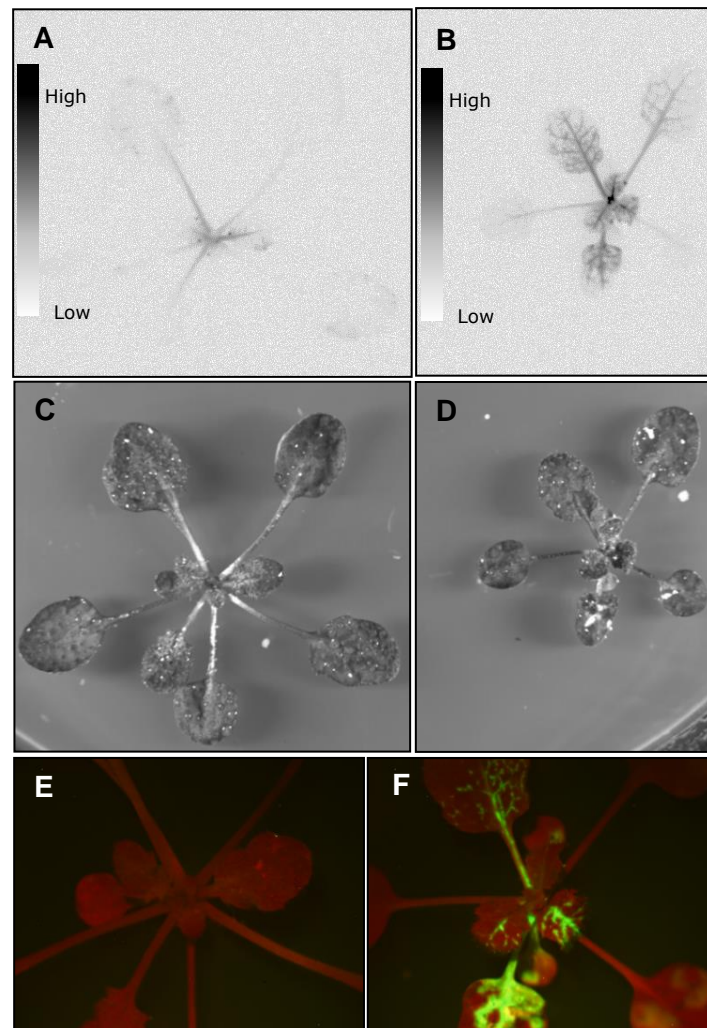


Figure 12. PPV-infected *Arabidopsis* plants carrying the amiR-LUC reporter system 14 DAI.

A. Luciferase activity assayed in a MOCK treated plant. Luciferin solution was applied 5 minutes before imaging. Exposure time: 10 min.

B. Luciferase activity from an infected plant. Plants showed stronger luminescence in the vascular tissues and mesophyll cells compared to non-infected plants. Luciferin solution was applied 5 minutes before imaging. Exposure time: 10 min.

C. Bright field picture of the plant used in luciferase activity assay in A.

D. Bright field picture of the plant used in luciferase activity assay in B.

E. MOCK treated plant imaged 14 DAI under a magnifying glass attached to a UV-light source. Red signal corresponds to chlorophyll fluorescence.

F. Spreading pattern of PPV in a PPV-infected plant, imaged 14 DAI under a magnifying glass attached to a UV-light source. PPV colonized the whole vasculature of the plant. Green signal corresponds to PPV-derived GFP fluorescence, while red signal corresponds to chlorophyll fluorescence

Plants were grown on soil, but for a better visualization of the luciferase activity, plants were cut by the stem and placed in a plate.

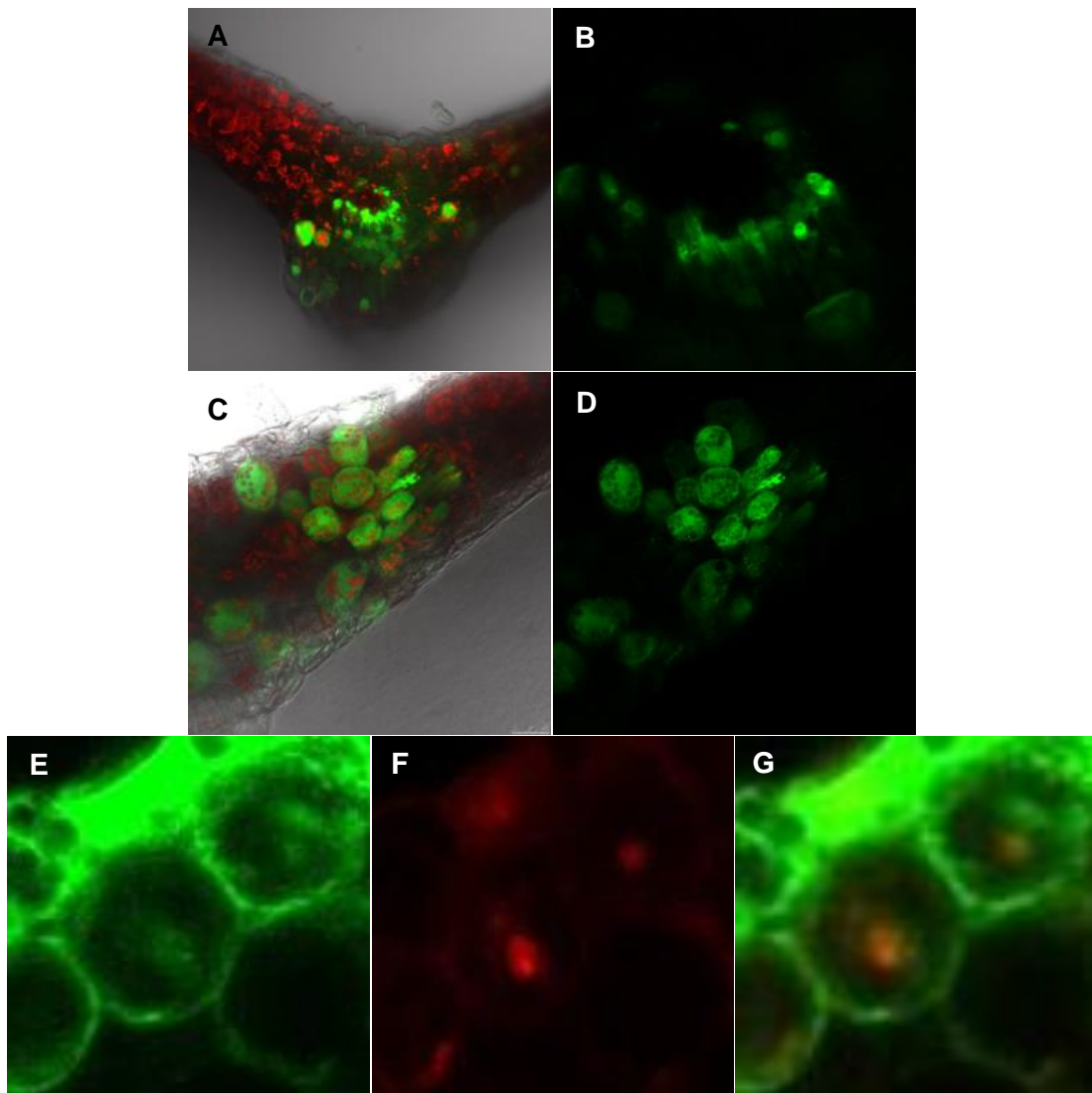


Figure 13. PPV-infected Arabidopsis plants carrying amiR-mScarlet-I reporter

- A.** Confocal laser scanning microscopy image showing GFP-PPV (green) and chlorophyll (red) in transversal sections of an infected leaf. The virus was observed in the vasculature cells.
- B.** Close up from **A** to highlight the vascular bundles. Image shows GFP channel.
- C.** Confocal laser scanning microscopy image showing GFP-PPV (green) and chlorophyll (red) in transversal sections of an infected leaf. The virus was additionally detected in mesophyll cells.
- D.** Same as C but showing GFP channel.
- E.** Confocal laser scanning microscopy images showing GFP-PPV (green) in mesophyll cells. Image show GFP channel.
- F.** Same as E but showing mScarlet-I channel. The image shows nuclei (red) from mesophyll cells. PPV presence led to the activation of mScarlet-I fluorescent signal in mesophyll cell nuclei.

1.4 RNA SILENCING MACHINERY IS DISMANTLED IN MESOPHYLL UPON BACTERIAL INFECTION

In order to determine the spatiotemporal pattern of *P. syringae* infection and to determine the effects of its BSRs delivery, 10 Arabidopsis plants carrying the amiR-LUC reporter system and 10 Arabidopsis plants carrying the amiR-mScarlet-I reporter system were grown on soil during 4-5 weeks under SD conditions and infected with a *Pto* DC3000 strain. Additionally, a mutant *Pto* DC3000 strain defective on the T3SS (*P. syringae* hrcC⁻) was included in the assays as negative control.

Pto DC3000 expresses different effectors during plant infection. Among them, AvrPtoB and HopT1-1 work as BSRs. AmiR-LUC reporter plants infected with *Pto* DC3000 strain showed a spotted pattern when assayed for luciferase activity at 3 DAI (Fig. 14 B). That pattern was absent in MOCK treated (Fig. 14 A) and *Pto* DC3000 hrcC⁻ strain infected plants (Fig. 14 C). That signal correlated with the presence of *Pto* DC3000 and its ability to deploy effectors. On the other hand, bacteria were not found under microscopy inspection of large areas lacking luciferase activity from infected plants with both *Pto* DC3000 strains or MOCK

treated plants. Additionally, in areas showing basal luciferase activity in MOCK treated and in plants infected with *Pto* DC3000 HrcC⁻ strain, bacteria were not present.

Nuclei from mesophyll cells showed an increase in fluorescence in amiR-mScarlet-I reporter plants infected with *Pto* DC3000 strain at 3 DAI (Fig. 14 H, K, N) compared to those from MOCK treated (Fig. 14 G, J, M) or plants infected with *Pto* DC3000 hrcC⁻ strain (Fig. 14 I, L, O), due to the amiR dysfunction. Again, this increase in fluorescent signal correlated with the presence of the bacteria and its ability to deploy effectors.

These results together, show that mesophyll cells are preferentially targeted by *Pto* DC3000 for BSRs deployment and that this is T3SS-dependent.

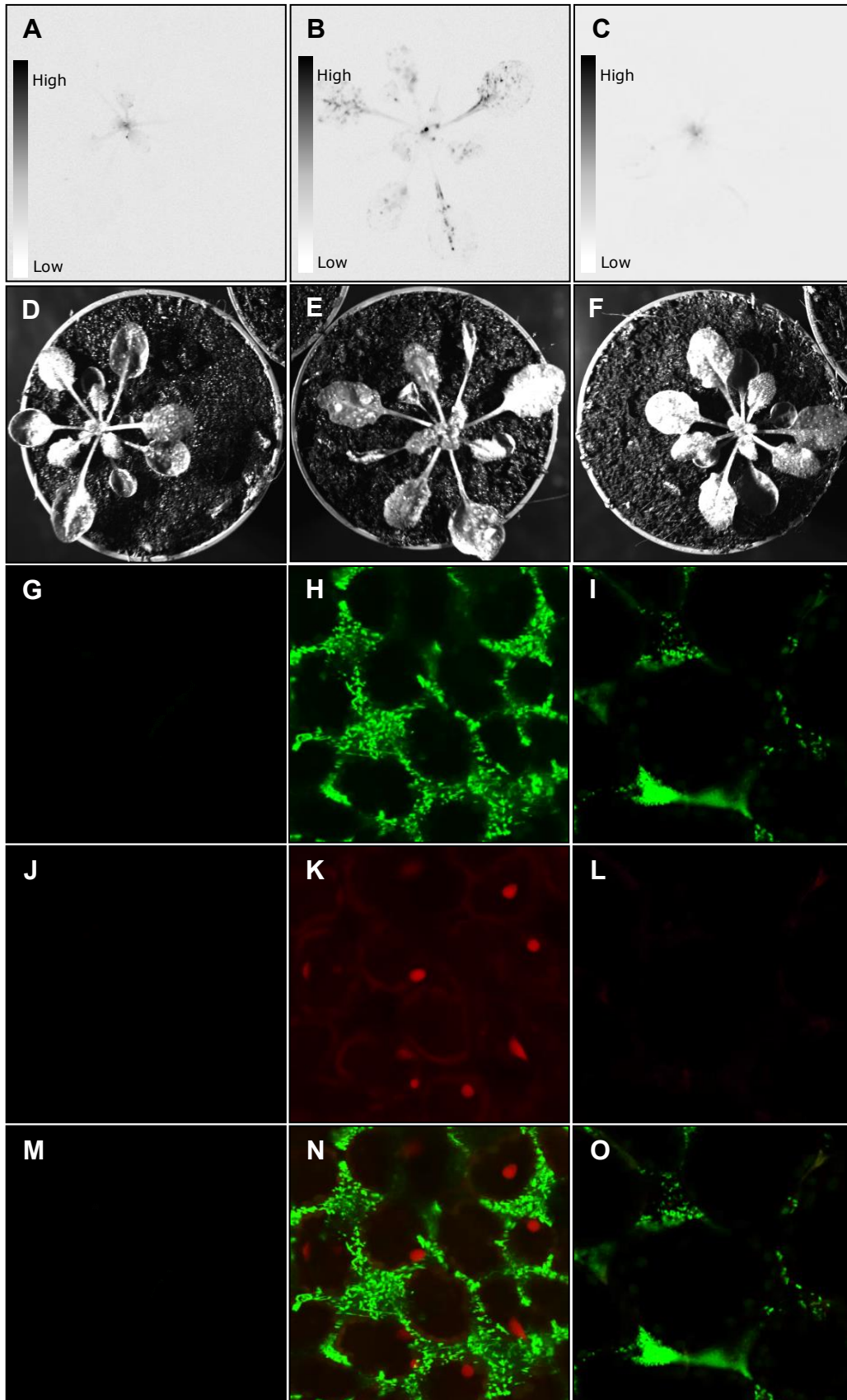


Figure 14. *Pseudomonas syringae* infection of Arabidopsis plants carrying the amiR reporter systems 3 DAI.

- A.** Luciferase activity from a MOCK treated plant. Luciferin solution was applied 5 minutes before imaging. Exposure time: 10 min.
- B.** Luciferase activity from an amiR-Luc reporter plant infected with *Pto* DC3000 strain. Luciferin solution was applied 5 minutes before imaging. Exposure time: 10 min.
- C.** Luciferase activity from an amiR-LUC reporter plant infected with *Pto* DC3000 hrcC⁻ strain. Similar luciferase signal was observed as in MOCK treated plants, due to its incapability to inject effectors. Luciferin solution was applied 5 minutes before image. Exposure time: 10 min.
- D.** Bright field image of the plant used in the luciferase activity assay in A.
- E.** Bright field image of the plant used in the luciferase activity assay in B.
- F.** Bright field image of the plant used in the luciferase activity assay in C.
- G.** Confocal laser scanning microscopy image showing a MOCK treated leaf from an amiR-mScarlet-I reporter plant. Image represents Z-stacks, showing GFP (green) channel.
- H.** Confocal laser scanning microscopy image showing an amiR-mScarlet-I reporter plant infected with *Pto* DC3000 strain. Bacteria were localized forming clusters around mesophyll cells. Image represents Z-stacks, showing GFP (green) channel.
- I.** Confocal laser scanning microscopy image showing an amiR-Scarlet-I reporter plant infected with *Pto* DC3000 HrcC⁻ strain. Bacteria were present forming groups around mesophyll cells. Image represent Z-stacks, showing GFP (green) channel.
- J.** Same as G but showing mScarlet-I (red) channel. Images represent Z-stacks.
- K.** Same as H but showing mScarlet-I (red) channel. Mesophyll nucleus (red). Images represent Z-stacks.
- L.** Same as H but showing mScarlet-I (red) channel. Images represent Z-stacks.
- M.** G, J merged channels.
- N.** H, K merged channels. mScarlet-I red signal increased only when *Pto* DC3000 was present (N compared to M) and just when the bacteria was able to inject the effectors through the T3SS (N compared to O).
- O.** I, L merged channels.

1.5 ASSAYING CELL-TYPE SPECIFICITY OF OOMYCETE-TRIGGERED SILENCING SUPPRESSION

The oomycete genus *Phytophthora* encompasses *Phytophthora* species which are able to synthesize cytoplasmic effectors working as SSs. These species include *P. sojae* which deploys PSR1 and PSR2 SSs and their orthologues in *P. parasitica* and *P. infestans*: PpPSR1L, PpPSR2, PiPSR1L and PiPSR2 (Qiao et al., 2013, 2015; Vries et al., 2017; Xiong et al., 2014). Additionally, *P. infestans* have at least another effector which also suppresses RNA silencing, Pi14054 (Vetukuri et al., 2017).

In order to determine whether the oomycete *P. Palmivora* produced specialized effectors affecting host-silencing machinery, amiR-mScarlet-I reporter plants were infected with an YFP-labelled strain of this plant pathogen. Thus, the use of a fluorescently labelled strain allowed us to determine the spatiotemporal pattern of *P. Palmivora* infection.

P. palmivora is a ubiquitous plant pathogen able to infect a wide range of hosts. During its life cycle, *P. palmivora* is able to form swimming zoospores from sporangia in wet soils or in water films on plant surfaces of plants to later spread by the action of water and wind. Released zoospores move across non-infected plant tissue and infect the plant through the production of a germ tube called appressoria. According to that, in order to mimic natural conditions, oomycete infections were performed by flooding plant seedlings with the solution containing zoospores, for both roots and leaves infections.

Root infection assays using amiR-mScarlet-I reporter plants, showed that cell viability was extremely affected in those areas showing a high concentration of oomycetes 24 hours after infection (Fig. 15 A, B, C). Accordingly, the detection of fluorescent nuclei under confocal microscopy was also compromised (Fig. 15 C). On the other hand, in those areas where a single oomycete was present (Fig. 15 D, E), no changes in the fluorescent signal were detected when comparing to MOCK treated plants (Fig 15 F).

Leaves from plants constitutively expressing mScarlet-I in cell nuclei but lacking the amiR (control plants), were used to evaluate the change of mScarlet-

I expression and infected along with amiR-mScarlet-I reporter plants. MOCK treated (Fig. 16 A) and infected amiR-mScarlet-I reporter plants (Fig. 16 B, C) displayed equivalent levels of fluorescent signals 24 hours after infection. Likewise, MOCK treated (Fig. 16 A) and infected amiR-mScarlet-I reporter plants (Fig. 16 B, C), displayed lower levels of fluorescent signals than MOCK treated control plants (Fig. 16 D) and infected control plants (Fig. 16 E, F), due to amiR regulation was not interrupted.

These preliminary results indicated that in both root and leaves infections, *P. palmivora* was not expressing any SS at the time the plants were observed, either because it lacks them or because the infection conditions were not the adequate for its detection.

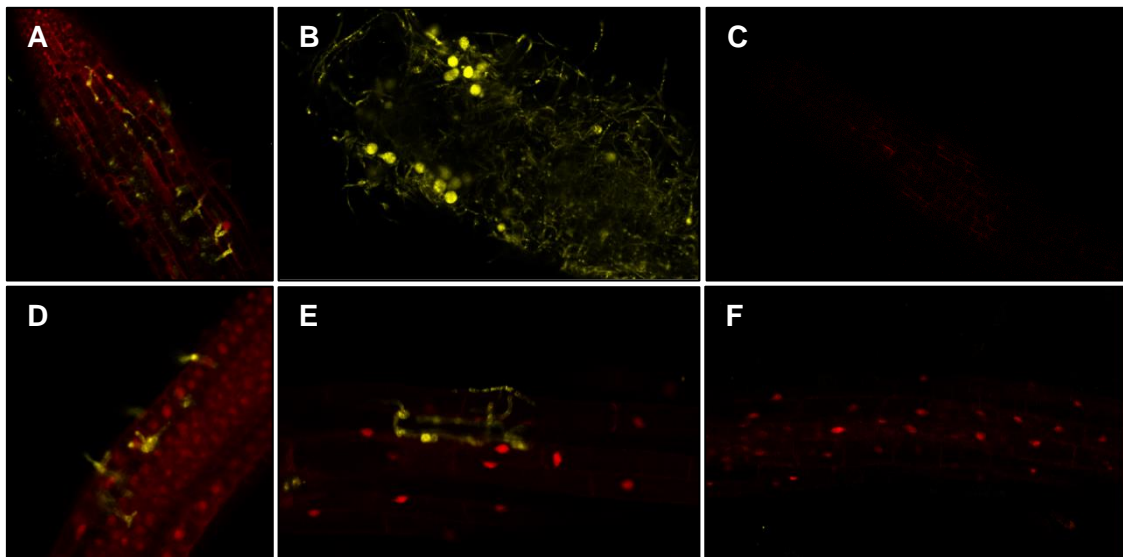


Figure 15. *Phytophthora palmivora* infection of amiR-mScarlet-I reporter plant roots 24 hours after infection.

A. Confocal laser scanning microscopy image showing an infection area of a root with a high concentration of *P. palmivora* (yellow). Red signal corresponds to mScarlet-I fluorescence signal. Image show YFP (yellow) channel and mScarlet-I (red) merged channels.

B. Confocal laser scanning microscopy image showing an infection area of a root with a high concentration of *P. palmivora* (yellow). Image show YFP (yellow) channel.

C. Same as B but showing mScarlet-I (red) channel. No nuclei were detected.

D. Confocal laser scanning microscopy image showing individual *P. palmivora* (yellow) infecting a root. Red signal corresponds to mScarlet-I fluorescence. Image show YFP (yellow) and mScarlet-I merged channels.

E. Confocal laser scanning microscopy image showing nucleus (red) of cell roots from plants infected with individual *P. palmivora* (yellow). Image show YFP (yellow) channel and mScarlet-I (red) merged channels.

F. Confocal laser scanning microscopy image showing nucleus (red) of cell roots from a MOCK treated plant. Nuclei showed same fluorescence signal as E. Image show YFP (yellow) channel and mScarlet-I (red) merged channels.

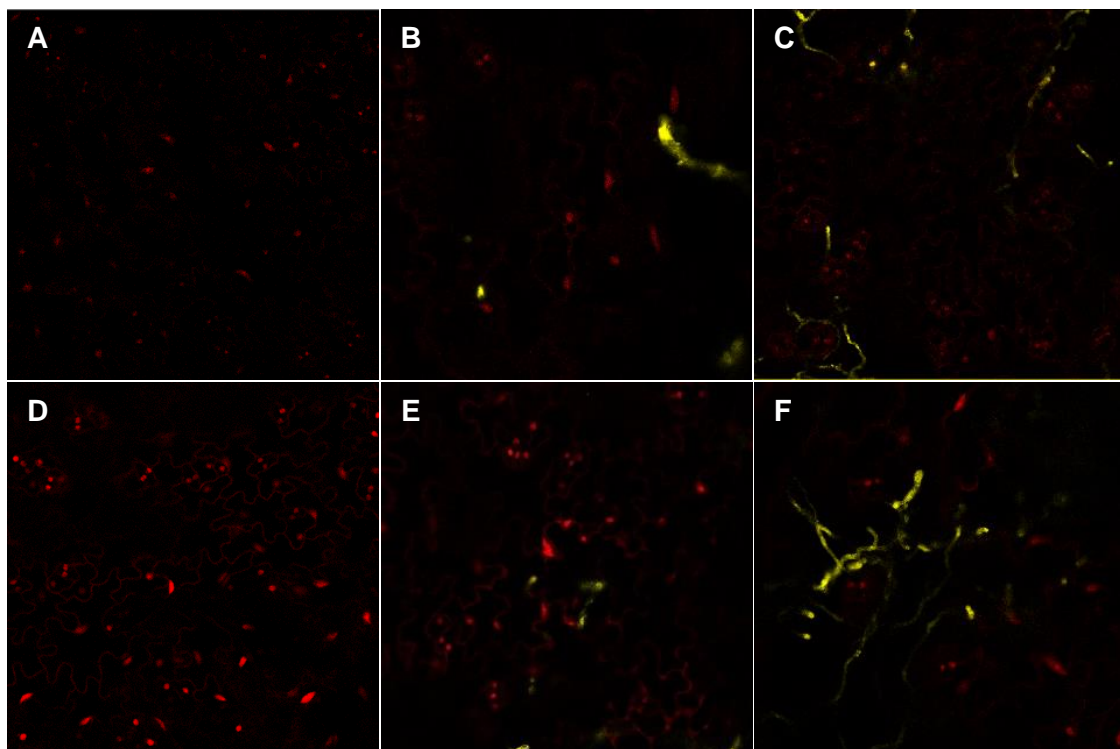


Figure 16. *Phytophthora palmivora* infection of leaves from (A, B, C) amiR-mScarlet-I reporter plants and (D, E, F) plants constitutively expressing mScarlet-I in cell nuclei but lacking the amiR (control plants), 24 hours after infection

A. Confocal laser scanning microscopy image showing leaf cell nucleus (red) of a MOCK treated mScarlet-I reporter plant. Image show mScarlet-I (red) channel

B. Confocal laser scanning microscopy image showing leaf cell nucleus of an infected mScarlet-I reporter plant. Individual *P. Palmivora* (yellow) were located on epidermis cells entering inside them. Image show YFP (yellow) channel and mScarlet-I (red) merged channels.

C. Confocal laser scanning microscopy image showing the leaf surface of an infected mScarlet-I reporter plant. Oomycetes (yellow) were present on the epidermis cells. Image show YFP (yellow) channel and mScarlet-I (red) merged channels.

D. Confocal laser scanning microscopy image showing leaf cell nucleus (red) of a MOCK treated control plant. Image show mScarlet-I (red) channel.

E. Confocal laser scanning microscopy image showing leaf cell nucleus (red) of an infected control plant. Individual *P. palmivora* (yellow) are located on epidermis cells, entering inside it. Image show YFP (yellow) channel and mScarlet-I (red) merged channels.

F. Confocal laser scanning microscopy image showing the leaf surface of an infected control plant. Mycelia from oomycetes (yellow) were present on epidermis cells. Image show YFP (yellow) channel and mScarlet-I (red) merged channels.

2. HOST CELL TYPE-SPECIFIC REPROGRAMMING IS TRIGGERED BY EFFECTORS WORKING AS SSs AGAINST THE RNA SILENCING MACHINERY

Among the different strategies employed by pathogens to colonize their hosts, the dismantling of host RNA silencing pathway by pathogen effectors working as SSs, is a conserved infection strategy. As shown before, pathogens may target different host cell-types for RNA silencing intervention. Since the set of sRNAs and their targets has been described to be cell-type specific, SS-triggered host cell reprogramming would potentially lead to different reprogramming outcomes. In order to determine cell-type specific responses to the presence of distinct SSs, a set of plant lines to surgically induced the expression of the different SS in different cell-types were developed using a two-components system. Those lines allowed the establishment of the temporal pattern and onset of miRNA dysfunction in each of those cell-types. On the other hand, the lines allowed the induction of SS-triggered reprogramming followed by transcriptomic assays to determine specific cellular responses.

To that end, three tasks were carried out: generation of plants conditionally expressing pathogen SSs, monitor the kinetics of inactivation of amiR function in amiR-mScarlet-I reporter plants and characterization of their transcriptome changes.

2.1 GENERATION OF PLANTS CONDITIONALLY EXPRESSING PATHOGEN SSs

In order to accomplish the desired spatiotemporal action of the SS Hc-Pro from TuMV and HopT1-1 from *Pto* DC3000 in the leaf cell-types in which natural infection events dismantle host RNA silencing machinery, promoters from marker genes for the cell-types of interest were combined with an inducible system of their expression, using the versatile modular GG system. The induction strategy was based on a two-component system approach (Schürholz et al., 2018). Within the two components, the first of the gene constructs was dedicated to define the

cellular niches where the system will be expressed, while the second one was devoted to induce the expression of the SSs upon stimuli application.

Niche-specific expression was achieved by searching in the literature (Cui et al., 2014; Ranjan et al., 2011; Sawchuk et al., 2008; Serna et al., 1997; Takahashi et al., 2000; Ursache et al., 2018) for promoters whose expression in leaves coincide with the different cell types where sRNA machinery was impaired during pathogen infection in the assays described in Objective 1. A collection of promoters was isolated and validated through its fusion to the GUS gene-coding region. GUS is the acronym for β -Glucuronidase, a gene from *Escherichia coli* that encodes a Glucuronidase, a sugar-consuming enzyme. Upon the presence of X-Gluc, the enzyme gives an insoluble indigo-blue precipitate at the site of GUS activity. GUS staining was performed in transgenic plants at different developmental stages, carrying the promoter sequences driving the GUS reporter gene and the promoter expression patterns were reflected by the activation of GUS (Fig. 17).

pCAB3, pSUC2 and pSultr2;2 were selected to generate the transgenic lines constitutively expressing the SSs, since as shown in Fig. 17, they drove gene expression to mesophyll, phloem companion and bundle sheath cells, the cellular domains where pathogens were found to interfere with RNA silencing in Objective 1.

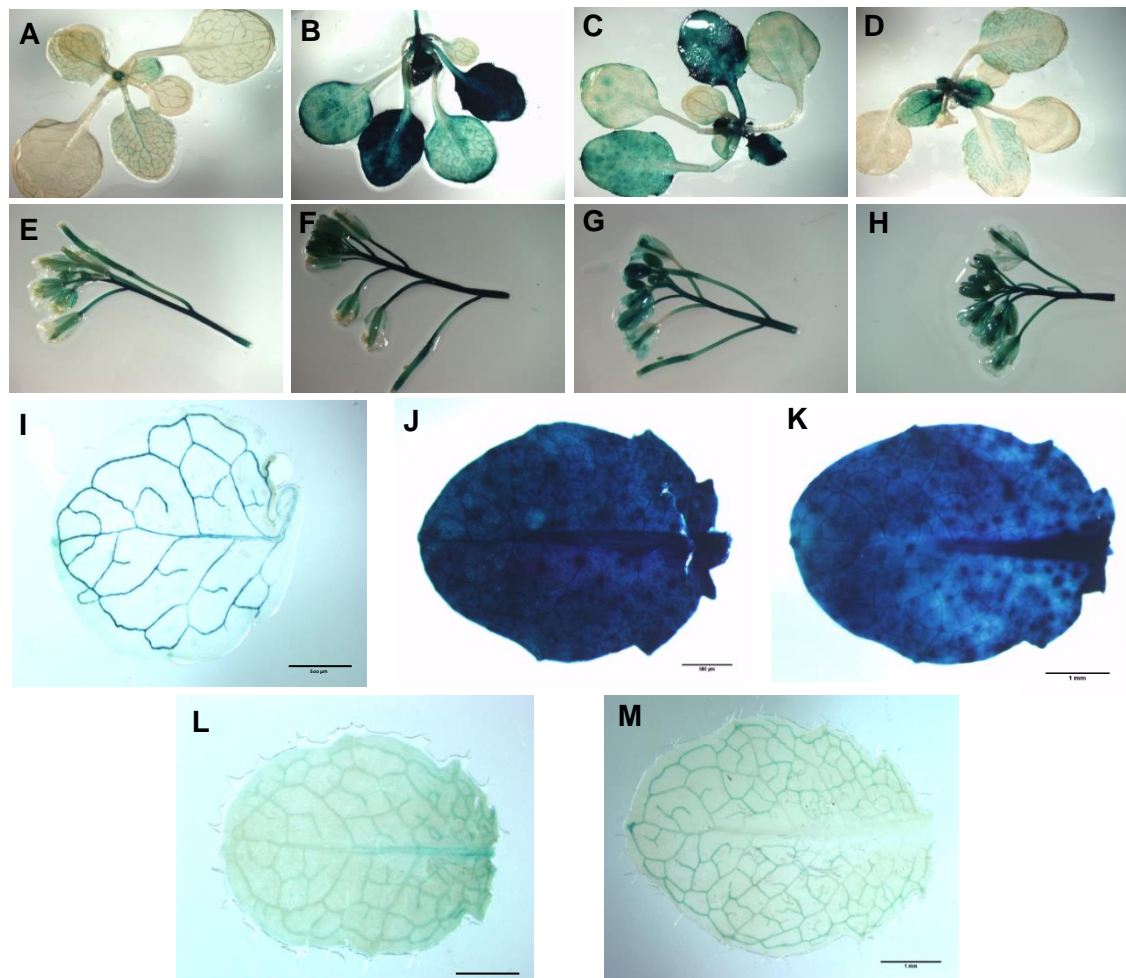


Figure 17. Expression of GUS reporter gene under the control of the selected promoters in transgenic Arabidopsis plants.

A, E, I. Expression of pSUC2::GUS in seedling (A), inflorescence (E) and leaf (I) in transgenic Arabidopsis plants.

B, F, J. Expression of pCAB3::GUS in seedling (B), inflorescence (F) and leaf (J) in transgenic Arabidopsis plants.

C, G. Expression of pCER6::GUS in seedling (C) and inflorescences (G) in transgenic Arabidopsis plants.

D, H. Expression of pCDC2A::GUS in seedling (D) and inflorescences (H) in transgenic Arabidopsis plants.

K. Expression of pRBCS1A::GUS in leaf in transgenic Arabidopsis plants.

L. Expression of pSCR::GUS in leaf in transgenic Arabidopsis plants.

M. Expression of pSultr2;2::GUS in leaf in transgenic Arabidopsis plants.

X-Gluc was used for histochemical staining to monitor GUS activity. Images were obtained under a magnifying glass attached to a bright-light source. Scale bar: I,J 500µm; K,L,M 1nm

The selected promoters drove the cell-type specific expression of a two-component system that triggered the expression of the SSs when activated by dexamethasone (DEX) application. That system relies on cell specific expression of a chimeric artificial TF GR-LhG4 that specifically recognizes pOp motifs within a synthetic promoter triggering the expression of the coding sequences under pOp control (Craft et al., 2005). In the first component of the gene constructs used to generate the transgenic plants, cell type-specific expression of the LhG4 synthetic transcription factor translationally fused to the ligand-binding domain of a rat glucocorticoid receptor (GR), was driven by CAB3, SUC2 and Sultr2;2 promoters. mScarlet-I, Hc-Pro and HopT1-1 SSs were cloned under the regulation of the pOp promoter in the second component. In absence of DEX, the GR domain sequesters the LhG4 trigger in the cytoplasm. Upon DEX treatment, LhG4 is translocated within the nucleus, binds to the pOp sequences and triggers the expression of the SSs.

In order to validate the two-component system and establish the conditions for the DEX treatment, plants carrying the two-component system in specific cell-types but bearing the mScarlet-I sequence instead of the SSs were treated with 10µM DEX. 24 hours after induction (HAI), plants carrying the pCAB3::GR-LhG4-pOp::NLS-mScarlet-I construct showed an activation of the fluorescence signal in mesophyll cells (Fig. 18 A) while in epidermal cells no fluorescence was detected (Fig. 18 B). That indicated the correct induction of the system in mesophyll cells, in which pathogens were found to interfere with host RNA silencing during natural infections (Fig. 13 C-G, Fig. 14 N, O).

In plants carrying the pSUC2::GR-LhG4-pOp::NLS-mScarlet-I and pSultr2;2::GR-LhG4-pOp::NLS-mScarlet-I constructs, 48 HAI were needed to observe an effect on the fluorescent signal. mScarlet signal was intense in phloem companion (Fig. 18 C, D) and bundle sheath cells (Fig. 18 E, F). Those

were the same cell-types where the virus was found to suppress host silencing in natural infections, besides mesophyll cells (Fig. 13 A, B, 18 D, F).

Once established the conditions for the DEX treatment, two different plant lines conditionally expressing the SSs in each specific cell-types, were treated with DEX. In order to select lines with no basal expression of the different transgenes but highly responsive to DEX treatment, the expression of Hc-Pro and HopT1-1 was assayed by qPCR. DEX and MOCK treated plants were collected 24 HAI for plants conditionally expressing Hc-Pro and HopT1-1 in mesophyll (Fig. 19 A, B) and 48 HAI for plants conditionally expressing Hc-Pro in vasculature (Fig. 19 C, D). After RNA isolation, cDNA synthesis and qPCR assays, lines showing the best induction and lowest background expression (shown in green in Figure 19), were selected for further experiments.

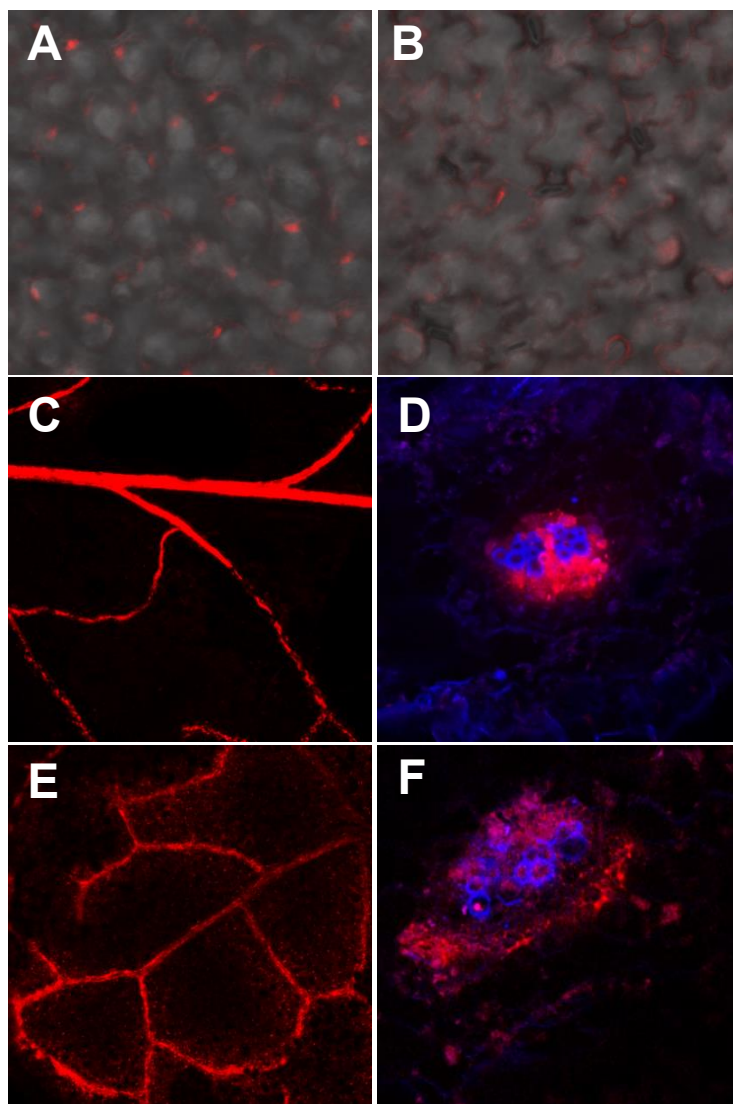


Figure 18. Plants conditionally expressing the mScarlet-I fluorescent protein in specific cell-types upon DEX treatment.

A. Mesophyll cells (grey) from a plant carrying the pCAB3::GR-LhG4-pOp::NLS-mScarlet-I construct 24 HAI. mScarlet-I induction was detected in nuclei from mesophyll cells. The image was obtained under confocal laser scanning microscope showing mScarlet-I and BF channels merged.

B. Epidermal cells (grey) from a plant carrying the pCAB3::GR-LhG4-pOp::NLS-mScarlet-I construct 24 HAI. No mScarlet-I induction was detected in epidermal cells. The image was obtained under confocal laser scanning microscope showing mScarlet-I and BF channels merged.

C. Confocal laser scanning microscopy image showing mScarlet-I fluorescent protein (red) induced in phloem companion cells at 48 HAI.

D. Transversal section of the leaf in C 48 HAI. mScarlet was located in phloem companion cells. The image was obtained under confocal laser scanning microscope showing mScarlet-I and UV channels merged.

E. Confocal laser scanning microscopy image showing mScarlet-I fluorescence (red) induced in bundle sheath cells 48 HAI.

F. Transversal section of the leaf in E 48 HAI. mScarlet-I was located in bundle sheath cells. The image was obtained under confocal laser scanning microscope showing mScarlet-I and UV channels merged.

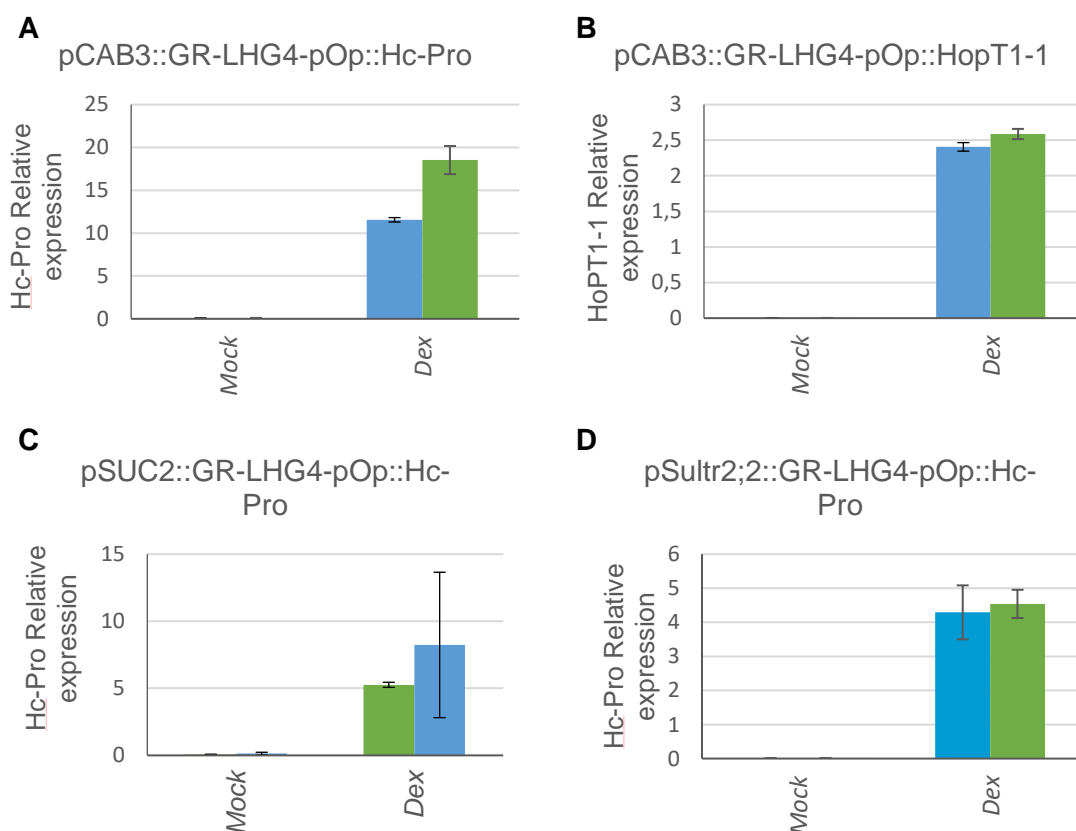


Figure 19. Relative expression levels of the SSs Hc-Pro (A, C, D) and HopT1-1 (B) in two (green/blue) homozygous T2 plant lines conditionally expressing the SSs in the specific cell-types. Images show the relative expression of SSs in non-treated (MOCK) and treated plants with DEX, 24 (A, B) and 48 (C, D) HAI. Results represent means (\pm SD) of three biological replicates.

2.2 KINETICS AND EFFICIENCY OF HOST SILENCING SUPPRESSION ARE SS-AND CELL-TYPE DEPENDENT

In order to establish the efficiency and kinetics of miRNA dysfunction due to the expression of SSs, plants conditionally expressing the different SSs in the specific cell types together with the amiR-mScarlet-I reporter system were treated with DEX and, the following days, analysed by confocal laser scanning microscopy (Fig. 20, 21). Cells where the SSs perturbed the miRNA machinery, increased the expression of mScarlet-I fluorescence due to amiR dysfunction.

MOCK treated plants presented background levels of mScarlet-I fluorescence (Fig. 20 A, B) in mesophyll cells, while an increase on that signal was readily observed 24 HAI in plants conditionally expressing the VSR Hc-Pro (Fig. 20 C, D) when compared. That increase in the fluorescence signal was more intense at 48 HAI (Fig. 20 G, H) compared to MOCK treated plants (Fig. 20 E, F).

On the other hand, in plants conditionally expressing the BSR HopT1-1 in mesophyll cells, minor changes in the fluorescent signal were detected 24 HAI (Fig. 20 K, L) compared to MOCK treated plants (Fig. 20 I, J). However, increase in the fluorescent signal was observed 48 HAI (Fig. 20 O, P) when compared to MOCK treated plants (Fig. 20 M, N). When compared to what it was observed in Hc-Pro (Fig. 20 A-H) inductions, the fluorescent signal was lower in HopT1-1 plants (Fig. 20 I-P).

Regarding to plants conditionally expressing the VSR Hc-Pro in vasculature cells, both expressing Hc-Pro in phloem companion (Fig. 21 C-D, G-H, K-L) and bundle sheath cells (Fig. 21 O-P, S-T, W-X) needed 96 HAI to show significant changes in mScarlet-I fluorescent signal, and hence, an impairment in miRNA silencing machinery, when compared with MOCK treated plants (Fig. 21 A-B, E-F, I-J for phloem companion cells and M-N, Q-R, U-V for bundle sheath cells).

Altogether, those results showed that different cell types had distinct sensitivities to silencing suppression with vascular-derived cell types being more refractory to the action of VSRs.

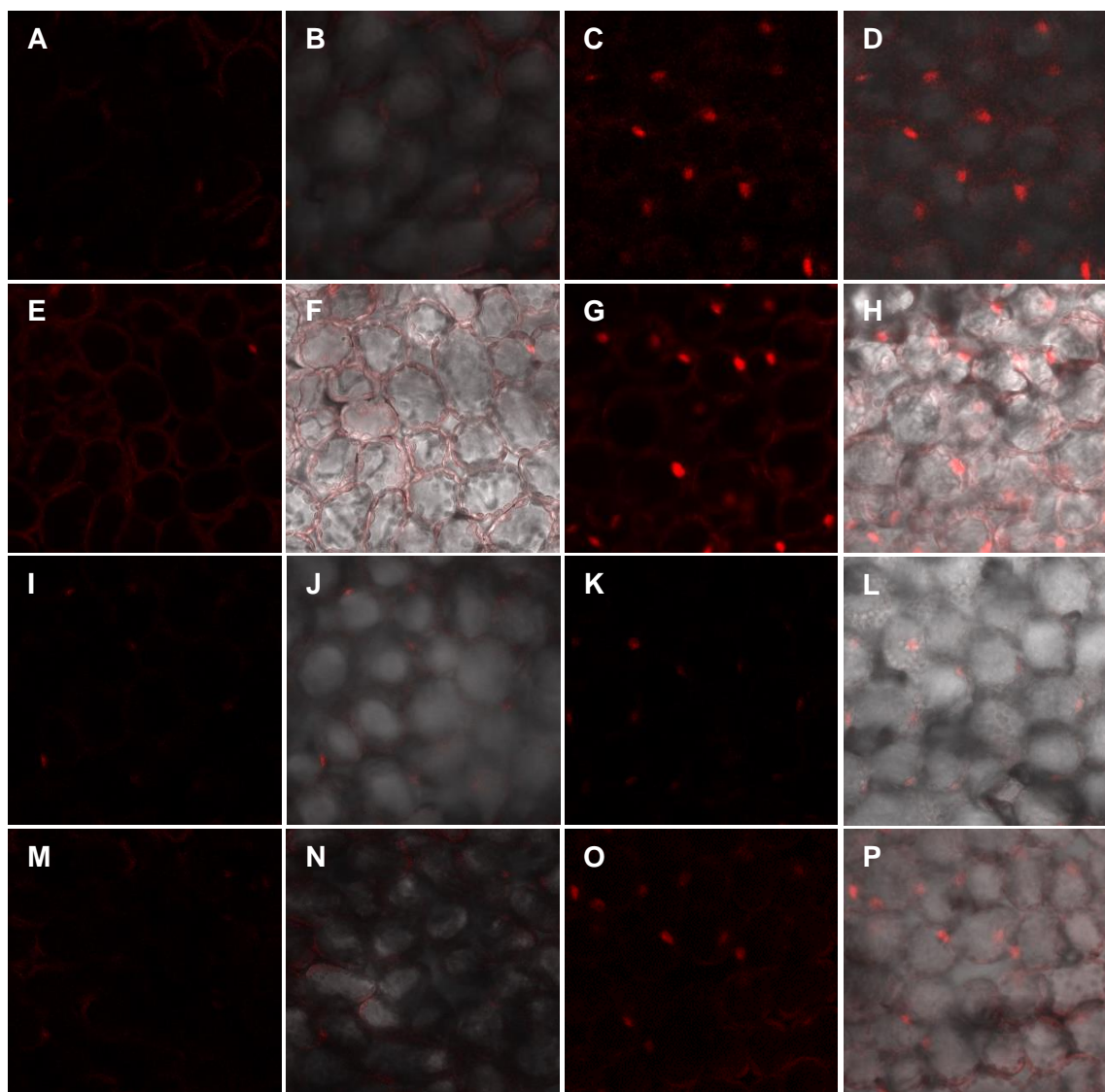


Figure 20. Time course of miRNA dysfunction in mesophyll cells from amiR-mScarlet-I reporter plants conditionally expressing SSs.

A. Confocal laser scanning microscopy image showing basal mScarlet-I fluorescence (red) in nuclei from mesophyll cells in MOCK treated plants conditionally expressing Hc-Pro 24 HAI.

B. Same as A but also showing bright field channel. Mesophyll cells are shown in grey.

C. Confocal laser scanning microscopy image showing mScarlet-I fluorescent protein (red) in nuclei from mesophyll cells in DEX treated plants conditionally expressing Hc-Pro 24 HAI. mScarlet-I fluorescence was increased compared to MOCK treated basal fluorescence.

D. C and bright field channel merged, showing mesophyll cells in grey.

E. Confocal laser scanning microscopy image showing basal mScarlet-I fluorescence (red) in nuclei from mesophyll cells in MOCK treated plants conditionally expressing Hc-Pro 48 HAI.

F. E and bright field channel merged, showing mesophyll cells in grey.

G. Confocal laser scanning microscopy image showing mScarlet-I fluorescence (red) in nuclei from mesophyll cells in DEX treated plants conditionally expressing Hc-Pro 48 HAI. mScarlet-I fluorescence was increased even more after 48 HAI.

H. G and bright field channel merged, showing mesophyll cells in grey.

I. Confocal laser scanning microscopy image showing basal mScarlet-I fluorescence (red) in nuclei from mesophyll cells in MOCK treated plants conditionally expressing HopT1-1 24 HAI.

J. I and bright field channel merged, showing mesophyll cells in grey.

K. Confocal laser scanning microscopy image showing mScarlet-I fluorescence (red) in nuclei from mesophyll cells in DEX treated plants conditionally expressing HopT1-1 24 HAI. mScarlet-I fluorescence remained at similar levels as observed in MOCK plants (I).

L. K and bright field channel merged, showing mesophyll cells in grey.

M. Confocal laser scanning microscopy image showing basal mScarlet-I fluorescence (red) in nuclei from mesophyll cells in MOCK treated plants conditionally expressing HopT1-1 48 HAI.

N. M and bright field channel merged, showing mesophyll cells in grey.

O. Confocal laser scanning microscopy image showing mScarlet-I fluorescence (red) in nuclei from mesophyll cells in DEX treated plants conditionally expressing HopT1-1 48 HAI. mScarlet-I fluorescence was increased compared with that observed in both MOCK plants (M) and treated plants 24 HAI (K).

P. O and bright field channel merged, showing mesophyll cells in grey.

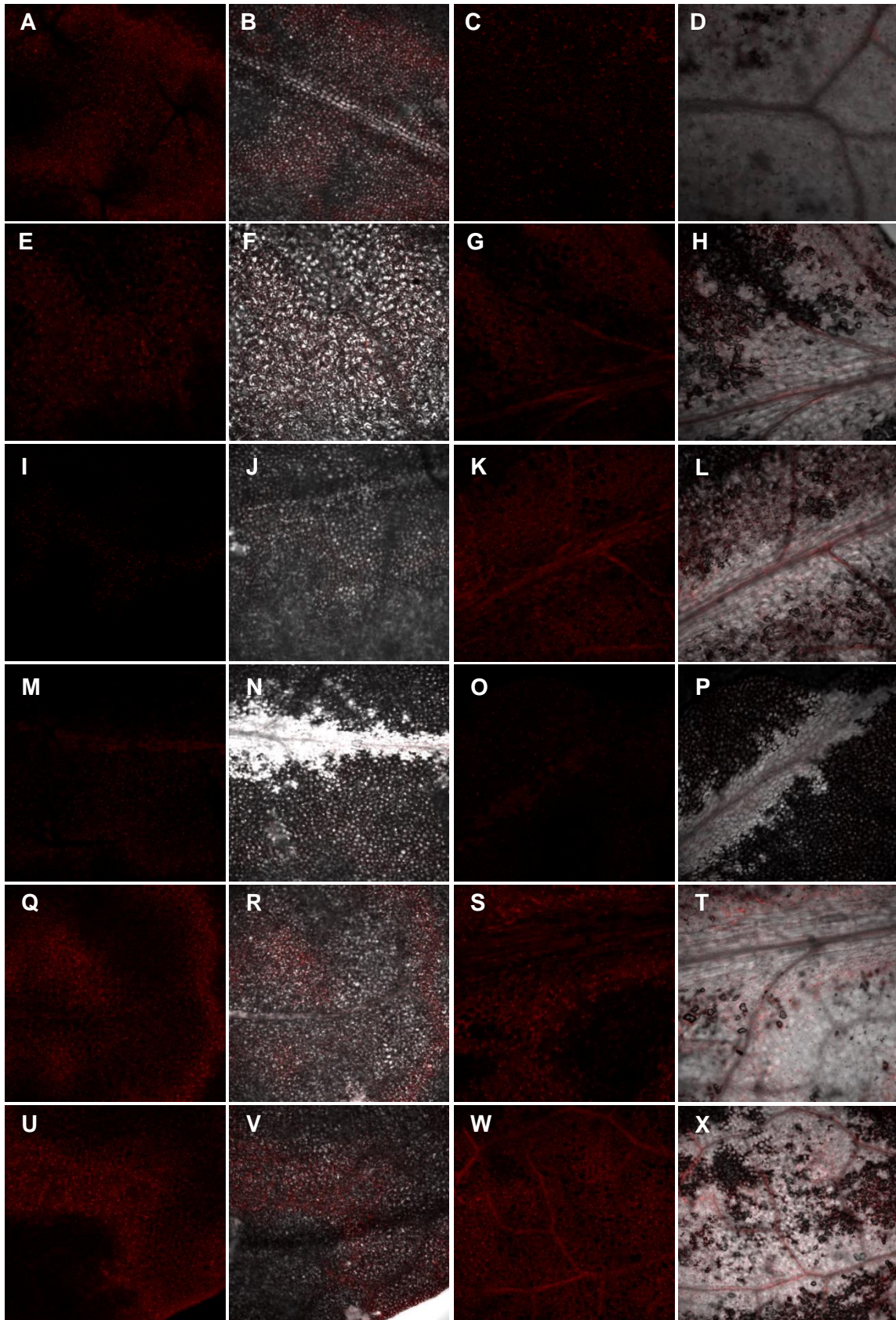


Figure 21. Time course of miRNA dysfunction in different vascular cell-types from amiR-mScarlet-I reporter plants conditionally expressing the VSR Hc-Pro.

- A.** Confocal laser scanning microscopy image showing mScarlet-I channel in red. Image shows a vascular bundle from a MOCK treated plant conditionally expressing Hc-Pro in phloem, 48 HAI.
- B.** Same as A but showing also bright field channel. Leaf cells are shown in grey.
- C.** Confocal laser scanning microscopy image showing mScarlet-I channel in red. Image shows a vascular bundle of a DEX treated plant conditionally expressing Hc-Pro in phloem, 48 HAI.
- D.** Same as C but showing also bright field channel. Leaf cells are shown in grey.
- E.** Confocal laser scanning microscopy image showing mScarlet-I channel in red. Image shows a vascular bundle from a MOCK treated plant conditionally expressing Hc-Pro in phloem, 72 HAI.
- F.** Same as E but showing also bright field channel. Leaf cells are shown in grey.
- G.** Confocal laser scanning microscopy image showing mScarlet-I channel in red. Image shows a vascular bundle from a DEX treated plant conditionally expressing Hc-Pro in phloem companion cells, 72 HAI. A small increase in mScarlet-I fluorescent signal was observed in phloem companion cells compared to previous images at shorter times.
- H.** Same as G but showing also bright field channel. Leaf cells are shown in grey.
- I.** Confocal laser scanning microscopy image showing mScarlet-I channel in red. Image shows a vascular bundle from a MOCK treated plant conditionally expressing Hc-Pro in phloem, 96 HAI.
- J.** Same as I but showing also bright field channel. Leaf cells are shown in grey.
- K.** Confocal laser scanning microscopy image showing mScarlet-I channel in red. Image show a vascular bundle from a DEX treated plant conditionally expressing Hc-Pro in phloem, 96 HAI. The increase of the mScarlet-I fluorescence signal in phloem cells became more evident that at 72 HAI (G).
- L.** Same as K but showing also bright field channel. Leaf cells are shown in grey.
- M.** Confocal laser scanning microscopy image showing mScarlet-I channel in red. Image shows a vascular bundle from a MOCK treated plant conditionally expressing Hc-Pro in bundle sheath cells, 48 HAI.
- N.** Same as M but showing also bright field channel. Leaf cells are shown in grey.

O. Confocal laser scanning microscopy image showing mScarlet-I channel in red. Image shows a vascular bundle from a DEX treated plant conditionally expressing Hc-Pro in bundle sheath cells, 48 HAI.

P. Same as O but showing also bright field channel. Leaf cells are shown in grey.

Q. Confocal laser scanning microscopy image showing mScarlet-I channel in red. Image shows a vascular bundle from a MOCK treated plant conditionally expressing Hc-Pro in bundle sheath cells, 72 HAI. The red signal observed corresponds to basal fluorescence from epidermal cells, previously observed in amiR-mScarlet-I reporter plants.

R. Same as Q but showing also bright field channel. Leaf cells are shown in grey.

S. Confocal laser scanning microscopy image showing mScarlet-I channel in red. Image shows a vascular bundle from a DEX treated plant conditionally expressing Hc-Pro in bundle sheath cells, 72 HAI. The red signal observed corresponds to basal fluorescence from epidermal cells, previously observed in amiR-mScarlet-I reporter plants.

T. Same as S but showing also bright field channel. Leaf cells are shown in grey.

U. Confocal laser scanning microscopy image showing mScarlet-I channel in red. Image shows a vascular bundle from a MOCK treated plant conditionally expressing Hc-Pro in bundle sheath cells, 96 HAI. The red signal observed corresponds to basal fluorescence from epidermal cells, previously observed in plants carrying amiR-mScarlet-I reporter system.

V. Same as U but showing also bright field channel. Leaf cells are shown in grey.

W. Confocal laser scanning microscopy image showing mScarlet-I channel in red. Image shows a vascular bundle from a DEX treated plant conditionally expressing Hc-Pro in bundle sheath cells, 96 HAI. Apart from the basal fluorescent signal in epidermal cells, an increase in the mScarlet-I signal was observed in vascular bundle cells.

X. Same as W but showing also bright field channel. Leaf cells are shown in grey.

2.3 SILENCING SUPPRESSION LEADS TO SPECIFIC CELL-TYPE AND SS-DEPENDENT REPROGRAMMING

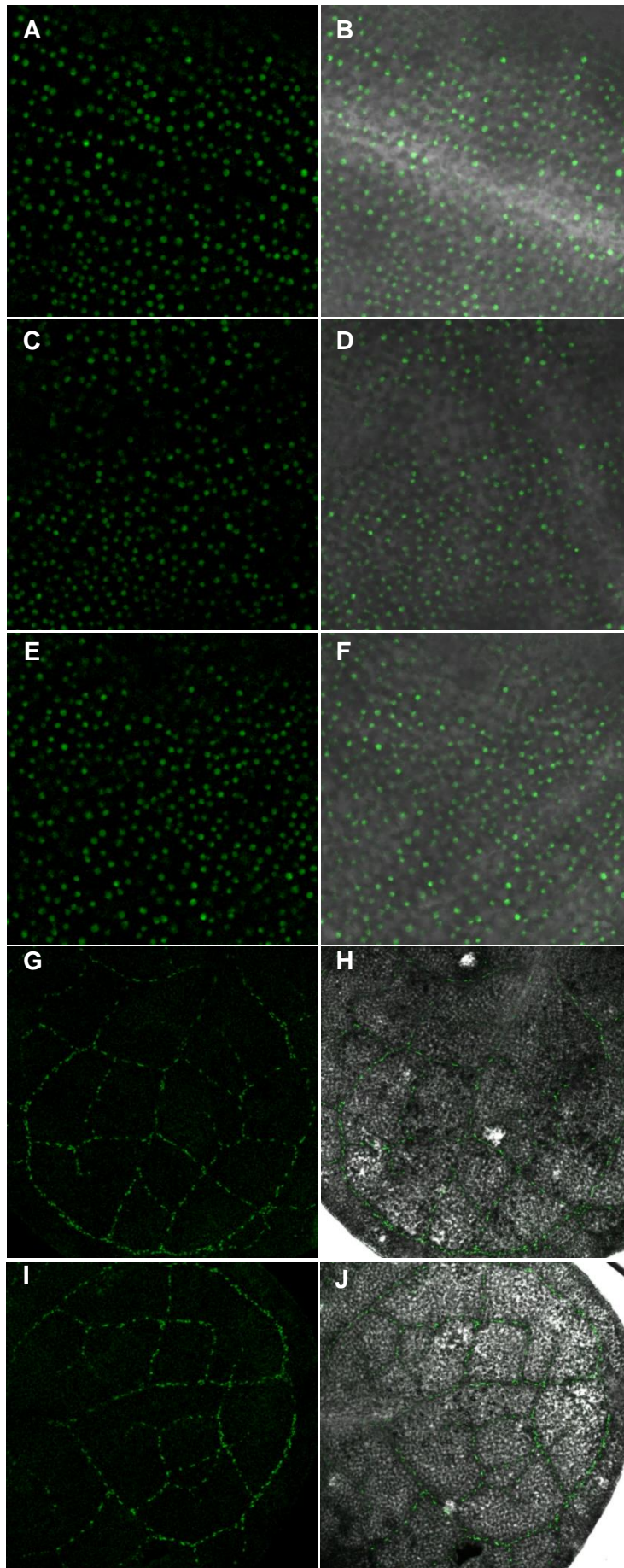
Once generated the stable lines conditionally expressing the SSs in the specific cell types and established the temporal pattern of miRNA dysfunction due to the expression of SSs, next step was to determine the transcriptome changes as consequence of SSs expression in host cells.

2.3.1 ISOLATION OF CELLS SHOWING sRNA MACHINERY DYSFUNCTIONS

Cells showing miRNA dysfunction and therefore, subjected to cell reprogramming were isolated by Fluorescence Activated Cell Sorting (FACS). FACS is a specialized class of flow cytometry, which sorts a subpopulation within a big population of cells using fluorescence labelling.

Plants conditionally expressing the different SSs in the specific cell types and the amiR-mScarlet-I reporter system assayed above could not be used to perform mScarlet-I-based FACS, since epidermal cells showed a higher background mScarlet-I signal (Fig. 21) that could affect the isolation of the desired cell types. Thus, plant lines crossed to amiR-Scarlet-I bearing plants and earlier characterized, were crossed to plant marker lines in which the different cell-type specific promoters were driving a nuclear located GFP (Fig. 22 C- F, I, J, M, N). GFP has been shown to be one of the best fluorescent markers to perform FACS. On the other hand, plants conditionally expressing mScarlet-I in the specific cell types and constitutively expressing GFP (Fig. 22 A, B, G, H, K, L) were also used as controls for RNA seq.

Firstly, induction of SSs in these plants was validated by qPCR. 24 HAI for plants conditionally expressing Hc-Pro and HopT1-1 and constitutively expressing GFP in mesophyll cells (Fig. 23 A, B) and 48 HAI for plants conditionally expressing Hc-Pro in vasculature (Fig. 23 C, D).



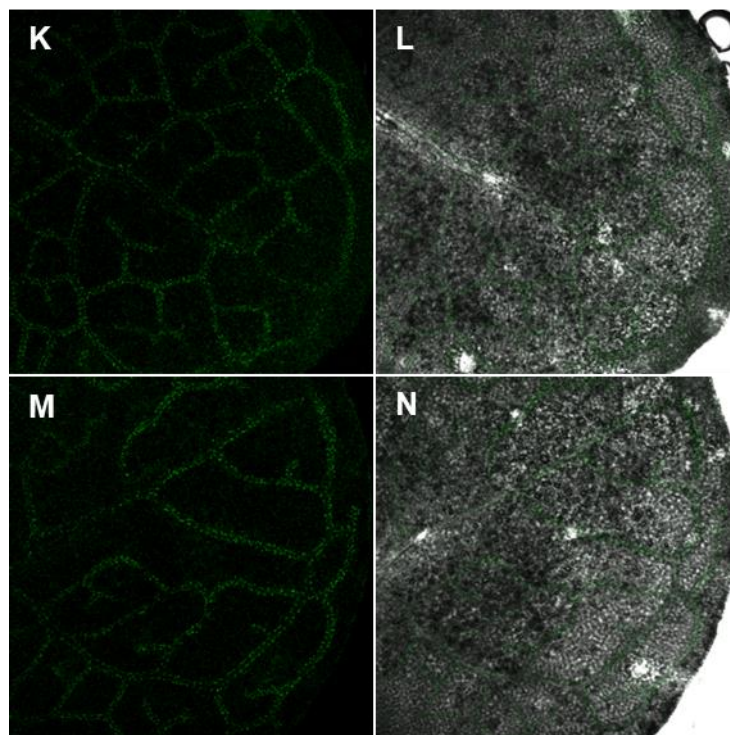


Figure 22. Plants conditionally expressing the mScarlet-I or SSs genes and constitutively expressing GFP gene in the specific cell-types not treated with DEX.

A. Confocal laser scanning microscopy image from a plant carrying the pCAB3::GR-LHG4-pOp::NLS-mScarlet-I and pCAB3::NLS-GFP constructs. Image shows GFP fluorescence (green) in nuclei from mesophyll cells, according to the constitutive expression of GFP in such cells.

B. Same as B but showing also bright field channel.

C. Confocal laser scanning microscopy image from a plant carrying the pCAB3::GR-LHG4-pOp::Hc-Pro and pCAB3::NLS-GFP constructs. Image shows GFP fluorescence (green) in nuclei from mesophyll cells, according to the constitutive expression of GFP in such cells.

D. Same as C but showing also bright field channel.

Images shows leaf 3.

E. Confocal laser scanning microscopy image from a plant carrying the pCAB3::GR-LHG4-pOp::HopT1-1 and pCAB3::NLS-GFP constructs. Image shows GFP fluorescence (green) in nuclei from mesophyll cells, according to the constitutive expression of GFP in such cells.

F. Same as E but showing also bright field channel.

G. Confocal laser scanning microscopy image from a plant carrying the pSUC2::GR-LHG4-pOp::NLS-mScarlet-I and pSUC2::NLS-GFP constructs. Image shows GFP fluorescence (green) in nuclei from of phloem companion cells, according to the constitutive expression of GFP in such cells.

H. Same as G but showing also bright field channel.

I. Confocal laser scanning microscopy image from a plant carrying the pSUC2::GR-LHG4-pOp::Hc-Pro and pSUC2::NLS-GFP construct. Image shows GFP fluorescence (green) in nuclei from phloem companion cells, according to the constitutive expression of GFP in such cells.

J. Same as I but showing also bright field channel.

K. Confocal laser scanning microscopy image from a plant carrying the pSultr2;2::GR-LHG4-pOp::NLS-mScarlet-I and pSultr2;2::NLS-GFP constructs. Image shows GFP fluorescence (green) in nuclei from bundle sheath cells, according to the constitutive expression of GFP in such cells.

L. Same as K but showing also bright field channel.

M. Confocal laser scanning microscopy image from a plant carrying the pSultr2;2::GR-LHG4-pOp::Hc-Pro and pSultr2;2::NLS-GFP constructs. Image shows GFP fluorescence (green) in nuclei from bundle sheath cells, according to the constitutive expression of GFP in such cells.

N. Same as M but showing also bright field channel.

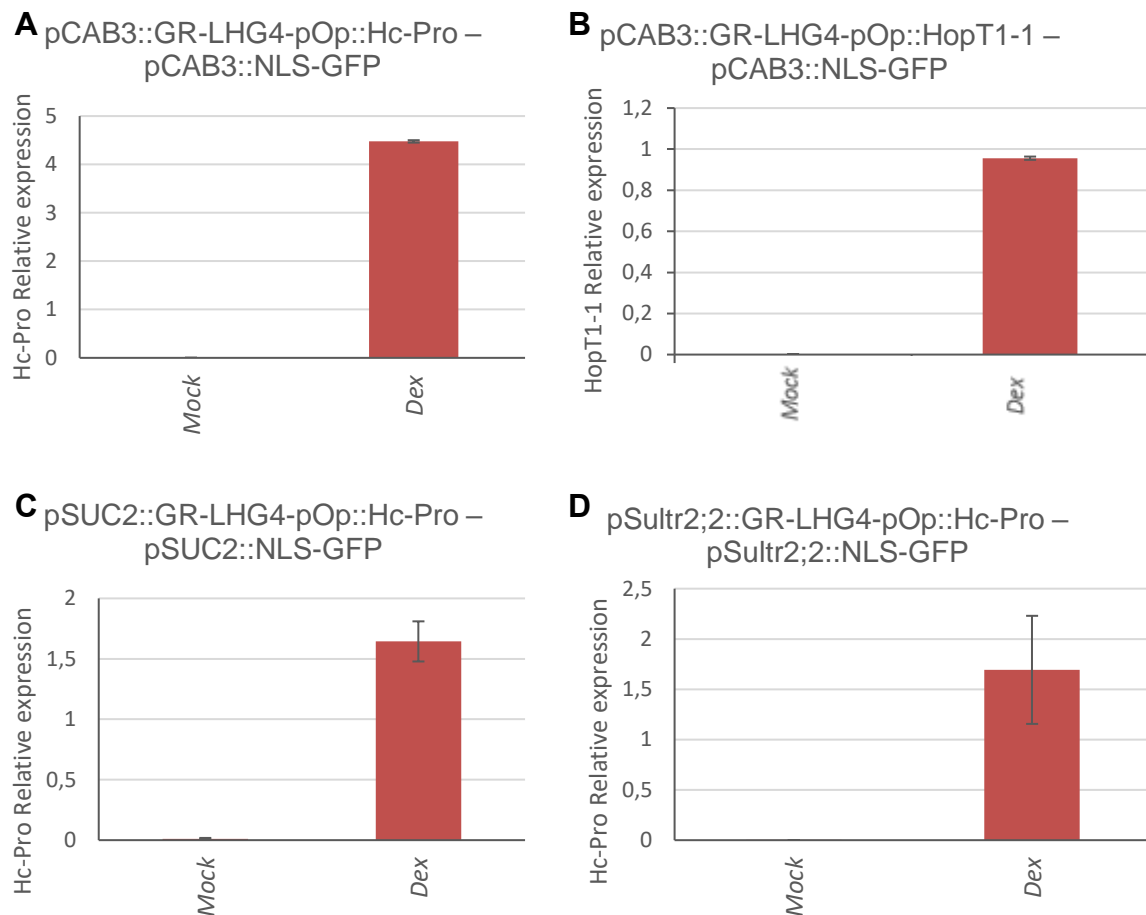


Figure 23. Relative expression levels of the SSs Hc-Pro (A, C, D) and HopT1-1 (B) in heterozygous F1 lines of plants conditionally expressing the SSs in the specific cell types and constitutively expressing GFP in such cells. Images show the relative expression of SSs in MOCK and DEX treated plants, 24 (A, B) and 48 (C, D) HAI. Results represent means (\pm SD) of three biological replicates.

2.3.2 HOPT1-1 INDUCTION HAS A LARGER IMPACT THAN HC-PRO IN TRANSCRIPTOME REPROGRAMMING IN MESHOPHYLL CELLS

Next, transcriptome reprogramming was assayed in the different cell types upon the induction of the different SSs along with those inducing mScarlet-I as control. To that aim, GFP-labelled protoplasts from 15 plants were isolated and 2000 cells were sorted at 24 HAI (that time point was chosen according to the

onset of dysfunction of miRNA dysfunction in that cell-type as observed in section 2.2). Leaves number 3 from 10 days old seedlings were used.

Hc-Pro induction in mesophyll cells resulted in transcriptomic reprogramming that encompassed 146 (Differentially expressed genes) DEG ($\text{padjust} < 0.1$; $\text{log}_2\text{foldchange} > 1$; annex 1). Among those, 12 genes were down-regulated while 134 were up-regulated (including the miR403 target and antiviral and antibacterial protein AGO2). Despite Hc-Pro was found to be expressed at higher levels in the isolated protoplasts (Fig. 24), HopT1-1 induction had a larger effect on mesophyll cells transcriptome when compared to what was found when Hc-Pro was induced 24 HAI (8038 DEG, 3724 up-regulated, 4357 down-regulated, $\text{padjust} < 0.05$; $\text{log}_2\text{foldchange} > 1$).

Transcriptome changes found in Hc-Pro expressing mesophyll cells were mostly included among those found when HopT1-1 was induced (58.33% within down- and 90.3% within up-regulated clusters, Fig. 25). Notably, among HopT1-1 both miR403 targets AGO2 and AGO3 were among the upregulated genes while just AGO2 was upregulated in Hc-Pro. That result suggested that HopT1-1 impact on host silencing was larger than that of Hc-Pro, despite that Hc-Pro expression levels were higher than those of HopT1-1 upon induction.

In order to define which processes were affected by the observed transcriptome changes as consequence of HopT1-1 induction, gene ontology (GO) enrichment analysis was performed using the online tool ShinyGO v.0.741 ($\text{p-value cut-off (FDR)} < 0.05$; <http://bioinformatics.sdstate.edu/go/>). Immunity, Proteasome activity and (endoplasmic reticulum) ER stress were found among the processes that were up-regulated, while photosynthesis, Chloroplast and plastid organization and protein translation related processes (ribosome biogenesis, rRNA processing...) were among the most representative down-regulated processes (Fig. 26).

Among the up-regulated immunity related genes there were elements involved both in PI and ETI, such as EF-TU receptor, NLRs WRKY TFs, Jasmonate (JA) and salicylate (SA) biosynthetic and signalling elements (both are hormones with core role in defence responses in plants) and markers, such as PR1, PR-4 and PR-5. Nevertheless, the flagellin receptor FLS2 was found to

be down-regulated. Among the upregulated NLRs, 8 were previously described as direct miR825-5p targets (At1g63730, At3g04220, At3g53480, At4g11170, At4g14370, At5g40060, At5g41550 and At5g51630) (López-Márquez et al., 2021) and 5 were predicted as miR472 targets (At1g12210, At1g12290, At1g15890, At1g61180 and At5g63020) (Boccaro et al., 2014).

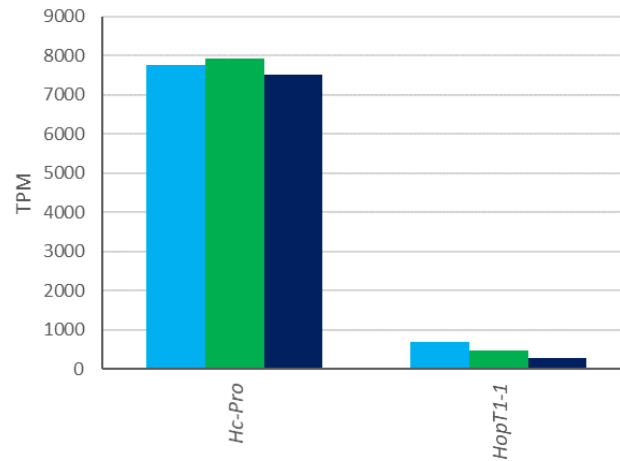


Figure 24. Hc-Pro showed higher expression levels (TPM, transcripts per million) after 24 HAI in mesophyll cells. TPM expression levels were established from RNA-seq results. Its bar represent values from 1 library.

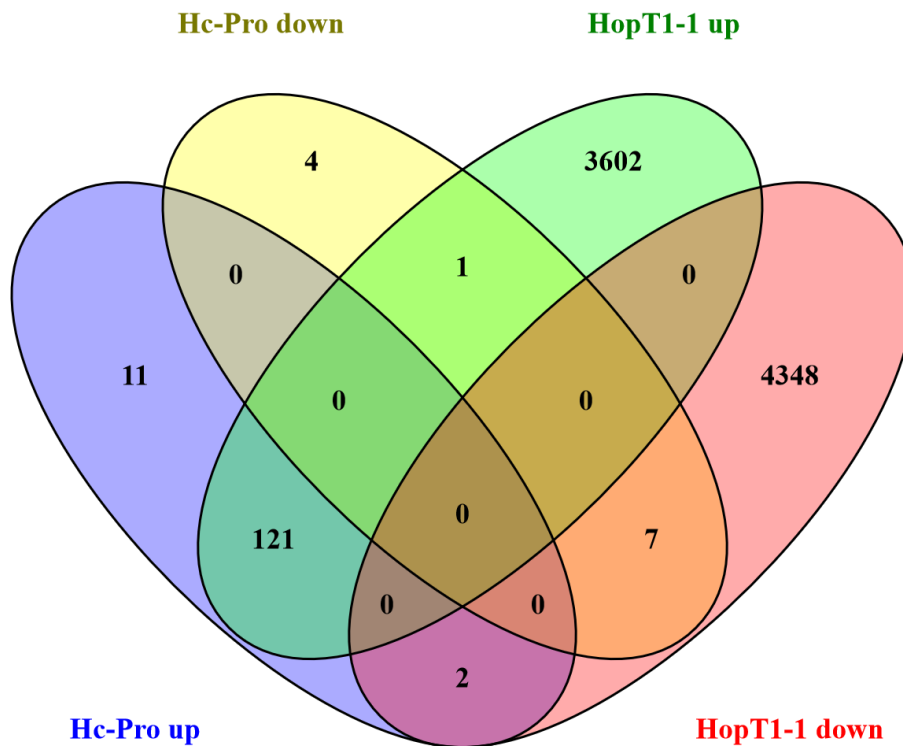


Figure 25. Transcriptome reprogramming resulting from HopT1-1 induction largely recapitulated changes observed upon Hc-Pro induction.

Venn diagram comparing DEG in both datasets showing that 58.33% of down-regulated genes are included in HopT1-1 downregulated genes ($p < 0.001$) while 90.3% of up-regulated genes from Hc-Pro were included in those found in HopT1-1 ($p < 1.36e-87$). Venn diagram was drawn using Venny 2.1.0 (<https://bioinfogp.cnb.csic.es/tools/venny/>)

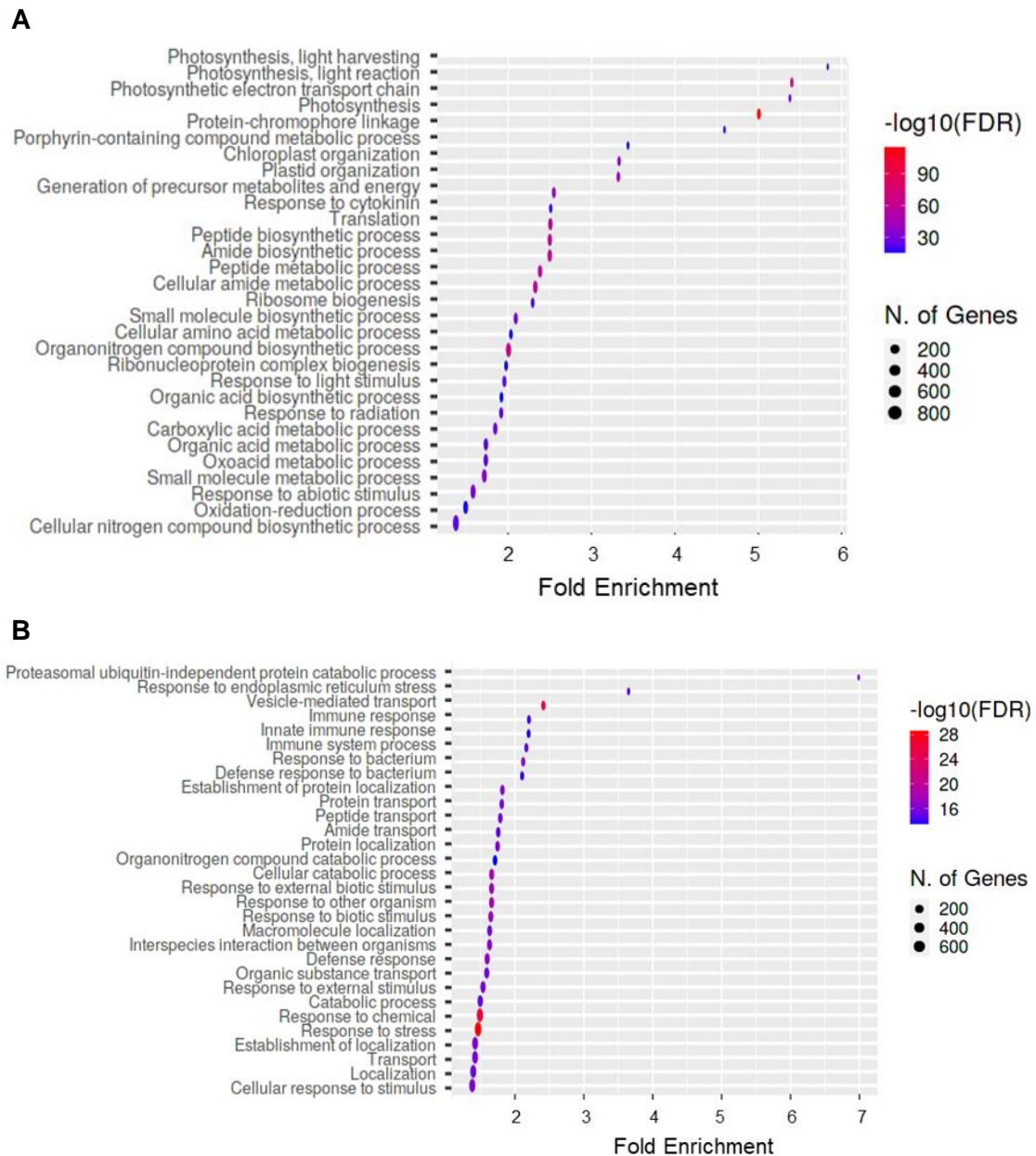


Figure 26. GO classification of Biological Functions to which DEG found as consequence of HopT1-1 induction in mesophyll cells belong.

A. Top 30 processes that were down-regulated (FDR<0.005).

B. Top 30 processes that were up-regulated (FDR<0.005).

The obtained results showed that the presence of SSs in plant mesophyll cells triggers host defence counter-counter measures. Those defensive measures are more pronounced when HopT1-1 is induced.

2.3.3 HC-PRO TRIGGERS CELL-TYPE SPECIFIC REPROGRAMMING

Besides mesophyll cells, Hc-Pro producing viruses were found to be present in vascular tissues where they impaired amiR-mediated regulation (Fig. 21). In order to define the transcriptome changes triggered by VSRs in two vascular cell-types, phloem companion and bundle sheath cells, Hc-Pro and mScarlet-I expression were induced. Protoplasts from 2000 GFP positive cells were isolated 96 HAI (time points were based on the onset of miRNA-dysfunction observed in section 2.2) and RNA isolation followed by Illumina-based transcriptome sequencing were performed.

Hc-pro induction resulted in minor transcriptional changes in both cell types, when compared to the ones observed in mesophyll cells. Hc-Pro levels were similar in mesophyll and phloem companion cells, while they were lower in bundle sheath cells (Fig. 27). Transcriptional reprogramming in bundle sheath cells encompassed 13 DEG (8 downregulated and 5 up-regulated genes, $p_{\text{adjust}} < 0.1$; $\log_2\text{foldchange} > 1$; Annex 1). Among those DEG FT-interacting protein 1 (FTIP1) was up-regulated.

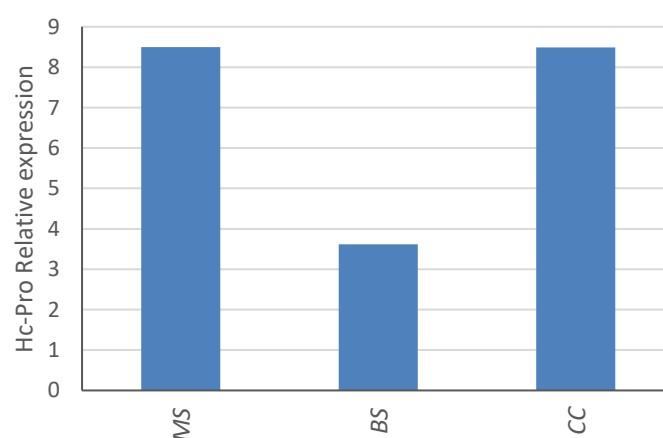


Figure 27. Hc-Pro expression in mesophyll and vascular cells. Log₂fold expression levels were established from RNA-seq results. MS stands for mesophyll cells, BS stands for bundle sheath cells and CC stands for companion cells

Likewise, transcriptome changes in phloem companion cells were very modest showing only 7 DEG (6 down-regulated and 1 up-regulated genes, $p_{\text{adjust}} < 0.1$; $\log_2 \text{foldchange} > 1$; Annex 1). Interestingly, the SUMO-activating enzyme SAE1B-2 (At5g50580) was the most repressed gene like it was the case for mesophyll cells (Annex 1).

Altogether, those results show that Hc-pro induction led to cell-type specific reprogramming and that vascular cell types were more refractory to the presence of that VSR than mesophyll cells (Fig. 28).

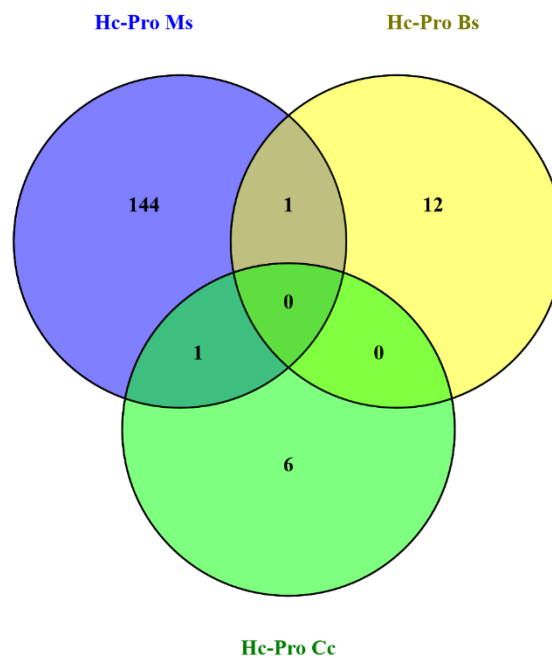


Figure 28. Hc-Pro-triggered reprogramming is cell-type specific.

Venn diagram was drawn using Venny 2.1.0 (<https://bioinfogp.cnb.csic.es/tools/venny/>). Ms stands for mesophyll cells, Bs stands for bundle sheath cells and CC stands for phloem companion cells.

3. CONSEQUENCES OF SSs-TRIGGERED HOST REPROGRAMMING FOR PATHOGEN INFECTION

The contribution from the different events triggered by SSs mediated reprogramming in plant defence was assayed by infecting plants conditionally expressing the different SSs with *Turnip Mosaic Virus* (TuMV), which carried the *Anthirrium majus* MYB-related Rosea 1 (Ros1) transcription factor. The expression of Ros1-TF leads to the accumulation of anthocyanins, facilitating to follow the progress of infection by naked eye (Bedoya et al., 2012). Plants conditionally expressing the SSs were treated with 5 μ M of DEX 1 DAI and twice per week after that. Plants conditionally expressing HopT1-1 in mesophyll were treated only once per week to reduce the macroscopic developmental deficiencies generated by the continuous induction of HopT1-1 expression. TuMV levels were monitored by qPCR.

When compared with control plants (Fig. 29 A), in which mScarlet-I was induced in mesophyll cells, induction of Hc-Pro did not lead to differences in TuMV-ROS1 levels (Fig. 29 B, D). On the other hand, induction of HopT1-1 majorly contributed to reduce the viral load (Fig. 29 C, D). Likewise, Hc-Pro induction in phloem companion (Fig. 30 B, C) and bundle sheath cells (Fig. 31 B, C) did not altered viral levels when compared with their corresponding controls (Fig. 30 A, C, 31 A, C).

Additionally, plants carrying mScarlet-I gene (Fig. 32 A), Hc-Pro (Fig. 32 B) and HopT1-1 (Fig. 32 C) inducible constructs under the control of the mesophyll specific CAB3 promoter, were infected with *Pto* DC3000. As it was found in TuMV-ROS1 infections, HopT1-1 induction resulted in an enhanced resistance against that bacterial pathogen and lower levels of *Pto* DC3000 (Fig. 32 D).

Those results confirm that HopT1-1-triggered host cell reprogramming enables a broad range defensive response that works as a counter-counter defence in response to the presence of SSs that strongly affect sRNA internal pathways.

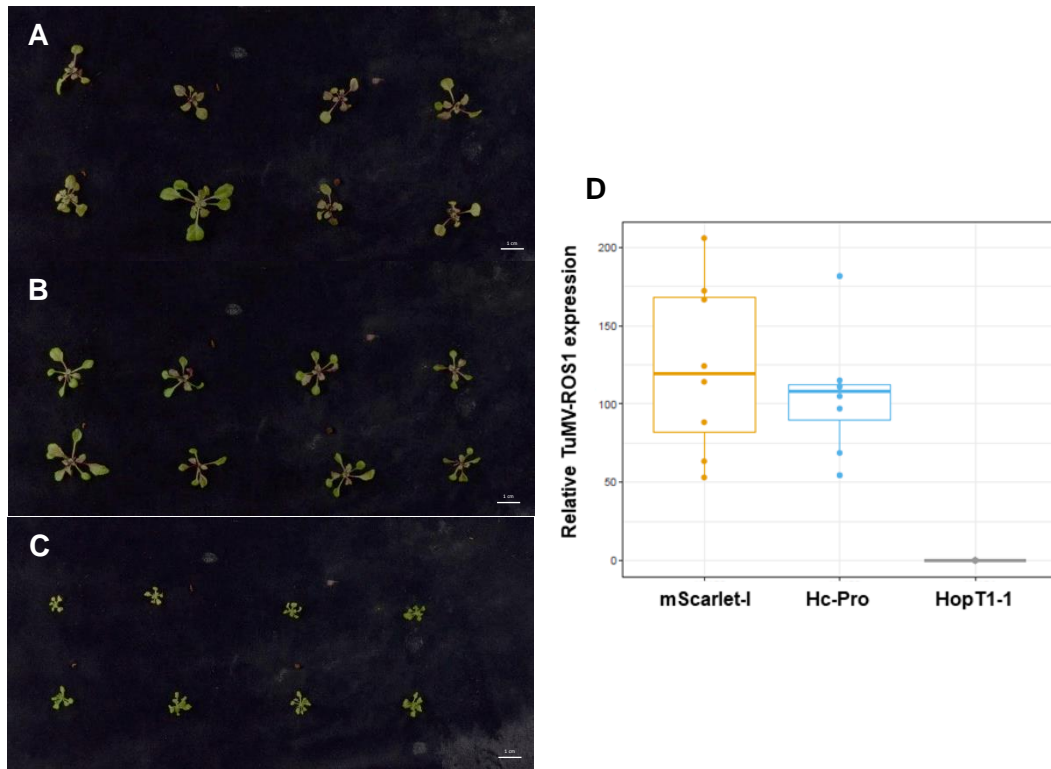


Figure 29. Hopt1-1 induction in mesophyll cells leads to enhance resistance against TuMV.

A. Plants conditionally expressing the mScarlet-I gene (control).

B. Plants conditionally expressing the VSR Hc-Pro.

C. Plants conditionally expressing the BSR HopT1-1 in mesophyll cells.

Plants were infected with TuMV-ROS1 and imaged 14 DAI. Scale bar: 1 cm

D. Relative expression of TuMV viral genome in 8 plants (dots) from each genotype.

Box plot was drawn using R. The horizontal line indicates the mean. Wilcoxon test was performed to determine the significant differences. mScarlet-I and Hc-Pro are not significantly different (p -value = 0.5737), while the difference between mScarlet-I and HopT1-1 is highly significant (p -value = 0.0001554).

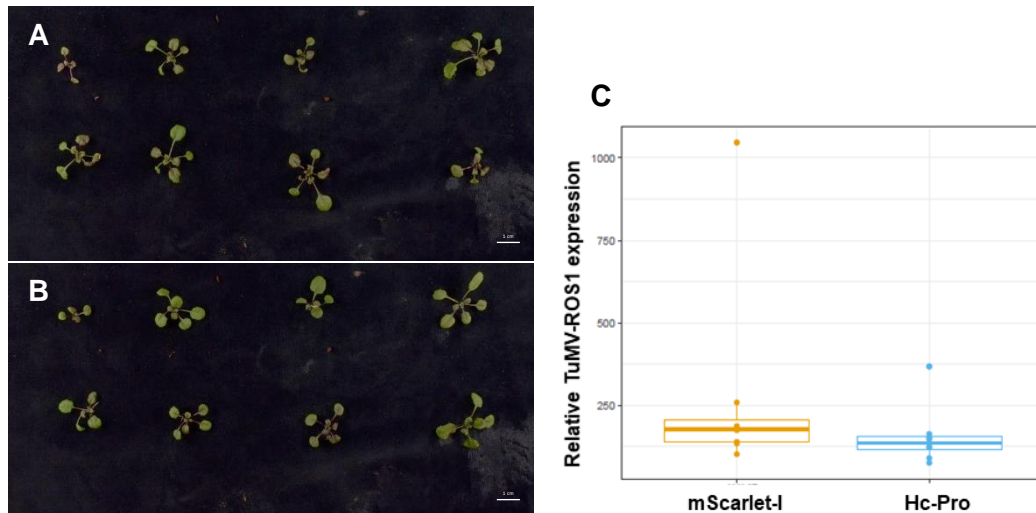


Figure 30. Hc-Pro induction in phloem companion cells had no effects in plant resistance against TuMV.

A. Plants conditionally expressing the mScarlet-I gene (control).

B. Plants conditionally expressing the VSR Hc-Pro in phloem companion cells infected with TuMV.

Plants were infected with TuMV-ROS1 and imaged 14 DAI. Scale bar: 1 cm

C. Relative expression of TuMV viral genome in 8 plants (dots) from each genotype.

Box plot was drawn using R. The horizontal line indicates the mean. Wilcoxon test was performed to determine the significant differences. Samples are not significantly different (p -value = 0.1605).

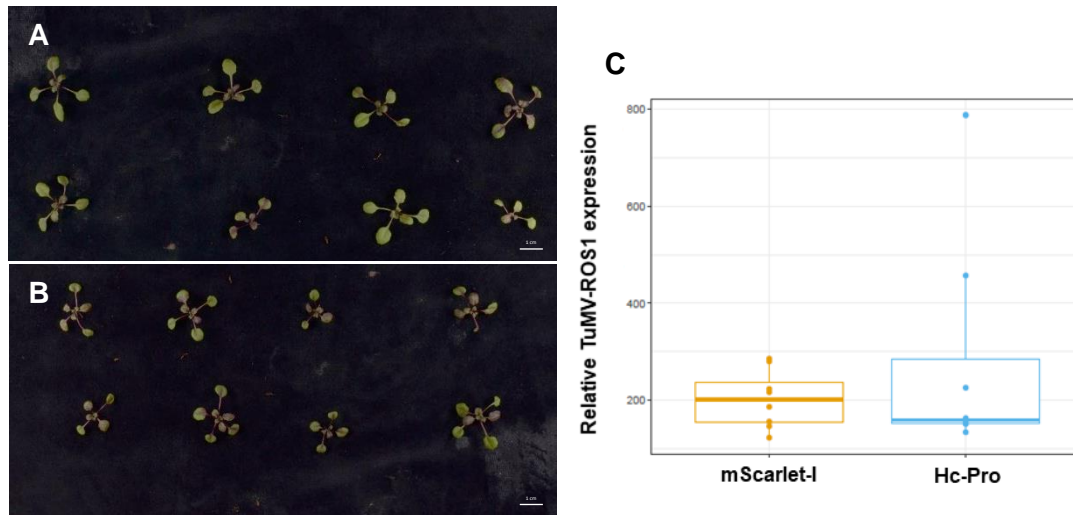


Figure 31. Hc-Pro induction in bundle sheath cells had no effects in plant resistance against TuMV.

A. Plants conditionally expressing the mScarlet-I gene (control).

B. Plants conditionally expressing the VSR Hc-Pro in bundle sheath cells infected with TuMV.

Plants were infected with TuMV-ROS1 and imaged 14 DAI. Scale bar: 1 cm

C. Relative expression of TuMV viral genome in 8 plants for each genotype.

Box plot was drawn using R. The horizontal line indicates the mean. Wilcoxon test was performed to determine the significant differences. Samples are not significantly different (p -value = 0.9591).

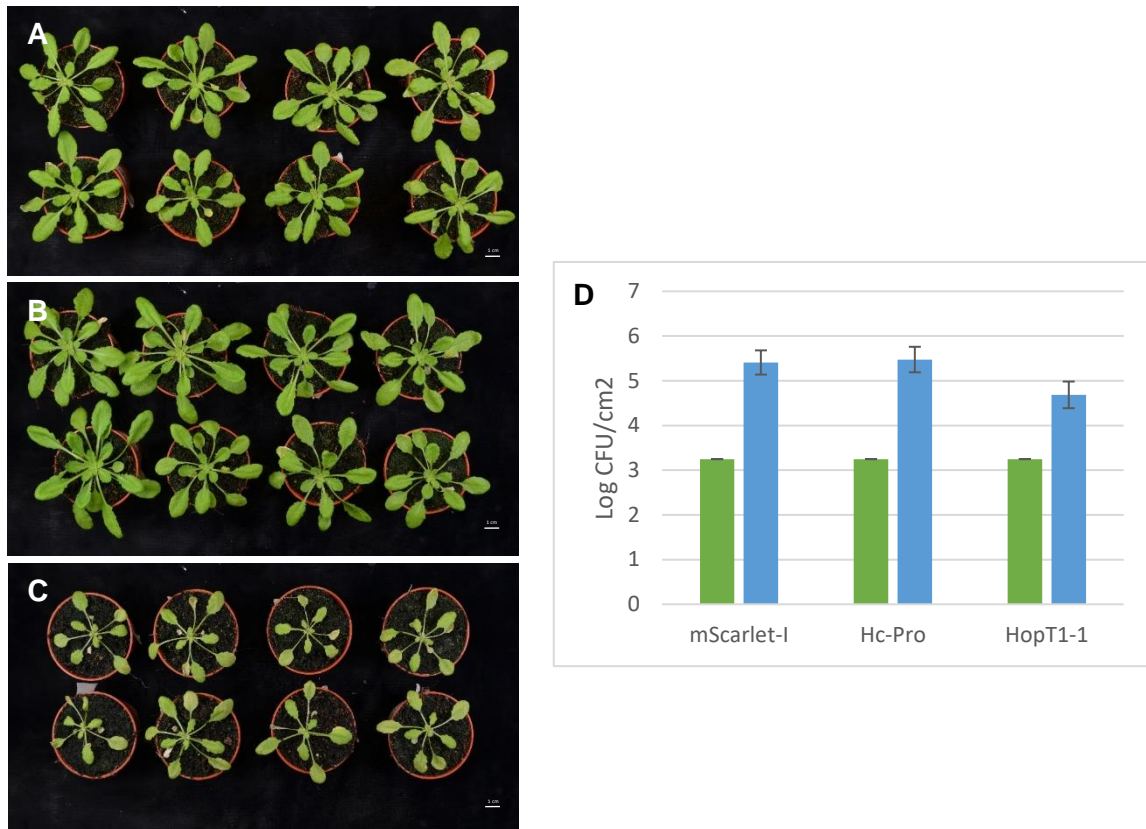


Figure 32. Hopt1-1 induction in mesophyll cells leads to enhance resistance against *Pto* DC 3000. 4-weeks-old plants conditionally expressing the **A.** mScarlet-I gene (control), **B.** the VSR Hc-Pro and **C.** the BSR HopT1-1 in mesophyll cells inoculated with *P. syringae* DC 3000.

Plants were inoculated by syringe-infiltration using an OD₆₀₀ 0,001. Scale bar: 1 cm

D. Log CFU/cm² calculated the day of infiltration (green) and 3 days after infiltration (blue). Bars represent means (\pm SD) of eight biological replicates.

DISCUSSION

Host RNA silencing suppression is a common strategy employed by pathogens as dissimilar as viruses, bacteria and oomycetes during their infections (Navarro et al., 2008; Pumpilin et al., 2013; Qiao et al., 2013). Those pathogens use different vectors for spreading between new hosts in which they interact with different cell types as consequence of their different colonization routes. Host cell types present distinctive transcriptomes, including specific sets of sRNAs and their targets. Pathogens can control the production of unrelated SSs that may target different steps within the host RNA silencing machinery, dismantling this defence system and also interfering with host cellular processes. Our current knowledge about the mode of action of those SSs, and the concomitant host cellular responses, in *A. thaliana* is largely derived from static studies neglecting the dynamics of such confrontation between host and pathogens. Thus, most of those studies rely on the constitutive expression of SSs leading to downstream effects in cell types that might not be their natural targets during natural infections.

In this study, I have focused on elucidating the cellular dynamics of RNA silencing suppression during the infection of three types of pathogens by defining which specific host cell types they target. Furthermore, I have determined the transcriptome changes derived from the presence of two viral and bacterial unrelated SSs in those specific cell types. Finally, I have assayed the contribution of cell-type SS-triggered reprogramming to counter-counter defence programs that enable increased resistance to pathogens.

Viruses from the *Potyviridae* family, such as TuMV and PPV, use aphids as vectors for their spread. Once inoculated in the host, those viruses are able to move cell-to-cell through plasmodesmata to finally move systemically through the plant vascular system and eventually colonize mesophyll cells. Using two different plant reporter systems based on luminescence (amiR-Luc) and fluorescence (amiR-mScarlet-I), it was found that the presence of a PPV-GFP labelled virus in vasculature and mesophyll cells correlated with higher levels of LUC and mScarlet-I expression as consequence of amiR dysfunction. Nevertheless, the cell-type specific induction of Hc-Pro VSR from TuMV in amiR-mScarlet-I reporter plants, showed that vascular tissues (bundle sheath and

phloem companion cells) are more refractory to Hc-Pro-mediated RNA silencing suppression. While 24 hours of induction were enough to observe the onset of amiR dysfunction in mesophyll cells, 96 hours were needed for the same to occur in vascular tissues. Accordingly, induction in mesophyll cells had a larger effect on host cell reprogramming at the transcriptome level. As part of such reprogramming, the miR403 and antiviral and antibacterial AGO2 gene was upregulated, along with the Jasmonate biosynthetic LOX 6 (At1g67560) and receptor COI1 (At2g39940) genes and several NLRs uniquely in mesophyll cells, while both vascular cell types also showed characteristic changes on their transcriptome. It is noteworthy that the most repressed gene in mesophyll and phloem companion cells is a subunit of a SUMO activating enzyme that participates in the conjugation of SUMO as part of protein posttranslational modifications (Castano-Miquel et al., 2013). Jasmonate biosynthetic and signalling pathways were shown to be upregulated in Arabidopsis plants constitutively expressing Hc-Pro (Endres et al., 2010).

Pseudomonas syringae is one of the most devastating plant pathogens and is thought to use rainfall and running waters for its spread between hosts. Once on the leaf surface, *P. syringae* enters the interstitial plant space through stomata that can be either open for plant transpiration or as consequence of bacterial molecular manipulation (Melotto et al., 2006). *Pto* DC3000 is able to produce at least three effectors with SS activity: AvrPto, HopN1 and HopT1-1 (Navarro et al., 2008). Those SS are translocated into host cells through the plasma membrane by the T3SS. Infection of amiR-LUC and amiR-mScarlet-I reporter plants with GFP-labelled *Pto* DC3000 showed that mesophyll cells were preferentially targeted for SSs depletion. GFP-labelled bacteria were found clustering around the plasma membrane of mesophyll cells coinciding with higher levels of both luciferase and nuclear located mScarlet-I. Instead, when a *Pto* DC3000 strain impaired on T3SS formation (*hrcC*⁻) was used, no difference on LUC or mScarlet-I activity were found, despite GFP-labelled cells were clustering around mesophyll cells. AmiR dysfunction and the concomitant increase on mScarlet-I activity, was readily detected 24 hours after HopT1-1 induction in mesophyll cells in amiR-mScarlet-I reporter plants. Despite the levels of mScarlet-I expression were lower as result of HopT1-1 induction when compared

to what was found in Hc-Pro induction, transcriptional reprogramming in mesophyll cells was significantly larger. HopT1-1 induction led to changes in the expression of 8081 genes, triggering ER stress, immune responses and repressing photosynthesis and translation (which could explain that mScarlet-I fluorescence was lower than in Hc-Pro-induced silencing suppression). Importantly, most of the transcriptional changes observed in mesophyll cells upon the induction of Hc-Pro, were included within those triggered by HopT1-1-mediated reprogramming. Moreover, when comparing HopT1-1 transcriptional reprogramming in mesophyll cells with that found as consequence of Hc-Pro constitutive expression in Arabidopsis plants (Toro et al., 2017), that overlap became clearer showing common increase in defence responses and inhibition of photosynthesis.

Since both Hc-Pro and HopT1-1 present GW motifs for AGO1 interaction (Pollari et al., 2020; Thiébeauld et al., 2021) and can potentially affect RISC assembly and loading, that result suggest that Hc-Pro would have evolved to minimize its impact on host sRNA pathways and that would happen when Hc-Pro is either expressed at higher levels, for longer times or in cell types others than the ones assayed in this study. That possibility is further supported by the fact that Hc-Pro seems to have primarily specialized in avoiding vsiRNA loading into RISC complexes by sRNA sequestration (Toro et al., 2017) and therefore, might preferentially affect to highly expressed plant miRNAs, such as those from our reporter plants or miR403. Additionally, Hc-Pro silencing suppressor activity has been shown to be tightly controlled likely to minimize its impact on host sRNA-regulated pathways to avoid counter-counter defence activation (Pasin et al., 2014; Pruss et al., 2004).

Based on those results, it is conceivable to speculate that the preference shown by Hc-Pro producing viruses to use vectors that mainly target host vascular tissues, such as aphids, is related to the fact that those are more refractory to the presence of Hc-Pro avoiding mesophyll cells where could potentially lead to host counter-counter defence and infection abrogation.

Accordingly, Hopt1-1 induction in mesophyll cells resulted in significantly higher defence against TuMV and *Pto* DC3000. Thus, in order to avoid host

counter-counter defence, *Pto* DC3000 must control the amount of HopT1-1 that is translocated into host cells and compensate its presence by the action of additional effectors that target central elements within that new layer of defence.

Host miRNA targets might have a central role in controlling that counter-counter defence mechanism. miR472 and miR825-5p NLR targets have shown to be involved in broad range resistance against virus, bacteria and fungal pathogens (Boccarda et al., 2014; López-Márquez et al., 2021; Nie et al., 2019). Likewise, miR403 regulated AGO2 is a central component of antiviral and antibacterial defence (Harvey et al., 2011; Manacorda et al., 2021; Xiaoming Zhang et al., 2011a). miRNA targeted TFs have also been involved in contributing to defence about several different pathogens. Therefore, the fast rate of evolutionary “birth and death” of miRNA genes in plants (Fahlgren et al., 2007) might reflect selection for those targeting genes involved in defence responses against pathogens that produce SSs as part of their infection strategy, such as Virus, bacteria and fungi. SS-triggered suppression of miRNA-mediated regulation would readily enable quick translation of otherwise repressed transcripts and enhanced defence responses.

Further studies will focus on establishing the role of miRNA-targeted TFs in silencing suppression-triggered host cell reprogramming and counter-counter defence.

CONCLUSIONS

Collectively, those results show that pathogen-mediated impairment of host RNA silencing triggers effective counter-counter defence in a cell type specific manner ensuing another step on the host-pathogen arms race. The main conclusions from this work are:

- Leaf mesophyll cells are commonly targeted by unrelated pathogens for host RNA silencing suppression.

- Vascular cell types are the most susceptible for virus expansion which correlates with their insensitivity to the presence of TuMV Hc-Pro.

- TuMV Hc-Pro has evolved to primarily avoid visRNA loading in functional RISC complexes and minimize its impact in host-regulated sRNA pathways avoiding counter-counter defence programs.

- HopT1-1 induction triggers major mesophyll cell reprogramming leading to counter-counter defence mechanisms.

- HopT1-1 has qualitatively similar albeit bigger impact on host sRNA-mediated pathways than TuMV Hc-Pro.

- HopT1-1-triggered reprogramming in mesophyll cells leads to Proteasome, ER stress and defence activation and energy deprivation (inhibition of photosynthesis and protein translation).

- HopT1-1 induction in mesophyll cells results in counter-counter defence mechanisms that abrogate both viral and bacterial infections.

- HopT1-1-triggered counter-counter defence encompasses activation of miRNA targets, such as AGO2, NLRs and TFs.

BIBLIOGRAPHY

- Alfano, J. R., & Collmer, A. (2004). TYPE III SECRETION SYSTEM EFFECTOR PROTEINS: Double Agents in Bacterial Disease and Plant Defense. *Http://Dx.Doi.Org/10.1146/Annurev.Phyto.42.040103.110731*, 42, 385–414. doi: 10.1146/ANNUREV.PHYTO.42.040103.110731
- Allen, E., Xie, Z., Gustafson, A. M., & Carrington, J. C. (2005). microRNA-Directed Phasing during Trans-Acting siRNA Biogenesis in Plants. *Cell*, 121(2), 207–221. doi: 10.1016/J.CELL.2005.04.004
- Anandalakshmi, R., Pruss, G. J., Ge, X., Marathe, R., Mallory, A. C., Smith, T. H., & Vance, V. B. (1998). A viral suppressor of gene silencing in plants. *Proceedings of the National Academy of Sciences*, 95(22), 13079–13084. doi: 10.1073/PNAS.95.22.13079
- Aranda, M. A., & Freitas-Astúa, J. (2017). Ecology and diversity of plant viruses, and epidemiology of plant virus-induced diseases. *Annals of Applied Biology*, 171(1), 1–4. doi: 10.1111/AAB.12361
- Arikiti, S., Xia, R., Kakrana, A., Huang, K., Zhai, J., Yan, Z., Valdés-López, O., Prince, S., Musket, T. A., Nguyen, H. T., Stacey, G., & Meyers, B. C. (2014). An Atlas of Soybean Small RNAs Identifies Phased siRNAs from Hundreds of Coding Genes. *The Plant Cell*, 26(12), 4584. doi: 10.1105/TPC.114.131847
- Asai, S., Furzer, O. J., Cevik, V., Kim, D. S., Ishaque, N., Goritschnig, S., Staskawicz, B. J., Shirasu, K., & Jones, J. D. G. (2018). A downy mildew effector evades recognition by polymorphism of expression and subcellular localization. *Nature Communications* 2018 9:1, 9(1), 1–11. doi: 10.1038/s41467-018-07469-3
- Axtell, M. J. (2013). Classification and Comparison of Small RNAs from Plants. *Http://Dx.Doi.Org/10.1146/Annurev-Arplant-050312-120043*, 64, 137–159. doi: 10.1146/ANNUREV-ARPLANT-050312-120043
- Azevedo, J., Garcia, D., Pontier, D., Ohnesorge, S., Yu, A., Garcia, S., Braun, L., Bergdoll, M., Hakimi, M. A., Lagrange, T., & Voinnet, O. (2010). Argonaute quenching and global changes in Dicer homeostasis caused by a pathogen-

- encoded GW repeat protein. *Genes & Development*, 24(9), 904–915. doi: 10.1101/GAD.1908710
- Bartels, S., & Boller, T. (2015). Quo vadis, Pep? Plant elicitor peptides at the crossroads of immunity, stress, and development. *Journal of Experimental Botany*, 66(17), 5183–5193. doi: 10.1093/JXB/ERV180
- Beck, M., Wyrsh, I., Strutt, J., Wimalasekera, R., Webb, A., Boller, T., & Robatzek, S. (2014). Expression patterns of FLAGELLIN SENSING 2 map to bacterial entry sites in plant shoots and roots. *Journal of Experimental Botany*, 65(22), 6487–6498. doi: 10.1093/JXB/ERU366
- Bedoya, L. C., Martínez, F., Orzáez, D., & Daròs, J.-A. (2012). Visual Tracking of Plant Virus Infection and Movement Using a Reporter MYB Transcription Factor That Activates Anthocyanin Biosynthesis. *Plant Physiology*, 158(3), 1130–1138. doi: 10.1104/PP.111.192922
- Boccaro, M., Sarazin, A., Thiébeauld, O., Jay, F., Voinnet, O., Navarro, L., & Colot, V. (2014). The Arabidopsis miR472-RDR6 Silencing Pathway Modulates PAMP- and Effector-Triggered Immunity through the Post-transcriptional Control of Disease Resistance Genes. *PLOS Pathogens*, 10(1), e1003883. doi: 10.1371/JOURNAL.PPAT.1003883
- Bologna, N. G., Iselin, R., Abriata, L. A., Sarazin, A., Pumplín, N., Jay, F., Grentzinger, T., Peraro, M. D., & Voinnet, O. (2018). Nucleo-cytosolic Shuttling of ARGONAUTE1 Prompts a Revised Model of the Plant MicroRNA Pathway. *Molecular Cell*, 69(4), 709-719.e5. doi: 10.1016/J.MOLCEL.2018.01.007
- Born, P. von, Bernardo-Faura, M., & Rubio-Somoza, I. (2018). An artificial miRNA system reveals that relative contribution of translational inhibition to miRNA-mediated regulation depends on environmental and developmental factors in *Arabidopsis thaliana*. *PLOS ONE*, 13(2), e0192984. doi: 10.1371/JOURNAL.PONE.0192984
- Borsani, O., Zhu, J., Verslues, P. E., Sunkar, R., & Zhu, J. K. (2005). Endogenous siRNAs Derived from a Pair of Natural cis-Antisense Transcripts Regulate

- Salt Tolerance in Arabidopsis. *Cell*, 123(7), 1279–1291. doi: 10.1016/J.CELL.2005.11.035
- Boutrot, F., & Zipfel, C. (2017). Function, Discovery, and Exploitation of Plant Pattern Recognition Receptors for Broad-Spectrum Disease Resistance. <https://doi.org/10.1146/Annurev-Phyto-080614-120106>, 55, 257–286. doi: 10.1146/ANNUREV-PHYTO-080614-120106
- Box, M. S., Coustham, V., Dean, C., & Mylne, J. S. (2011). Protocol: A simple phenol-based method for 96-well extraction of high quality RNA from Arabidopsis. *Plant Methods* 2011 7:1, 7(1), 1–10. doi: 10.1186/1746-4811-7-7
- Breakfield, N. W., Corcoran, D. L., Petricka, J. J., Shen, J., Sae-Seaw, J., Rubio-Somoza, I., Weigel, D., Ohler, U., & Benfey, P. N. (2012). High-resolution experimental and computational profiling of tissue-specific known and novel miRNAs in Arabidopsis. *Genome Research*, 22(1), 163–176. doi: 10.1101/GR.123547.111
- Brioudes, F., Jay, F., Sarazin, A., Grentzinger, T., Devers, E. A., & Voinnet, O. (2021). HASTY, the Arabidopsis EXPORTIN5 ortholog, regulates cell-to-cell and vascular microRNA movement. *The EMBO Journal*, 40(15), e107455. doi: 10.15252/EMBJ.2020107455
- Brosnan, C. A., Sarazin, A., Lim, P., Bologna, N. G., Hirsch-Hoffmann, M., & Voinnet, O. (2019). Genome-scale, single-cell-type resolution of microRNA activities within a whole plant organ. *The EMBO Journal*, 38(13), e100754. doi: 10.15252/EMBJ.2018100754
- Budak, H., & Akpinar, B. A. (2015). Plant miRNAs: biogenesis, organization and origins. *Functional & Integrative Genomics* 2015 15:5, 15(5), 523–531. doi: 10.1007/S10142-015-0451-2
- Burguán, J., & Havelda, Z. (2011). Viral suppressors of RNA silencing. *Trends in Plant Science*, 16(5), 265–272. doi: 10.1016/J.TPLANTS.2011.02.010

- Cambiagno, D. A., Giudicatti, A. J., Arce, A. L., Gagliardi, D., Li, L., Yuan, W., Lundberg, D. S., Weigel, D., & Manavella, P. A. (2021). HASTY modulates miRNA biogenesis by linking pri-miRNA transcription and processing. *Molecular Plant*, *14*(3), 426–439. doi: 10.1016/J.MOLP.2020.12.019
- Cao, Y., Liang, Y., Tanaka, K., Nguyen, C. T., Jedrzejczak, R. P., Joachimiak, A., & Stacey, G. (2014). The kinase LYK5 is a major chitin receptor in Arabidopsis and forms a chitin-induced complex with related kinase CERK1. *ELife*, *3*. doi: 10.7554/ELIFE.03766
- Carella, P., Gogleva, A., Hoey, D. J., Bridgen, A. J., Stolze, S. C., Nakagami, H., & Schornack, S. (2019). Conserved Biochemical Defenses Underpin Host Responses to Oomycete Infection in an Early-Divergent Land Plant Lineage. *Current Biology*, *29*(14), 2282-2294.e5. doi: 10.1016/J.CUB.2019.05.078
- Castano-Miquel, L., Seguí, J., Manrique, S., Teixeira, I., Carretero-Paulet, L., Atencio, F., & Lois, L. M. (2013). Diversification of SUMO-Activating Enzyme in Arabidopsis: Implications in SUMO Conjugation. *Molecular Plant*, *6*(5), 1646–1660. doi: 10.1093/MP/SST049
- Chandran, V., Wang, H., Gao, F., Cao, X.-L., Chen, Y.-P., Li, G.-B., Zhu, Y., Yang, X.-M., Zhang, L.-L., Zhao, Z.-X., Zhao, J.-H., Wang, Y.-G., Li, S., Fan, J., Li, Y., Zhao, J.-Q., Li, S.-Q., & Wang, W.-M. (2019). miR396-OsGRFs Module Balances Growth and Rice Blast Disease-Resistance. *Frontiers in Plant Science*, *0*, 1999. doi: 10.3389/FPLS.2018.01999
- Chen, T., Nomura, K., Wang, X., Sohrabi, R., Xu, J., Yao, L., Paasch, B. C., Ma, L., Kremer, J., Cheng, Y., Zhang, L., Wang, N., Wang, E., Xin, X.-F., & He, S. Y. (2020). A plant genetic network for preventing dysbiosis in the phyllosphere. *Nature* *2020* *580:7805*, *580*(7805), 653–657. doi: 10.1038/s41586-020-2185-0
- Chinchilla, D., Zipfel, C., Robatzek, S., Kemmerling, B., Nürnberger, T., Jones, J. D. G., Felix, G., & Boller, T. (2007). A flagellin-induced complex of the receptor FLS2 and BAK1 initiates plant defence. *Nature* *2007* *448:7152*, *448*(7152), 497–500. doi: 10.1038/nature05999

- Cianciotto, N. P., & White, R. C. (2017). Expanding Role of Type II Secretion in Bacterial Pathogenesis and Beyond. *Infection and Immunity*, *85*(5). doi: 10.1128/IAI.00014-17
- Craft, J., Samalova, M., Baroux, C., Townley, H., Martinez, A., Jepson, I., Tsiantis, M., & Moore, I. (2005). New pOp/LhG4 vectors for stringent glucocorticoid-dependent transgene expression in Arabidopsis. *The Plant Journal*, *41*(6), 899–918. doi: 10.1111/J.1365-313X.2005.02342.X
- Cui, H., Kong, D., Liu, X., & Hao, Y. (2014). SCARECROW, SCR-LIKE 23 and SHORT-ROOT control bundle sheath cell fate and function in Arabidopsis thaliana. *The Plant Journal*, *78*(2), 319–327. doi: 10.1111/TPJ.12470
- Deslandes, L., & Rivas, S. (2012). Catch me if you can: bacterial effectors and plant targets. *Trends in Plant Science*, *17*(11), 644–655. doi: 10.1016/J.TPLANTS.2012.06.011
- Ding, S. W., & Voinnet, O. (2007). Antiviral Immunity Directed by Small RNAs. *Cell*, *130*(3), 413–426. doi: 10.1016/J.CELL.2007.07.039
- Duan, C.-G., Fang, Y.-Y., Zhou, B.-J., Zhao, J.-H., Hou, W.-N., Zhu, H., Ding, S.-W., & Guo, H.-S. (2012). Suppression of Arabidopsis ARGONAUTE1-Mediated Slicing, Transgene-Induced RNA Silencing, and DNA Methylation by Distinct Domains of the Cucumber mosaic virus 2b Protein. *The Plant Cell*, *24*(1), 259–274. doi: 10.1105/TPC.111.092718
- Emonet, A., Zhou, F., Vacheron, J., Heiman, C. M., Dénervaud Tendon, V., Ma, K. W., Schulze-Lefert, P., Keel, C., & Geldner, N. (2021). Spatially Restricted Immune Responses Are Required for Maintaining Root Meristematic Activity upon Detection of Bacteria. *Current Biology*, *31*(5), 1012-1028.e7. doi: 10.1016/J.CUB.2020.12.048
- Endres, M. W., Gregory, B. D., Gao, Z., Foreman, A. W., Mlotshwa, S., Ge, X., Pruss, G. J., Ecker, J. R., Bowman, L. H., & Vance, V. (2010). Two Plant Viral Suppressors of Silencing Require the Ethylene-Inducible Host Transcription Factor RAV2 to Block RNA Silencing. *PLOS Pathogens*, *6*(1), e1000729. doi: 10.1371/JOURNAL.PPAT.1000729

- Fahlgren, N., Howell, M. D., Kasschau, K. D., Chapman, E. J., Sullivan, C. M., Cumbie, J. S., Givan, S. A., Law, T. F., Grant, S. R., Dangl, J. L., & Carrington, J. C. (2007). High-Throughput Sequencing of Arabidopsis microRNAs: Evidence for Frequent Birth and Death of MIRNA Genes. *PLOS ONE*, *2*(2), e219. doi: 10.1371/JOURNAL.PONE.0000219
- Fang, Y.-Y., Zhao, J.-H., Liu, S.-W., Wang, S., Duan, C.-G., & Guo, H.-S. (2016). CMV2b-AGO Interaction Is Required for the Suppression of RDR-Dependent Antiviral Silencing in Arabidopsis. *Frontiers in Microbiology*, *0*(AUG), 1329. doi: 10.3389/FMICB.2016.01329
- Fei, Q., Xia, R., & Meyers, B. C. (2013). Phased, Secondary, Small Interfering RNAs in Posttranscriptional Regulatory Networks. *The Plant Cell*, *25*(7), 2400–2415. doi: 10.1105/TPC.113.114652
- Garcia-Ruiz, H., Carbonell, A., Hoyer, J. S., Fahlgren, N., Gilbert, K. B., Takeda, A., Giampetruzzi, A., Ruiz, M. T. G., McGinn, M. G., Lowery, N., Baladejo, M. T. M., & Carrington, J. C. (2015). Roles and Programming of Arabidopsis ARGONAUTE Proteins during Turnip Mosaic Virus Infection. *PLOS Pathogens*, *11*(3), e1004755. doi: 10.1371/JOURNAL.PPAT.1004755
- Ge, Y., Han, J., Zhou, G., Xu, Y., Ding, Y., Shi, M., Guo, C., & Wu, G. (2018). Silencing of miR156 confers enhanced resistance to brown planthopper in rice. *Planta* *2018 248:4*, *248*(4), 813–826. doi: 10.1007/S00425-018-2942-6
- Giner, A., Lakatos, L., García-Chapa, M., López-Moya, J. J., & Burgyán, J. (2010). Viral Protein Inhibits RISC Activity by Argonaute Binding through Conserved WG/GW Motifs. *PLOS Pathogens*, *6*(7), e1000996. doi: 10.1371/JOURNAL.PPAT.1000996
- Glick, E., Zrachya, A., Levy, Y., Mett, A., Gidoni, D., Belausov, E., Citovsky, V., & Gafni, Y. (2008). Interaction with host SGS3 is required for suppression of RNA silencing by tomato yellow leaf curl virus V2 protein. *Proceedings of the National Academy of Sciences*, *105*(1), 157–161. doi: 10.1073/PNAS.0709036105
- Grant-Downton, R., Kourmpetli, S., Hafidh, S., Khatab, H., le Trionnaire, G., Dickinson, H., & Twell, D. (2013). Artificial microRNAs reveal cell-specific

differences in small RNA activity in pollen. *Current Biology*, 23(14), R599–R601. doi: 10.1016/J.CUB.2013.05.055

Haas, G., Azevedo, J., Moissiard, G., Geldreich, A., Himber, C., Bureau, M., Fukuhara, T., Keller, M., & Voinnet, O. (2015). Nuclear import of CaMV P6 is required for infection and suppression of the RNA silencing factor DRB4. *The EMBO Journal*, 34(20), 2591–2592. doi: 10.15252/EMBJ.201570060

Harvey, J. J. W., Lewsey, M. G., Patel, K., Westwood, J., Heimstädt, S., Carr, J. P., & Baulcombe, D. C. (2011). An Antiviral Defense Role of AGO2 in Plants. *PLOS ONE*, 6(1), e14639. doi: 10.1371/JOURNAL.PONE.0014639

Held, M. A., Penning, B., Brandt, A. S., Kessans, S. A., Yong, W., Scofield, S. R., & Carpita, N. C. (2008). Small-interfering RNAs from natural antisense transcripts derived from a cellulose synthase gene modulate cell wall biosynthesis in barley. *Proceedings of the National Academy of Sciences*, 105(51), 20534–20539. doi: 10.1073/PNAS.0809408105

Hu, S.-F., Wei, W.-L., Hong, S.-F., Fang, R.-Y., Wu, H.-Y., Lin, P.-C., Sanobar, N., Wang, H.-P., Sulistio, M., Wu, C.-T., Lo, H.-F., & Lin, S.-S. (2020). Investigation of the effects of P1 on HC-pro-mediated gene silencing suppression through genetics and omics approaches. *Botanical Studies* 2020 61:1, 61(1), 1–18. doi: 10.1186/S40529-020-00299-X

Ivanov, K. I., Eskelin, K., Bašić, M., De, S., Löhmus, A., Varjosalo, M., & Mäkinen, K. (2016). Molecular insights into the function of the viral RNA silencing suppressor HCPro. *The Plant Journal*, 85(1), 30–45. doi: 10.1111/TPJ.13088

Jamous, R. M., Boonrod, K., Fuellgrabe, M. W., Ali-Shtayeh, M. S., Krczal, G., & Wassenegger, M. (2011). The helper component-proteinase of the Zucchini yellow mosaic virus inhibits the Hua Enhancer 1 methyltransferase activity in vitro. *Journal of General Virology*, 92(9), 2222–2226. doi: 10.1099/VIR.0.031534-0

Janjusevic, R., Abramovitch, R. B., Martin, G. B., & Stebbins, C. E. (2006). A Bacterial Inhibitor of Host Programmed Cell Death Defenses Is an E3 Ubiquitin Ligase. *Science*, 311(5758), 222–226. doi: 10.1126/SCIENCE.1120131

- Jones, J. D. G., & Dangl, J. L. (2006). The plant immune system. *Nature* 2006 444:7117, 444(7117), 323–329. doi: 10.1038/nature05286
- Jubic, L. M., Saile, S., Furzer, O. J., el Kasmi, F., & Dangl, J. L. (2019). Help wanted: helper NLRs and plant immune responses. *Current Opinion in Plant Biology*, 50, 82–94. doi: 10.1016/J.PBI.2019.03.013
- Katiyar-Agarwal, S., Morgan, R., Dahlbeck, D., Borsani, O., Villegas, A., Zhu, J.-K., Staskawicz, B. J., & Jin, H. (2006). A pathogen-inducible endogenous siRNA in plant immunity. *Proceedings of the National Academy of Sciences*, 103(47), 18002–18007. doi: 10.1073/PNAS.0608258103
- Kendall, A., McDonald, M., Bian, W., Bowles, T., Baumgarten, S. C., Shi, J., Stewart, P. L., Bullitt, E., Gore, D., Irving, T. C., Havens, W. M., Ghabrial, S. A., Wall, J. S., & Stubbs, G. (2008). Structure of Flexible Filamentous Plant Viruses. *Journal of Virology*, 82(19), 9546–9554. doi: 10.1128/JVI.00895-08
- Kontra, L., Csorba, T., Tavazza, M., Lucioli, A., Tavazza, R., Moxon, S., Tisza, V., Medzihradzsky, A., Turina, M., & Burgyán, J. (2016). Distinct Effects of p19 RNA Silencing Suppressor on Small RNA Mediated Pathways in Plants. *PLOS Pathogens*, 12(10), e1005935. doi: 10.1371/JOURNAL.PPAT.1005935
- Kroon, L. P. N. M., Brouwer, H., Cock, A. W. A. M. de, & Govers, F. (2012). The Genus *Phytophthora* Anno 2012. [Http://Dx.Doi.Org/10.1094/PHYTO-01-11-0025](http://Dx.Doi.Org/10.1094/PHYTO-01-11-0025), 102(4), 348–364. doi: 10.1094/PHYTO-01-11-0025
- Lakatos, L., Csorba, T., Pantaleo, V., Chapman, E. J., Carrington, J. C., Liu, Y.-P., Dolja, V. v, Calvino, L. F., López-Moya, J. J., & Burgyán, J. (2006). Small RNA binding is a common strategy to suppress RNA silencing by several viral suppressors. *The EMBO Journal*, 25(12), 2768–2780. doi: 10.1038/SJ.EMBOJ.7601164
- Lampropoulos, A., Sutikovic, Z., Wenzl, C., Maegele, I., Lohmann, J. U., & Forner, J. (2013). GreenGate - A Novel, Versatile, and Efficient Cloning System for Plant Transgenesis. *PLOS ONE*, 8(12), e83043. doi: 10.1371/JOURNAL.PONE.0083043

- Lansac, M., Eyquard, J. P., Salvador, B., Garcia, J. A., le Gall, O., Decroocq, V., & Schurdi-Levraud Escalettes, V. (2005). Application of GFP-tagged Plum pox virus to study Prunus–PPV interactions at the whole plant and cellular levels. *Journal of Virological Methods*, *129*(2), 125–133. doi: 10.1016/J.JVIROMET.2005.05.016
- Li, L., Yi, H., Xue, M., & Yi, M. (2017). miR398 and miR395 are involved in response to SO₂ stress in *Arabidopsis thaliana*. *Ecotoxicology* *2017* *26*:9, *26*(9), 1181–1187. doi: 10.1007/S10646-017-1843-Y
- Li, X., Lin, H., Zhang, W., Zou, Y., Zhang, J., Tang, X., & Zhou, J.-M. (2005). Flagellin induces innate immunity in nonhost interactions that is suppressed by *Pseudomonas syringae* effectors. *Proceedings of the National Academy of Sciences*, *102*(36), 12990–12995. doi: 10.1073/PNAS.0502425102
- Li, Yan, Zhang, Q., Zhang, J., Wu, L., Qi, Y., & Zhou, J.-M. (2010). Identification of MicroRNAs Involved in Pathogen-Associated Molecular Pattern-Triggered Plant Innate Immunity. *Plant Physiology*, *152*(4), 2222–2231. doi: 10.1104/PP.109.151803
- Li, Yang, Basavappa, M., Lu, J., Dong, S., Cronkite, D. A., Prior, J. T., Reinecker, H.-C., Hertzog, P., Han, Y., Li, W.-X., Cheloufi, S., Karginov, F. v., Ding, S.-W., & Jeffrey, K. L. (2016). Induction and suppression of antiviral RNA interference by influenza A virus in mammalian cells. *Nature Microbiology* *2016* *2*:3, *2*(3), 1–9. doi: 10.1038/nmicrobiol.2016.250
- Lin, P.-C., Lu, C.-W., Shen, B.-N., Lee, G.-Z., Bowman, J. L., Arteaga-Vazquez, M. A., Liu, L.-Y. D., Hong, S.-F., Lo, C.-F., Su, G.-M., Kohchi, T., Ishizaki, K., Zachgo, S., Althoff, F., Takenaka, M., Yamato, K. T., & Lin, S.-S. (2016). Identification of miRNAs and Their Targets in the Liverwort *Marchantia polymorpha* by Integrating RNA-Seq and Degradome Analyses. *Plant and Cell Physiology*, *57*(2), 339–358. doi: 10.1093/PCP/PCW020
- Lin, W., Li, B., Lu, D., Chen, S., Zhu, N., He, P., & Shan, L. (2014). Tyrosine phosphorylation of protein kinase complex BAK1/BIK1 mediates *Arabidopsis* innate immunity. *Proceedings of the National Academy of Sciences*, *111*(9), 3632–3637. doi: 10.1073/PNAS.1318817111

- López-Márquez, D., Del-Espino, Á., López-Pagán, N., Rodríguez-Negrete, E. A., Rubio-Somoza, I., Ruiz-Albert, J., Bejarano, E. R., & Beuzón, C. R. (2021). miR825-5p targets the TIR-NBS-LRR gene MIST1 and down-regulates basal immunity against *Pseudomonas syringae* in *Arabidopsis*. *Journal of Experimental Botany*, 72(20), 7316–7334. doi: 10.1093/JXB/ERAB354
- López-Salmerón, V., Schürholz, A.-K., Li, Z., Schlamp, T., Wenzl, C., Lohmann, J. U., Greb, T., & Wolf, S. (2019). Inducible, Cell Type-Specific Expression in *Arabidopsis thaliana* Through LhGR-Mediated Trans-Activation. *JoVE (Journal of Visualized Experiments)*, 2019(146), e59394. doi: 10.3791/59394
- Manacorda, C. A., Tasselli, S., Marano, M. R., & Asurmendi, S. (2021). TuMV infection alters miR168/AGO1 and miR403/AGO2 systems regulation in *Arabidopsis*. *BioRxiv*, 2021.02.17.431672. doi: 10.1101/2021.02.17.431672
- Manavella, P. A., Hagmann, J., Ott, F., Laubinger, S., Franz, M., MacEk, B., & Weigel, D. (2012). Fast-Forward Genetics Identifies Plant CPL Phosphatases as Regulators of miRNA Processing Factor HYL1. *Cell*, 151(4), 859–870. doi: 10.1016/J.CELL.2012.09.039
- Matzke, M., Kanno, T., Daxinger, L., Huettel, B., & Matzke, A. J. (2009). RNA-mediated chromatin-based silencing in plants. *Current Opinion in Cell Biology*, 21(3), 367–376. doi: 10.1016/J.CEB.2009.01.025
- McGowan, J., & Fitzpatrick, D. A. (2017). Genomic, Network, and Phylogenetic Analysis of the Oomycete Effector Arsenal. *MSphere*, 2(6). doi: 10.1128/MSPHERE.00408-17
- Melotto, M., Underwood, W., Koczan, J., Nomura, K., & He, S. Y. (2006). Plant Stomata Function in Innate Immunity against Bacterial Invasion. *Cell*, 126(5), 969–980. doi: 10.1016/J.CELL.2006.06.054
- Meng, Y., & Shao, C. (2012). Large-Scale Identification of Mirtrons in *Arabidopsis* and Rice. *PLOS ONE*, 7(2), e31163. doi: 10.1371/JOURNAL.PONE.0031163
- Mérai, Z., Kerényi, Z., Molnár, A., Barta, E., Válóczy, A., Bisztray, G., Havelda, Z., Burgyán, J., & Silhavy, D. (2005). Aureusvirus P14 Is an Efficient RNA

Silencing Suppressor That Binds Double-Stranded RNAs without Size Specificity. *Journal of Virology*, 79(11), 7217. doi: 10.1128/JVI.79.11.7217-7226.2005

Mingot, A., Valli, A., Rodamilans, B., León, D. S., Baulcombe, D. C., García, J. A., & López-Moya, J. J. (2016). The P1N-PISPO trans-Frame Gene of Sweet Potato Feathery Mottle Potyvirus Is Produced during Virus Infection and Functions as an RNA Silencing Suppressor. *Journal of Virology*, 90(7), 3543–3557. doi: 10.1128/JVI.02360-15

Miska, E. A., Alvarez-Saavedra, E., Abbott, A. L., Lau, N. C., Hellman, A. B., McGonagle, S. M., Bartel, D. P., Ambros, V. R., & Horvitz, H. R. (2007). Most *Caenorhabditis elegans* microRNAs Are Individually Not Essential for Development or Viability. *PLOS Genetics*, 3(12), e215. doi: 10.1371/JOURNAL.PGEN.0030215

Monteiro, F., & Nishimura, M. T. (2018). Structural, Functional, and Genomic Diversity of Plant NLR Proteins: An Evolved Resource for Rational Engineering of Plant Immunity. <https://doi.org/10.1146/Annurev-Phyto-080417-045817>, 56, 243–267. doi: 10.1146/ANNUREV-PHYTO-080417-045817

Morris, C. E., Kinkel, L. L., Xiao, K., Prior, P., & Sands, D. C. (2007). Surprising niche for the plant pathogen *Pseudomonas syringae*. *Infection, Genetics and Evolution*, 7(1), 84–92. doi: 10.1016/J.MEEGID.2006.05.002

Navarro, L., Dunoyer, P., Jay, F., Arnold, B., Dharmasiri, N., Estelle, M., Voinnet, O., & Jones, J. D. G. (2006). A Plant miRNA Contributes to Antibacterial Resistance by Repressing Auxin Signaling. *Science*, 312(5772), 436–439. doi: 10.1126/SCIENCE.1126088

Navarro, L., Jay, F., Nomura, K., He, S. Y., & Voinnet, O. (2008). Suppression of the MicroRNA Pathway by Bacterial Effector Proteins. *Science*, 321(5891), 964–967. doi: 10.1126/SCIENCE.1159505

Ngou, B. P. M., Ahn, H.-K., Ding, P., & Jones, J. D. G. (2021). Mutual potentiation of plant immunity by cell-surface and intracellular receptors. *Nature* 2021 592:7852, 592(7852), 110–115. doi: 10.1038/s41586-021-03315-7

- Nie, P., Chen, C., Yin, Q., Jiang, C., Guo, J., Zhao, H., & Niu, D. (2019). Function of miR825 and miR825* as Negative Regulators in *Bacillus cereus* AR156-elicited Systemic Resistance to *Botrytis cinerea* in *Arabidopsis thaliana*. *International Journal of Molecular Sciences* 2019, Vol. 20, Page 5032, 20(20), 5032. doi: 10.3390/IJMS20205032
- Niu, D., Xia, J., Jiang, C., Qi, B., Ling, X., Lin, S., Zhang, W., Guo, J., Jin, H., & Zhao, H. (2016). *Bacillus cereus* AR156 primes induced systemic resistance by suppressing miR825/825* and activating defense-related genes in *Arabidopsis*. *Journal of Integrative Plant Biology*, 58(4), 426–439. doi: 10.1111/JIPB.12446
- Padmanabhan, M. S., Ma, S., Burch-Smith, T. M., Czymmek, K., Huijser, P., & Dinesh-Kumar, S. P. (2013). Novel Positive Regulatory Role for the SPL6 Transcription Factor in the N TIR-NB-LRR Receptor-Mediated Plant Innate Immunity. *PLOS Pathogens*, 9(3), e1003235. doi: 10.1371/JOURNAL.PPAT.1003235
- Parys, K., Colaianni, N. R., Lee, H.-S., Hohmann, U., Edelbacher, N., Trgovcevic, A., Blahovska, Z., Lee, D., Mechtler, A., Muhari-Portik, Z., Madalinski, M., Schandry, N., Rodríguez-Arévalo, I., Becker, C., Sonnleitner, E., Korte, A., Bläsi, U., Geldner, N., Hothorn, M., ... Belkhadir, Y. (2021). Signatures of antagonistic pleiotropy in a bacterial flagellin epitope. *Cell Host & Microbe*, 29(4), 620-634.e9. doi: 10.1016/J.CHOM.2021.02.008
- Pasin, F., Simón-Mateo, C., & García, J. A. (2014). The Hypervariable Amino-Terminus of P1 Protease Modulates Potyviral Replication and Host Defense Responses. *PLOS Pathogens*, 10(3), e1003985. doi: 10.1371/JOURNAL.PPAT.1003985
- Peragine, A., Yoshikawa, M., Wu, G., Albrecht, H. L., & Poethig, R. S. (2004). SGS3 and SGS2/SDE1/RDR6 are required for juvenile development and the production of trans-acting siRNAs in *Arabidopsis*. *Genes & Development*, 18(19), 2368–2379. doi: 10.1101/GAD.1231804
- Pérez-Cañamás, M., & Hernández, C. (2015). Key Importance of Small RNA Binding for the Activity of a Glycine-Tryptophan (GW) Motif-containing Viral

Suppressor of RNA Silencing *. *Journal of Biological Chemistry*, 290(5), 3106–3120. doi: 10.1074/JBC.M114.593707

Pfeilmeier, S., Caly, D. L., & Malone, J. G. (2016). Bacterial pathogenesis of plants: future challenges from a microbial perspective. *Molecular Plant Pathology*, 17(8), 1298–1313. doi: 10.1111/MPP.12427

Pollari, M., De, S., Wang, A., & Mäkinen, K. (2020). The potyviral silencing suppressor HCPro recruits and employs host ARGONAUTE1 in pro-viral functions. *PLOS Pathogens*, 16(10), e1008965. doi: 10.1371/JOURNAL.PPAT.1008965

Preiss, W., & Jeske, H. (2003). Multitasking in Replication Is Common among Geminiviruses. *Journal of Virology*, 77(5), 2972–2980. doi: 10.1128/JVI.77.5.2972-2980.2003

Pruss, G. J., Lawrence, C. B., Bass, T., Li, Q. Q., Bowman, L. H., & Vance, V. (2004). The potyviral suppressor of RNA silencing confers enhanced resistance to multiple pathogens. *Virology*, 320(1), 107–120. doi: 10.1016/J.VIROL.2003.11.027

Pumplin, N., & Voinnet, O. (2013). RNA silencing suppression by plant pathogens: defence, counter-defence and counter-counter-defence. *Nature Reviews Microbiology* 2013 11:11, 11(11), 745–760. doi: 10.1038/nrmicro3120

Qiao, Y., Liu, L., Xiong, Q., Flores, C., Wong, J., Shi, J., Wang, X., Liu, X., Xiang, Q., Jiang, S., Zhang, F., Wang, Y., Judelson, H. S., Chen, X., & Ma, W. (2013). Oomycete pathogens encode RNA silencing suppressors. *Nature Genetics* 2013 45:3, 45(3), 330–333. doi: 10.1038/ng.2525

Qiao, Y., Shi, J., Zhai, Y., Hou, Y., & Ma, W. (2015). Phytophthora effector targets a novel component of small RNA pathway in plants to promote infection. *Proceedings of the National Academy of Sciences*, 112(18), 5850–5855. doi: 10.1073/PNAS.1421475112

- Raja, P., Sanville, B. C., Buchmann, R. C., & Bisaro, D. M. (2008). Viral Genome Methylation as an Epigenetic Defense against Geminiviruses. *Journal of Virology*, *82*(18), 8997–9007. doi: 10.1128/JVI.00719-08
- Ranjan, A., Fiene, G., Fackendahl, P., & Hoecker, U. (2011). The Arabidopsis repressor of light signaling SPA1 acts in the phloem to regulate seedling de-etiolation, leaf expansion and flowering time. *Development*, *138*(9), 1851–1862. doi: 10.1242/DEV.061036
- Rodríguez-Herva, J. J., González-Melendi, P., Cuartas-Lanza, R., Antúnez-Lamas, M., Río-Alvarez, I., Li, Z., López-Torrejón, G., Díaz, I., Pozo, J. C. del, Chakravarthy, S., Collmer, A., Rodríguez-Palenzuela, P., & López-Solanilla, E. (2012). A bacterial cysteine protease effector protein interferes with photosynthesis to suppress plant innate immune responses. *Cellular Microbiology*, *14*(5), 669–681. doi: 10.1111/J.1462-5822.2012.01749.X
- Rogers, K., & Chen, X. (2013). Biogenesis, Turnover, and Mode of Action of Plant MicroRNAs. *The Plant Cell*, *25*(7), 2383–2399. doi: 10.1105/TPC.113.113159
- Roux, M., Schwessinger, B., Albrecht, C., Chinchilla, D., Jones, A., Holton, N., Malinovsky, F. G., Tör, M., de Vries, S., & Zipfel, C. (2011). The Arabidopsis Leucine-Rich Repeat Receptor-Like Kinases BAK1/SERK3 and BKK1/SERK4 Are Required for Innate Immunity to Hemibiotrophic and Biotrophic Pathogens. *The Plant Cell*, *23*(6), 2440–2455. doi: 10.1105/TPC.111.084301
- Rubio-Somoza, I., & Weigel, D. (2011). MicroRNA networks and developmental plasticity in plants. *Trends in Plant Science*, *16*(5), 258–264. doi: 10.1016/J.TPLANTS.2011.03.001
- Rubio-Somoza, I., Zhou, C.-M., Confraria, A., Martinho, C., von Born, P., Baena-Gonzalez, E., Wang, J.-W., & Weigel, D. (2014). Temporal Control of Leaf Complexity by miRNA-Regulated Licensing of Protein Complexes. *Current Biology*, *24*(22), 2714–2719. doi: 10.1016/J.CUB.2014.09.058

- Saijo, Y., Loo, E. P., & Yasuda, S. (2018). Pattern recognition receptors and signaling in plant–microbe interactions. *The Plant Journal*, *93*(4), 592–613. doi: 10.1111/TPJ.13808
- Salvador-Guirao, R., Baldrich, P., Weigel, D., Rubio-Somoza, I., & Segundo, B. S. (2017). The MicroRNA miR773 Is Involved in the Arabidopsis Immune Response to Fungal Pathogens. <https://doi.org/10.1094/MPMI-05-17-0108-R>, *31*(2), 249–259. doi: 10.1094/MPMI-05-17-0108-R
- Sanobar, N., Lin, P.-C., Pan, Z.-J., Fang, R.-Y., Tjita, V., Chen, F.-F., Wang, H.-C., Tsai, H.-L., Wu, S.-H., Shen, T.-L., Chen, Y.-H., & Lin, S.-S. (2021). Investigating the Viral Suppressor HC-Pro Inhibiting Small RNA Methylation through Functional Comparison of HEN1 in Angiosperm and Bryophyte. *Viruses* 2021, Vol. 13, Page 1837, *13*(9), 1837. doi: 10.3390/V13091837
- Sawchuk, M. G., Donner, T. J., Head, P., & Scarpella, E. (2008). Unique and Overlapping Expression Patterns among Members of Photosynthesis-Associated Nuclear Gene Families in Arabidopsis. *Plant Physiology*, *148*(4), 1908–1924. doi: 10.1104/PP.108.126946
- Schürholz, A.-K., López-Salmerón, V., Li, Z., Forner, J., Wenzl, C., Gaillochet, C., Augustin, S., Barro, A. V., Fuchs, M., Gebert, M., Lohmann, J. U., Greb, T., & Wolf, S. (2018). A Comprehensive Toolkit for Inducible, Cell Type-Specific Gene Expression in Arabidopsis. *Plant Physiology*, *178*(1), 40–53. doi: 10.1104/PP.18.00463
- Serna, L., & Fenoll, C. (1997). Tracing the ontogeny of stomatal clusters in Arabidopsis with molecular markers. *The Plant Journal*, *12*(4), 747–755. doi: 10.1046/J.1365-313X.1997.12040747.X
- Shiboleth, Y. M., Haronsky, E., Leibman, D., Arazi, T., Wassenegger, M., Whitham, S. A., Gaba, V., & Gal-On, A. (2007). The Conserved FRNK Box in HC-Pro, a Plant Viral Suppressor of Gene Silencing, Is Required for Small RNA Binding and Mediates Symptom Development. *Journal of Virology*, *81*(23), 13135–13148. doi: 10.1128/JVI.01031-07
- Shivaprasad, P. v., Chen, H.-M., Patel, K., Bond, D. M., Santos, B. A. C. M., & Baulcombe, D. C. (2012). A MicroRNA Superfamily Regulates Nucleotide

- Binding Site–Leucine-Rich Repeats and Other mRNAs. *The Plant Cell*, 24(3), 859–874. doi: 10.1105/TPC.111.095380
- Smith, L. M., Burbano, H. A., Wang, X., Fitz, J., Wang, G., Ural-Blimke, Y., & Weigel, D. (2015). Rapid divergence and high diversity of miRNAs and miRNA targets in the Camelinae. *The Plant Journal*, 81(4), 597–610. doi: 10.1111/TPJ.12754
- Soto-Suárez, M., Baldrich, P., Weigel, D., Rubio-Somoza, I., & San Segundo, B. (2017). The Arabidopsis miR396 mediates pathogen-associated molecular pattern-triggered immune responses against fungal pathogens. *Scientific Reports 2017 7:1*, 7(1), 1–14. doi: 10.1038/srep44898
- T, I., MA, T., & O, V. (2017). Biochemical and genetic functional dissection of the P38 viral suppressor of RNA silencing. *RNA (New York, N.Y.)*, 23(5), 639–654. doi: 10.1261/RNA.060434.116
- Takahashi, H., Watanabe-Takahashi, A., Smith, F. W., Blake-Kalff, M., Hawkesford, M. J., & Saito, K. (2000). The roles of three functional sulphate transporters involved in uptake and translocation of sulphate in Arabidopsis thaliana. *The Plant Journal*, 23(2), 171–182. doi: 10.1046/J.1365-313X.2000.00768.X
- Thiébeauld, O., Charvin, M., Rastogi, M. S., Yang, F., Pontier, D., Pouzet, C., Bapaume, L., Ameseffe, D., Li, G., Deslandes, L., Lagrange, T., Alfano, J. R., & Navarro, L. (2021). A bacterial GW-effector directly targets Arabidopsis Argonaute 1 to suppress PAMP-triggered immunity and cause disease. *BioRxiv*, 215590. doi: 10.1101/215590
- Thines Marco, M., & Kamoun, S. (2010). Oomycete–plant coevolution: recent advances and future prospects. *Current Opinion in Plant Biology*, 13(4), 427–433. doi: 10.1016/J.PBI.2010.04.001
- Todesco, M., Rubio-Somoza, I., Paz-Ares, J., & Weigel, D. (2010). A Collection of Target Mimics for Comprehensive Analysis of MicroRNA Function in Arabidopsis thaliana. *PLOS Genetics*, 6(7), e1001031. doi: 10.1371/JOURNAL.PGEN.1001031

- Toro, F. J. del, Donaire, L., Aguilar, E., Chung, B.-N., Tenllado, F., & Canto, T. (2017). Potato Virus Y HCPro Suppression of Antiviral Silencing in *Nicotiana benthamiana* Plants Correlates with Its Ability To Bind In Vivo to 21- and 22-Nucleotide Small RNAs of Viral Sequence. *Journal of Virology*, *91*(12), 367–384. doi: 10.1128/JVI.00367-17
- Ursache, R., Andersen, T. G., Marhavý, P., & Geldner, N. (2018). A protocol for combining fluorescent proteins with histological stains for diverse cell wall components. *The Plant Journal*, *93*(2), 399–412. doi: 10.1111/TPJ.13784
- Valli, A. A., Gallo, A., Rodamilans, B., López-Moya, J. J., & García, J. A. (2018). The HCPro from the Potyviridae family: an enviable multitasking Helper Component that every virus would like to have. *Molecular Plant Pathology*, *19*(3), 744–763. doi: 10.1111/MPP.12553
- Valli, A., García, J. A., & López-Moya, J. J. (2015). Potyviridae. *ELS*, 1–10. doi: 10.1002/9780470015902.A0000755.PUB3
- Várallyay, É., & Havelda, Z. (2013). Unrelated viral suppressors of RNA silencing mediate the control of ARGONAUTE1 level. *Molecular Plant Pathology*, *14*(6), 567–575. doi: 10.1111/MPP.12029
- Várallyay, É., Válóczy, A., Ágyi, Á., Burgyán, J., & Havelda, Z. (2017). Plant virus-mediated induction of miR168 is associated with repression of ARGONAUTE1 accumulation. *The EMBO Journal*, *36*(11), 1641–1642. doi: 10.15252/EMBJ.201797083
- Vaucheret, H., Vazquez, F., Crété, P., & Bartel, D. P. (2004). The action of ARGONAUTE1 in the miRNA pathway and its regulation by the miRNA pathway are crucial for plant development. *Genes & Development*, *18*(10), 1187–1197. doi: 10.1101/GAD.1201404
- Vetukuri, R. R., Whisson, S. C., & Grenville-Briggs, L. J. (2017). Phytophthora infestans effector Pi14054 is a novel candidate suppressor of host silencing mechanisms. *European Journal of Plant Pathology* 2017 149:3, *149*(3), 771–777. doi: 10.1007/S10658-017-1222-9

- Vries, S. de, Dahlen, J. K. von, Uhlmann, C., Schnake, A., Kloesges, T., & Rose, L. E. (2017). Signatures of selection and host-adapted gene expression of the *Phytophthora infestans* RNA silencing suppressor PSR2. *Molecular Plant Pathology*, *18*(1), 110–124. doi: 10.1111/MPP.12465
- Wang, Linping, Poque, S., Laamanen, K., Saarela, J., Poso, A., Laitinen, T., & Valkonen, J. P. T. (2021). In Vitro Identification and In Vivo Confirmation of Inhibitors for Sweet Potato Chlorotic Stunt Virus RNA Silencing Suppressor, a Viral RNase III. *Journal of Virology*, *95*(12). doi: 10.1128/JVI.00107-21
- Wang, Liping, Ding, Y., He, L., Zhang, G., Zhu, J.-K., & Lozano-Duran, R. (2020). A virus-encoded protein suppresses methylation of the viral genome through its interaction with AGO4 in the Cajal body. *ELife*, *9*, 1–21. doi: 10.7554/ELIFE.55542
- Wang, S., Boevink, P. C., Welsh, L., Zhang, R., Whisson, S. C., & Birch, P. R. J. (2017). Delivery of cytoplasmic and apoplastic effectors from *Phytophthora infestans* haustoria by distinct secretion pathways. *New Phytologist*, *216*(1), 205–215. doi: 10.1111/NPH.14696
- Waqar, I. (2018). Plant disease epidemiology: disease triangle and forecasting mechanisms in highlights. *Hosts and Viruses*, *5*(1), 7–11.
- Whisson, S. C., Boevink, P. C., Moleleki, L., Avrova, A. O., Morales, J. G., Gilroy, E. M., Armstrong, M. R., Grouffaud, S., van West, P., Chapman, S., Hein, I., Toth, I. K., Pritchard, L., & Birch, P. R. J. (2007). A translocation signal for delivery of oomycete effector proteins into host plant cells. *Nature* *2007* *450*:7166, *450*(7166), 115–118. doi: 10.1038/nature06203
- Xiang, T., Zong, N., Zou, Y., Wu, Y., Zhang, J., Xing, W., Li, Y., Tang, X., Zhu, L., Chai, J., & Zhou, J. M. (2008). *Pseudomonas syringae* Effector AvrPto Blocks Innate Immunity by Targeting Receptor Kinases. *Current Biology*, *18*(1), 74–80. doi: 10.1016/J.CUB.2007.12.020
- Xiong, Q., Ye, W., Choi, D., Wong, J., Qiao, Y., Tao, K., Wang, Y., & Ma, W. (2014). *Phytophthora* Suppressor of RNA Silencing 2 Is a Conserved RxLR Effector that Promotes Infection in Soybean and *Arabidopsis thaliana*.

[Http://Dx.Doi.Org/10.1094/MPMI-06-14-0190-R](http://dx.doi.org/10.1094/MPMI-06-14-0190-R), 27(12), 1379–1389. doi: 10.1094/MPMI-06-14-0190-R

Yamada, K., Yamaguchi, K., Shirakawa, T., Nakagami, H., Mine, A., Ishikawa, K., Fujiwara, M., Narusaka, M., Narusaka, Y., Ichimura, K., Kobayashi, Y., Matsui, H., Nomura, Y., Nomoto, M., Tada, Y., Fukao, Y., Fukamizo, T., Tsuda, K., Shirasu, K., ... Kawasaki, T. (2016). The Arabidopsis CERK1-associated kinase PBL27 connects chitin perception to MAPK activation. *The EMBO Journal*, 35(22), 2468–2483. doi: 10.15252/EMBJ.201694248

Yang, C.-Y., Huang, Y.-H., Lin, C.-P., Lin, Y.-Y., Hsu, H.-C., Wang, C.-N., Liu, L.-Y. D., Shen, B.-N., & Lin, S.-S. (2015). MicroRNA396-Targeted SHORT VEGETATIVE PHASE Is Required to Repress Flowering and Is Related to the Development of Abnormal Flower Symptoms by the Phyllody Symptoms1 Effector. *Plant Physiology*, 168(4), 1702–1716. doi: 10.1104/PP.15.00307

Yin, H., Hong, G., Li, L., Zhang, X., Kong, Y., Sun, Z., Li, J., Chen, J., & He, Y. (2019). miR156/SPL9 Regulates Reactive Oxygen Species Accumulation and Immune Response in *Arabidopsis thaliana*. [Https://Doi.Org/10.1094/PHYTO-08-18-0306-R](https://doi.org/10.1094/PHYTO-08-18-0306-R), 109(4), 632–642. doi: 10.1094/PHYTO-08-18-0306-R

Yuan, M., Jiang, Z., Bi, G., Nomura, K., Liu, M., Wang, Y., Cai, B., Zhou, J.-M., He, S. Y., & Xin, X.-F. (2021). Pattern-recognition receptors are required for NLR-mediated plant immunity. *Nature* 2021 592:7852, 592(7852), 105–109. doi: 10.1038/s41586-021-03316-6

Zeng, Y., & Cullen, B. R. (2004). Structural requirements for pre-microRNA binding and nuclear export by Exportin 5. *Nucleic Acids Research*, 32(16), 4776–4785. doi: 10.1093/NAR/GKH824

Zhai, J., Jeong, D.-H., Paoli, E. de, Park, S., Rosen, B. D., Li, Y., González, A. J., Yan, Z., Kitto, S. L., Grusak, M. A., Jackson, S. A., Stacey, G., Cook, D. R., Green, P. J., Sherrier, D. J., & Meyers, B. C. (2011). MicroRNAs as master regulators of the plant NB-LRR defense gene family via the

production of phased, trans-acting siRNAs. *Genes & Development*, 25(23), 2540–2553. doi: 10.1101/GAD.177527.111

Zhang, P., Jia, Y., Shi, J., Chen, C., Ye, W., Wang, Y., Ma, W., & Qiao, Y. (2019). The WY domain in the Phytophthora effector PSR1 is required for infection and RNA silencing suppression activity. *New Phytologist*, 223(2), 839–852. doi: 10.1111/NPH.15836

Zhang, Xiaoming, Du, P., Lu, L., Xiao, Q., Wang, W., Cao, X., Ren, B., Wei, C., & Li, Y. (2008). Contrasting effects of HC-Pro and 2b viral suppressors from Sugarcane mosaic virus and Tomato aspermy cucumovirus on the accumulation of siRNAs. *Virology*, 374(2), 351–360. doi: 10.1016/J.VIROL.2007.12.045

Zhang, Xiaoming, Zhao, H., Gao, S., Wang, W. C., Katiyar-Agarwal, S., Huang, H. da, Raikhel, N., & Jin, H. (2011a). Arabidopsis Argonaute 2 Regulates Innate Immunity via miRNA393*-Mediated Silencing of a Golgi-Localized SNARE Gene, MEMB12. *Molecular Cell*, 42(3), 356–366. doi: 10.1016/J.MOLCEL.2011.04.010

Zhang, Xiaoming, Zhao, H., Gao, S., Wang, W.-C., Katiyar-Agarwal, S., Huang, H.-D., Raikhel, N., & Jin, H. (2011b). Arabidopsis Argonaute 2 Regulates Innate Immunity via miRNA393*-Mediated Silencing of a Golgi-Localized SNARE Gene, MEMB12. *Molecular Cell*, 42(3), 356–366. doi: 10.1016/J.MOLCEL.2011.04.010

Zhang, Xiuren, Henriques, R., Lin, S.-S., Niu, Q.-W., & Chua, N.-H. (2006). Agrobacterium-mediated transformation of Arabidopsis thaliana using the floral dip method. *Nature Protocols* 2006 1:2, 1(2), 641–646. doi: 10.1038/nprot.2006.97

Zhang, Y., Xia, R., Kuang, H., & Meyers, B. C. (2016). The Diversification of Plant NBS-LRR Defense Genes Directs the Evolution of MicroRNAs That Target Them. *Molecular Biology and Evolution*, 33(10), 2692–2705. doi: 10.1093/MOLBEV/MSW154

Zheng, L., Zhang, C., Shi, C., Yang, Z., Wang, Y., Zhou, T., Sun, F., Wang, H., Zhao, S., Qin, Q., Qiao, R., Ding, Z., Wei, C., Xie, L., Wu, J., & Li, Y. (2017).

Rice stripe virus NS3 protein regulates primary miRNA processing through association with the miRNA biogenesis factor OsDRB1 and facilitates virus infection in rice. *PLOS Pathogens*, 13(10), e1006662. doi: 10.1371/JOURNAL.PPAT.1006662

Zheng, Z., Wang, N., Jalajakumari, M., Blackman, L., Shen, E., Verma, S., Wang, M.-B., & Millar, A. A. (2020). miR159 Represses a Constitutive Pathogen Defense Response in Tobacco. *Plant Physiology*, 182(4), 2182–2198. doi: 10.1104/PP.19.00786

Zhou, F., Emonet, A., Tendon, V. D., Marhavy, P., Wu, D., Lahaye, T., & Geldner, N. (2020). Co-occurrence of Damage and Microbial Patterns Controls Localized Immune Responses in Roots. *Cell*, 180(3), 440-453.e18. doi: 10.1016/J.CELL.2020.01.013

Zhou, J. M., & Zhang, Y. (2020). Plant Immunity: Danger Perception and Signaling. *Cell*, 181(5), 978–989. doi: 10.1016/J.CELL.2020.04.028

Zou, Y., Wang, S., Zhou, Y., Bai, J., Huang, G., Liu, X., Zhang, Y., Tang, D., & Lu, D. (2018). Transcriptional Regulation of the Immune Receptor FLS2 Controls the Ontogeny of Plant Innate Immunity. *The Plant Cell*, 30(11), 2779–2794. doi: 10.1105/TPC.18.00297

ANNEX

Annex 1 **DEG RNA-seq** is provided in an accompanying Excel File. If you cannot access to it, request it sending an email to ignacio.rubio@cragenomica.es.

